CELLULAR MECHANISMS UNDERLYING HOMEOSTATIC AND CROSS-MODAL PLASTICITY IN MOUSE PRIMARY VISUAL CORTEX

by

Gabriela Rodríguez

A dissertation submitted to Johns Hopkins University in conformity with the requirements for the degree of Doctor of Philosophy.

Baltimore, MD

April, 2018

Abstract

The brain has an essential ability to modify and reorganize synaptic connections according to experience. Sensory experience, in particular, is required for the formation of cortical circuits during early postnatal development and for their regulation throughout life. Synaptic connections are modified according to experience through two mechanisms, synapse-specific (Hebbian) and global (homeostatic) plasticity, which must work in harmony to achieve optimal processing. Sensory loss causes brain-wide adaptations that engage both types of synaptic plasticity. In the deprived cortex, homeostatic mechanisms of plasticity regulate synaptic function after prolonged periods of sensory loss, whereas spared cortical areas undergo compensatory cross-modal synaptic plasticity. We have utilized rodent primary visual cortex (V1) to investigate the mechanisms that mediate these compensatory changes after sensory loss. Here, we demonstrate the indispensable role of NMDARs in both types of plasticity. First, we provide evidence for the requirement of NMDARs in homeostatic synaptic plasticity after uni-modal sensory loss (dark exposure). In parallel, we induced cross-modal plasticity in V1 of adult mice by deafening animals older than 3 months (P90-120). Inspired by previous work showing synaptic strengthening in the feedforward thalamic input after cross-modal sensory deprivation (Petrus et al., 2014), we investigated the molecular mechanisms underlying this post- critical period plasticity. We show that cross-modal TC plasticity in the adult brain is driven mainly by the resurgence of NMDAR-dependent LTP at TC synapses, with no modulation on feedforward inhibition. Moreover, we demonstrate *in vivo* functional

consequences of deafening on V1 by using ocular dominance plasticity (ODP) as a model. Briefly, we show that deafening accelerates ODP in adult V1 by promoting open-eye potentiation during monocular deprivation (MD). Taken together, our results indicate that both uni-modal and cross-modal plasticity rely on similar molecular mechanisms to adapt to changes in the environment. They also provide insights into the brain's ability to adapt beyond the critical period and suggest cross-modal sensory deprivation may be an effective way to re-engage plasticity in the adult brain.

Dissertation committee: Hey-Kyoung Lee, Ph. D. (advisor, primary reader)

Kristina Nielsen, Ph. D. (secondary reader)

Alfredo Kirkwood, Ph. D. (Chair)

David Linden, Ph. D.

Acknowledgements

First and foremost, I would like to thank my family for supporting me in countless ways throughout the graduate school rollercoaster.

My dad for instilling in me a curious spirit and endorsing my passions in life.

My mom for teaching me there are no limits and pushing me to be my best.

My grandmother for showing me what unconditional love and resilience are.

My fiancé for believing in me when I doubted myself.

Second, I would like to thank my advisor Hey-Kyoung Lee for initially taking a chance on a student with no neuroscience background and guiding me through a journey into the brain. Thank you for your patience, time, guidance, optimism, and showing me that women in science can have it all (a successful career, a family and fashion style).

Third, I would like to thank past and present members of the Lee and Kirkwood labs who helped shape and guide these studies. In particular, Varun for becoming the brother I never had and sharing every step of this experience with me. Trinh for being part of my Baltimore family. Michelle, Bryce, Daniel, Emily and Jess for scientific and “not-so-scientific” discussions and outings. Thank you all for creating an enjoyable working environment.

Fourth, I would like to thank my thesis advisory committee members Alfredo, Kristina and David for your stimulating scientific commentary, invaluable feedback and constant encouragement.

Finally, I would like to thank my fur babies Nena, Scarzy and Cleo for reminding me of the small joys in life.

TABLE OF CONTENTS

List of Figures

Chapter 1: General Introduction

Section 1: Mechanisms of long-lasting synaptic plasticity: An overview

An essential feature of brain function is the capacity of neuronal connections, or synapses, to be modified according to experience. The ability of synapses to adjust their strength is referred to as synaptic plasticity, and it is thought to underlie fundamental processes such as sensory perception, development, learning and memory. Several mechanisms have been proposed and observed experimentally that allow for changes of synaptic strength or efficacy with neuronal activity. Fully understanding the mechanisms that govern synaptic plasticity will have a profound impact on our views of normal brain function, development, and the aspects that might go awry after injury or disorders of the nervous system. The first section of this chapter will focus on discussing some of the mechanisms that are known to underlie long lasting synaptic plasticity and the second section will discuss the mechanisms responsible for the homeostatic adjustment of synaptic strength, which provides stability to neural circuits

Subsection 1: Input specific synaptic plasticity

i. Long-term potentiation (LTP)

The idea that changes in synaptic activity could lead to changes in connection strength was initially proposed by Ramon y Cajal in 1911. Donald Hebb later proposed a mechanism by which synapses between neurons that had coincident or correlated activity would grow stronger (Morris, 1999), better recognized as the phrase “neurons that fire together wire together”. Experimental

evidence for activity-induced synaptic changes was first observed in the hippocampus of rabbits in which repeated electrical stimulation of the presynaptic perforant path induced an increase in the postsynaptic excitatory response in the dentate gyrus (Bliss and Gardner-Medwin, 1973). The expression “long-term potentiation (LTP)” was then used to describe the results from these experiments since the enhanced response could last hours.

At the molecular level, N-methyl-D-aspartate receptors (NMDARs) have been found to act as the synaptic “coincidence detector” for LTP. The biophysical properties of NMDARs allow these proteins to detect coincident glutamate release and postsynaptic activity. NMDARs are tetrameric proteins that require glutamate binding as well as a change in membrane potential in order to become fully active. The change in voltage is required to remove magnesium ions that block the NMDARs channel under resting membrane potential (Mayer et al., 1984). Therefore, presynaptic glutamate release as well as postsynaptic depolarization must occur within a very narrow time-window in order for these receptors to open and allow influx of ions into postsynaptic compartments.

The influx of calcium is key for the expression of LTP since it activates a cascade of kinases that play critical roles in the transduction mechanisms that lead to synapse modification. One major kinase implicated in LTP is calcium/calmodulin dependent protein kinase II (CaMKII) which can activate downstream effectors through phosphorylation events and undergoes autophosphorylation after calcium influx (Lisman et al., 2012; Peter et al., 1998). The importance of CaMKII for this process is highlighted by several independent studies in which blockade of CaMKII

activity inhibited LTP (Frankland et al., 2001; Malenka and Bear, 2004; Malinow et al., 1989; Otmakhov et al., 1997) or a postsynaptic loading of constitutively active CaMKII promoted and occluded LTP (Lledo et al., 1995; Monyer et al., 1994; Pettit et al., 1994; Pi et al., 2010). The ability of CaMKII to autophosphorylate allows it to become independent of calmodulin, which initially regulates CamKII activation in response to calcium influx, and remain active long after calcium has initially entered the cell. At this point CaMKII plays dual roles in facilitating LTP. First, CaMKII activity leads to an activation of downstream effectors that participate in cellular processes leading to changes in synaptic strength. One effector of CaMKII is α-amino-3-hydroxy-5-methyl-4-isoxazolepropionic acid receptors (AMPARs) subunit GluA1, which can be phosphorylated at residues serine 818 (S818) and S831 by CaMKII and protein kinase C (PKC) (Boehm et al., 2006). In addition, GluA1 is phosphorylated on S845 (Esteban et al., 2003; Lee et al., 2003) by protein kinase A (PKA) (Boehm et al., 2006; Roche et al., 1996). Phosphorylation of these residues have been shown to promote the insertion of AMPARs in the postsynaptic density (PSD) or to increase AMPAR open channel probability (Goel et al., 2011; Lee and Kirkwood, 2011). Second, fully phosphorylated CaMKII gets incorporated into the PSD and serves as a scaffold for newly inserted AMPARs (Lisman and Zhabotinsky, 2001; Lisman et al., 2012). Both of these processes converge to increase the number of stable AMPARs at the PSD resulting in a more robust response to glutamate release (Henley and Wilkinson, 2013; Lu and Roche, 2012).

The previously described postsynaptic processes have been the most widely studied mechanisms of synaptic strengthening. However, other

mechanisms have also been implicated in synaptic potentiation. One such example is the modification of synaptic strength by retrograde messengers like nitric oxide (NO) and brain-derived neurotrophic factor (BDNF). In these cases, calcium influx, through NMDARs or voltage gated calcium channels (VGCC), into the postsynaptic space is still required, but the ultimate locus of LTP expression is presynaptic and involves regulation of neurotransmitter release. In the case of NO signaling, calcium influx activates NO synthase in the postsynaptic neuron. NO is then able to diffuse to the presynaptic terminal resulting in an increase in glutamate release (Huang, 1997). BDNF signaling, on the other hand, mainly requires a local increase in calcium concentration before it is released from the postsynaptic compartment. It acts through TrkB receptors in the presynaptic terminal, ultimately increasing the probability of glutamate release (Regehr et al., 2009; Walz et al., 2006)

NMDAR-independent LTP has also been reported in several areas of the rodent brain (Huemmeke et al., 2002; Sarihi et al., 2008; Wang et al., 2016). This involves the activation of group 1 metabotropic glutamate receptors (mGluRs), which are generally found at perisynaptic sites. It is therefore hypothesized to be suitable for detecting high activity that can result in spill-over of glutamate to the periphery of synapses. Consistent with this idea, blockade of mGluRs has been shown to abolish LTP induced by strong, high frequency stimulation (Wang et al., 2016). The involvement of mGluRs in LTP induction was initially demonstrated to be predominant in excitatory inputs onto interneurons in the hippocampus (Perez et al., 2001). However, more recent data suggest that this mechanism is present

at a broad range of excitatory synapses (Anwyl, 2009). Group 1 mGluR-dependent LTP not only requires strong and prolonged glutamate release, but also the influx of calcium into the postsynaptic area, as is the case for NMDAR-dependent LTP (Anwyl, 2009). This type of LTP is mediated through either activation of mGluR1 or mGluR5, results in the potentiation of AMPARs or NMDARs function and can be expressed both pre- and post-synaptically (Anwyl, 2009). Currently, most data support mGluR1-dependent LTP to be expressed presynaptically, while mGluR5-dependent LTP is expressed postsynaptically and results in potentiation of both AMPAR and NMDAR function (Anwyl, 2009).

There are many other signaling pathways that have been implicated in LTP, but it is debatable whether they are required or simply play a modulatory role (Lee, 2006). However, there is overall consensus from several studies that both transcription and protein synthesis are necessary for the late phase of LTP maintenance that can last weeks (Abraham and Williams, 2008; Sutton et al., 2006). Transcription factors such as cAMP response element-binding protein (CREB) and zif/268 are activated following LTP induction and disruption of these molecules inhibits late-phase LTP (Bourtchuladze et al., 1994; Jones et al., 2001). Similarly, application of protein synthesis inhibitors impairs the persistence of LTP (Abraham and Williams, 2003; Frey et al., 1988). Thus, transcription and *de novo* protein synthesis are necessary to consolidate the changes caused by coincident activity during plasticity induction.

In most cases the changes in synaptic strength resulting from LTP are considered to be: input specific, associative, and cooperative. Input specificity

refers to a mechanism that particularly affects active synapses, and it is thought to augment the information storage capacity of neurons. In a mechanism that is input specific a single neuron can store different types of information across distinct synapses on the same cell responding to various stimuli (Citri and Malenka, 2008). Associativity relates to the ability to strengthen weak inputs if they are activated in association with stronger ones, and is thought to form the cellular basis for associative learning (Citri and Malenka, 2008). Cooperativity means that a crucial number of axons onto a neuron must be activated simultaneously in order to achieve LTP. This implies that there is a threshold level of postsynaptic activation that is necessary for inducing LTP (Citri and Malenka, 2008).

ii. Long-term depression (LTD)

Just as evidence for LTP was starting to surface, Gunter Stent proposed an opposite idea about changes in synaptic strength. In 1973 he postulated that connections between neurons with anti-correlated activity should weaken. Evidence supporting this prediction came from experiments done in hippocampal slices which demonstrated that low frequency electrical stimulation could induce a prolonged decrease in the efficiency of excitatory synaptic responses (Dudek and Bear, 1992). Low frequency stimulation likely produces a pattern of activity that consistently fails to sufficiently drive the postsynaptic neuron. Dudek and colleagues went on to name this type of change LTD. They also showed that its induction was specific to stimulated inputs and required NMDARs, similar to LTP (Dudek and Bear, 1992). Also, similar to LTP induction, LTD was shown to require calcium influx into the postsynaptic dendrite, since loading neurons with 1,2-bis(*o*-

aminophenoxy)ethane-*N*,*N*,*N′*,*N′*-tetraacetic acid (BAPTA) prevented synaptic depression (Mulkey and Malenka, 1992).

The fact that both LTP and LTD induction depend on similar molecular players suggested that the triggers for synaptic plasticity are shared and present at multiple synapses, but activation of NMDARs or postsynaptic increase in calcium alone does not determine the direction of the synaptic change. Indeed, further research into mechanisms of synaptic plasticity demonstrated that the magnitude of calcium increase in the postsynaptic compartment and the level of NMDAR activation determined the polarity of synaptic plasticity. First, Cummings and colleagues showed that strong and brief stimuli, which normally induce LTP, could generate LTD if stimulation occurred in the presence of submaximal doses of an NMDARs antagonist, but not when NMDARs were completely blocked. This result indicates that although NMDARs are indeed required for both LTP/LTD, the degree of NMDAR activation dictates the direction of synaptic plasticity (Artola and Singer, 1993; Cho et al., 2001; Cummings et al., 1996). Later, another group used intracellular calcium (Ca^{2+}) uncaging to manipulate the temporal profile and magnitude of intracellular calcium concentration ($[Ca^{2+}]$) increases, and showed that prolonged mild increases in $[Ca^{+2}]$ lead to LTD while short, large changes in $[Ca^{2+}]$ produce LTP (Yang et al., 1999).

Despite the common requirement for NMDAR activation and intracellular Ca^{2+} increase, mechanisms of LTD diverge from those of LTP downstream of Ca^{2+} changes. Postsynaptic loading of phosphatase inhibitors blocks LTD induction, which is different from the requirement of protein kinases in LTP (Kirkwood and

Bear, 1994a; Mulkey et al., 1994). Two main phosphatases, calcineurin and PP1, are implicated in the induction of LTD (Mulkey et al., 1994). The main targets for phosphatases during LTD are the AMPAR GluA1 subunit and CaMKII (Lee et al., 2000, 1998). Dephosphorylating GluR1 S845 is particularly important for LTD, leading to synaptic AMPAR endocytosis and thus weakening excitatory synaptic transmission (Lee et al., 2000).

These findings, together with what has been described for LTP, compose the current model for NMDAR-dependent long-term plasticity (Fig.1.1). Since both LTP and LTD share required molecular components, the temporal increase in calcium concentration at the postsynaptic compartment dictates which pathway dominates. In essence, because the affinity of phosphatases for calcium is lower, the LTD pathway can be activated at lower increases in $[Ca^{2+}]$ while activation of LTP requires brief, but robust changes in $[Ca^{2+}]$ (Winder and Sweatt, 2001).

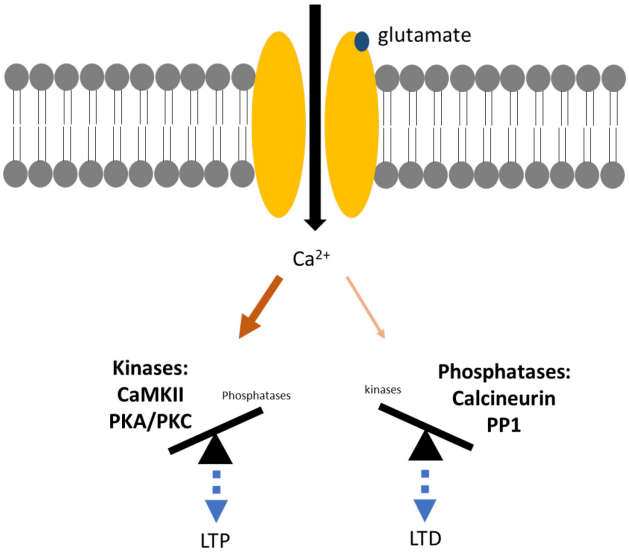

Figure 1.1: **Canonical mechanism for NMDAR-dependent LTP and LTD induction** (yellow transmembrane protein represents NMDAR). The amount of intracellular calcium determines whether kinase or phosphatase activity dominate signaling and thus, whether LTP or LTD are triggered.

Similar to LTP, NMDAR-independent forms of LTD have also been reported. It is now understood that stimulation of group 1 mGluRs can induce LTD. The first indication of mGluR-

dependent forms of LTD came from experiments in which group 1 mGluR antagonist could block LTD in the hippocampus (Stanton et al., 1991). The expression mechanisms underlying mGluR-dependent LTD involves endocytosis of synaptic AMPAR (Lüscher and Huber, 2010), which is a shared downstream mechanism with NMDAR-dependent LTD. In general, the activation of mGluRs coupled to Gq proteins induce release of intracellular calcium and synthesis of proteins that lead to or participate in AMPAR endocytosis (Huber et al., 2000). The main difference between mGluR and NMDAR dependent LTD is that activation of mGluRs leads to dissociation of GluA2 from GRIP, a synaptic AMPAR stabilizing protein, while activation of NMDARs results in regulation of AMPARs GluA1. Since each of these mechanisms regulate the internalization of different populations of AMPARs it is thought that each pathway participates in forms of LTD that are functionally distinct (Casimiro et al., 2011).

Subsection 2: Homeostatic synaptic plasticity

Although the flexibility of synapses to undergo input-specific and activity-dependent changes is imperative for brain function, it is equally important to keep neural systems working within a dynamic range. It was quickly realized that neural networks modified purely by Hebbian (LTP/LTD) mechanisms would face an inherent positive-feedback loop that would cause instability and limit information storage (Abbott and Nelson, 2000). In essence, as connections become stronger, the firing rate of the postsynaptic cell increases, potentially leading to increased coincidence between pre- and post- synaptic activity, which itself would allow for more LTP. The opposite could apply to neurons whose inputs have undergone

LTD leading to lower firing rates, which would decrease the probability of coincident activation and thus more synaptic weakening. Ultimately, in either case, this would lead to networks in which activity is saturated or minimized, and synaptic strengths are stuck at either extreme. Therefore, several mechanisms have been proposed to be at play to counteract the effects of excessive LTP/LTD in order to maintain neuronal homeostasis. One commonality between these homeostatic mechanisms is that they should operate at longer timescales than LTP/LTD in order to achieve stability, but the mechanisms by which stability is achieved vary.

i. Sliding threshold

One homeostatic mechanism is the "sliding threshold" model, which was proposed by Bienenstock, Cooper and Munro in 1982 (also known as BCM theory or metaplasticity). In this model, the threshold of activity required for inducing LTP/LTD changes according to the history of postsynaptic activity levels (Abraham and Bear, 1996; Bienenstock et al., 1982; Cooper and Bear, 2012). If neuronal activity surpasses the value for the threshold then LTP is induced, otherwise LTD is preferred. The value for the activity threshold is not constant and it is projected to "slide" to higher values after prolonged periods of high postsynaptic firing or to lower values after periods of reduced activity (Bienenstock et al., 1982).

The predictions from this model were initially tested in rat visual cortex, in which prolonged visual deprivation can reduce neuronal activity and re-exposure to light can induce high levels of activation. Indeed, the induction of LTP was viable at lower stimulation frequencies after light deprivation and required higher frequencies after light re-exposure (Kirkwood et al., 1996). These results

demonstrated that the threshold of neuronal activity for inducing LTP can change in a predictable way according to the history of neuronal activity.

NMDARs are considered to underlie the mechanism that “slides” the threshold for LTP since the magnitude of their activation dictates whether LTD or LTP is induced. NMDARs are tetrameric proteins that require an obligatory NR1 subunit in association with NR2 or NR3 components (Quinlan et al., 1999; Vicini et al., 1998). Four different types of NR2 subunits (a-d) can be incorporated and each one determines the functional properties of the NMDAR. NR2b-containing receptors have overall slower kinetics than those with NR2a and thus result in longer periods of synaptic calcium influx, which can ultimately promote LTP (Carmignoto and Vicini, 1992). It has been shown that the NR2a/NR2b ratio increases with visual experience resulting in shorter periods of calcium influx with NMDAR activation (Philpot et al., 2001, 2003; Quinlan et al., 1999) and thus favoring LTD over LTP (Shouval et al., 2002). Furthermore, visual deprivation prevents this switch, suggesting that the modification threshold for synaptic plasticity mainly changes in response to changes in neuronal activity (Carmignoto and Vicini, 1992; Fox et al., 1991; Quinlan et al., 1999).

An alternative mechanism involved in sliding the threshold for synaptic plasticity is the “pull-push” hypothesis, which argues that different neuromodulators can gate LTP/ LTD expression (Seol et al., 2007). In particular, several studies have demonstrated the ability of certain neuromodulators acting on G-protein coupled receptors (GPCRs) to promote LTP/LTD by affecting AMPAR phosphorylation (Huang et al., 2012; Seol et al., 2007). For example, GPCRs

linked to Gs and downstream adenylyl cyclase signaling promote LTP, while those linked to Gq and downstream phospholipase C (PLC) activation promote LTD (Huang et al., 2012). Moreover, activating each of these cascades triggers global LTP and LTD respectively, similar to what has been described for other forms of homeostatic synaptic plasticity like synaptic scaling (Huang et al., 2012). The main difference between the NMDAR-dependent mechanism of sliding the threshold and the "pull-push" model is that the former changes induction mechanisms of Hebbian plasticity while the latter regulates forms of expression.

Changes in the excitation to inhibition (E/I) balance can ultimately affect the output of neurons, and thus modify the threshold for synaptic plasticity. For example, studies in hippocampal slices have shown that increasing inhibitory transmission by application of muscimol increases the range of frequencies that produce LTD while decreasing inhibition by application of picrotoxin decreases that range and favors the induction of LTP (Steele and Mauk, 1999). In addition, BDNF, which can regulate the maturation of γ-aminobutyric acid (GABA)-ergic inputs, has also been implicated in modifying the threshold for synaptic plasticity (Huang et al., 1999; Huber et al., 1998). Visual cortical slices incubated with BDNF exhibit LTP with "weak" tetanic stimulus and show reduced LTD with LFS (1Hz) (Huber et al., 1998).

ii. Synaptic scaling

Another model of homeostatic plasticity termed "synaptic scaling" was proposed based on evidence from experiments in dissociated cultured neurons, in which pharmacological manipulation of synaptic activity resulted in compensatory

changes of synaptic strength (Turrigiano et al., 1998). In this model, synaptic strength is globally adjusted, by insertion or removal of AMPARs, to stabilize firing rates. Since the scaling process affects all synapses onto a neuron equally, it allows neurons to regulate firing rate while maintaining relative synaptic strength intact. This mechanism ensures that information storage and processing are not disrupted by changes in synaptic weights after homeostatic adaptations (Turrigiano, 2008).

Several studies in dissociated cultured neurons have shown that prolonged blockade of inhibitory inputs, which caused an overall increase in activity, resulted in weaker synapses as measured by a decrease in the amplitude of miniature excitatory postsynaptic currents (mEPSCS) (Lissin et al., 1998; O'Brien et al., 1998; Turrigiano et al., 1998). In contrast, blocking action potential firing or glutamate transmission through AMPARs caused the opposite effect (Lissin et al., 1998; O'Brien et al., 1998; Turrigiano et al., 1998). mEPSCs are postsynaptic currents that represent the response to individual vesicles released spontaneously under blockade of action potentials and thus are a measure of the unit strength of a synapse. mEPSC frequency and amplitude provide information about possible pre- and post-synaptic modifications of a synapse, respectively. Changes in mEPSC frequency are generally interpreted as changes in either presynaptic release probability or an alteration in synaptic contacts (Murthy et al., 2001). Differences in mEPSC amplitude are usually taken as representative of changes in the number or conductance of postsynaptic AMPARs (O'Brien et al., 1998). In the above-mentioned experiments, mEPSC amplitudes underwent multiplicative

modification after changes in neuronal activity without major regulation of event frequency, which suggests a postsynaptic locus of expression.

In vivo manipulations of neuronal activity can result in similar changes in mEPSCs, indicating that the “synaptic scaling” mechanism is not a mere artifact of cultured networks. Sensory manipulations have been a popular model used to study homeostatic changes *in vivo*, since deprivation or re-exposure to a sensory stimulus can mimic reduction or increase in neuronal activity, respectively (Czepita et al., 1994). Visual deprivation, through intraocular tetrodotoxin (TTX) injection or dark rearing (DR), results in increased mEPSC amplitude of inputs onto neurons within the primary visual cortex (V1) (Desai et al., 2002a; Goel and Lee, 2007), while re-exposure to light, after a period of dark rearing, results in decreased synaptic strength (Gao et al., 2010; Goel and Lee, 2007). It is important to note that TTX application to neuronal cultures and sensory deprivation could have significantly different consequences on neuronal activity. While TTX abolishes firing altogether, sensory deprivation would reduce sensory-evoked firing without abolishing activity from other sources, including spontaneous activity. Therefore, the molecular players found to be important for scaling after TTX incubation could be different than those at play *in vivo* even if the final consequences on synaptic strength are similar.

In general terms, the mechanisms underlying homeostatic synaptic scaling must include an “activity sensor” and subsequently a signal leading to the expression of changes in synaptic strength. Currently, there is evidence supporting the role of several molecules involved in synaptic scaling. It is pertinent to note that

the mechanisms underlying up- and downscaling are known to be asymmetric and thus each require a distinct set of signal molecules.

One molecule of interest in upscaling is the cytokine tumor necrosis factor (TNF-α), which is secreted by glial cells (Bessis et al., 2007). Neuronal cultures in which glia are unable to express TNF-α fail to respond accordingly to prolonged blockade of action potentials (Stellwagen and Malenka, 2006). Another released molecule thought to be involved in homeostatic synaptic upscaling is BDNF. Incubation with exogenous BDNF prevents upscaling after prolonged activity blockade (Rutherford et al., 1998). The bulk release of both of these compounds could account for the global changes associated with synaptic scaling. Other molecules that influence synaptic upscaling include beta-integrins and MHC1. The expression or localization of these molecules can be regulated by activity, which was the first evidence suggesting that they might play a role in scaling. For one, surface levels of beta-integrins are regulated by neuronal activity and ultimately result in altered regulation of AMPAR endocytosis (Cingolani et al., 2008). For the other, MHC1 expression is increased after activity blockade and it is believed to participate in scaling and morphological changes associated with it (Goddard et al., 2007). Additionally, phosphorylation events that promote AMPAR synaptic content, like GluA1-S845 phosphorylation, are also required for synaptic upscaling (Goel et al., 2011). Although the previously described molecules seem to be important for upscaling following decreased activity, they are either not required or have not been tested for their role in downscaling.

The mechanisms underlying downscaling have been proposed to require a different signal than the ones mentioned above. The expression of immediate early genes (IEGs), like activity-regulated cytoskeletal protein (Arc), Homer1a and Plk2, is directly involved in downscaling after periods of heightened activity. Evidence supporting this shows that overexpression of either Arc, Homer1a or Plk2 leads to synaptic depression, and knockouts of either Arc, Homer1a or Plk2 prevent downscaling (Gao et al., 2010; Hu et al., 2010; Rial Verde et al., 2006; Seeburg and Sheng, 2008; Shepherd et al., 2006). The expression of all three proteins increases after heightened activity and has been implicated in regulating AMPAR endocytosis. Their mechanisms of action, however, seem to be quite different. Arc interacts with endocytic machinery that regulates GLuA1 AMPARs. Upon heightened activity, Arc protein levels increase, which leads to higher rates of AMPAR endocytosis (Gao et al., 2010; Nikolaienko et al., 2017; Shepherd et al., 2006). Plk2 expression is thought to lead to a decrease in surface GluA2 AMPAR by disrupting its interaction with NSF, an ATPase involved in membrane fusion and AMPAR stabilization (Evers et al., 2010). Homer1a, on the other hand, competitively disrupts the mGluR complex with Shank-PSD95-NMDARs, leading to GluA2 dephosphorylation (Siddoway et al., 2014).

The search for the “activity sensor” has been more problematic, since it requires an understanding of what type of activity is being monitored. Initial reports affirmed that postsynaptic firing was a determinant factor that drives synaptic scaling. For example, blocking somatic spikes by TTX perfusion is sufficient to scale up synapses (Ibata et al., 2008), while optogenetic activation of the

postsynaptic neuron is sufficient to drive synaptic downscaling (Goold and Nicoll, 2010). However, more recent studies have challenged this idea by demonstrating that glutamate release and activation of glutamate receptors are required for synaptic scaling to occur. These experiments demonstrated that blocking AMPARs is sufficient to lead to upscaling even when firing rates were clamped to normal levels in a closed-loop system (Fong et al., 2015). Note that both, alterations in postsynaptic firing or changes in glutamatergic input, have the potential to alter calcium concentrations inside the cell. The changes in intracellular calcium could be the condition that is ultimately monitored, although there is debate as to what is the exact source of Ca^{2+} (Turrigiano, 2008).

The source of calcium leading to scaling could be VGCC, NMDARs, intracellular stores or a combination of these. Some evidence supports the role of VGCC, in particular L-type Ca^{2+} channels. Ibata and colleagues showed that blockade of L-type Ca^{2+} channels could induce synaptic upscaling in cultured neurons (Ibata et al., 2008). However, this has not been tested *in vivo*. In the case of NMDARs, the evidence is controversial. Indeed, NMDARs have been shown to be co-regulated with AMPAR after prolonged periods of altered activity (Mu et al., 2003; Watt et al., 2000), but whether their activation is required for scaling is unclear. *In vitro* studies using dissociated cortical neuronal cultures have shown that prolonged NMDAR blockade by itself does not induce upscaling (Leslie et al., 2001; Turrigiano et al., 1998). These results are opposed by studies performed in dissociated hippocampal neuronal cultures in which blockade of NMDARs does result in an increase of mEPSC amplitude (Kato et al., 2007). Additionally, other

studies in dissociated hippocampal cultures have shown NMDAR blockade to accelerate synaptic scaling induced by TTX activity blockade (Sutton et al., 2006). The discrepancy between these data could be due to differences in the brain regions from which the cultures are derived. Alternatively, each manipulation, abolishing action potentials by TTX or doing it in combination with NMDAR blockade, could engage different mechanisms of homeostatic plasticity

Although the previously mentioned *in vitro* studies have advanced our understanding of synaptic scaling mechanisms, the bath application of TTX essentially abolishes neuronal activity, which is quite different from what is possible with *in vivo* manipulations such as dark exposure (DE). Therefore, the mechanisms that govern homeostatic synaptic plasticity *in vivo* could differ from those described thus far. One group reduced NMDAR permeability to calcium *in vivo* and showed that this manipulation resulted in decreased AMPAR currents in the hippocampus (Pawlak et al., 2005). These results suggest that the calcium influx through NMDARs might be important for regulating scaling of AMPAR currents. However, this study did not address the possible lack of NMDAR-dependent LTP with reduced Ca^{2+} permeability, which could also result in low AMPAR currents. Clearly, the controversy pertaining the role of NMDAR-mediated signaling in synaptic scaling requires more specific and direct testing *in vivo*. I have addressed this issue in Chapter 2 and will further discuss my findings there. Briefly, we report a requirement for NMDAR activation in pyramidal neurons of rodent V1 to undergo homeostatic synaptic plasticity *in vivo.*

iii. Spike-timing Dependent Plasticity (STDP)

Unlike synaptic scaling, STDP is a Hebbian mechanism that can self-regulate and prevent continuous positive feedback. It relies on the theoretical premise that a delicate balance between LTP and LTD can result in consistently appropriate levels of synaptic drive (Abbott and Nelson, 2000). STDP refers to a mechanism that regulates synaptic strength according to the temporal relationship between pre- and post-synaptic activity. In general, presynaptic activity that precedes postsynaptic depolarization will induce LTP and the opposite order leads to LTD (Feldman, 2012; Linden, 1999). Independent studies have shown the precision of timing by describing the induction of LTP when the EPSP preceded the post-synaptic spike by 10 ms, but no change in response if the time was extended to 100 ms (Magee and Johnston, 1997; Markram et al., 1997). On the other hand, LTD is induced when postsynaptic spikes precede EPSPs by 20-100 ms (Bi and Poo, 1998; Feldman, 2012; Markram et al., 1997; Song et al., 2000).

In terms of homeostasis, one property this mechanism offers is a stringent temporal constraint for the induction of plasticity. Therefore, one way in which excessive LTP/LTD are prevented is by limiting their induction to a particular time requirement. Another major homeostatic feature of STDP relates to its ability to immediately counteract the increased probability of coincident firing after LTP induction which leads to its inherent positive feedback (Abbott and Nelson, 2000). Experiments done in cortical layer 2/3 (L2/3) neurons have shown that increased random spiking preferentially results in LTD based on the longer window for LTD induction (Feldman, 2000, 2012). This implies that a neuron receiving prolonged

high synaptic drive will initially increase its firing rate, but eventually this activity will become random and uncorrelated with the postsynaptic response and thus, the inputs will weaken (Feldman, 2000). Weakening of the inputs will result in less efficacy at driving the postsynaptic neuron. At this point, only the inputs that are able to produce a postsynaptic spike preceded by an EPSP within a short amount of time will undergo potentiation. Therefore, STDP can impose a balance between LTP/LTD and stabilize neuronal activity without the need for additional mechanisms.

STDP can result from two main mechanisms. In all cases, the backpropagating action potential (bAP) is a necessary component for STDP induction. Magee and colleagues demonstrated that STDP can be dependent on NMDAR activation as well as local postsynaptic spiking. During pre-leading-post conditions, the EPSP and the bAP coincide, leading to a strong NMDAR-dependent calcium signal. On the other hand, in post-leading-pre conditions the bAP coincides with activity only after an initial strong depolarization has occurred, therefore this produces either modest influx through NMDAR or inactivates them (Feldman, 2012; Linden, 1999). A different form of STDP utilizes two different coincidence detectors to produce NMDAR-dependent LTP and mGluR-dependent LTD. In this case LTP occurs in the same way as described previously, but coincident activation of mGluRs and voltage sensitive calcium channels (VSCC) lead to LTD through the release of endocannabinoid transmitter which activates presynaptic CB1 receptors and ultimately decreases probability of release (Feldman, 2012).

iv. E/I maintenance

Although the initial studies regarding homeostatic synaptic plasticity focused on studying excitatory synapses, neurons are embedded in a network composed of both excitatory and inhibitory inputs. Therefore, in order to stabilize a neural network both types of inputs must be regulated in harmony. Stemming from the premise that homeostatic mechanisms must counteract extremes in neuronal activity it follows that inhibitory inputs could be modulated to directly oppose overall excitatory drive. The overall inhibitory tone within a network depends on several factors including direct inhibition onto excitatory cells and the excitatory drive onto inhibitory neurons.

In fact, GABAergic inputs onto excitatory neurons have been shown to be under strong homeostatic control *in vitro* and *in vivo*. Work done in cultured neurons revealed that TTX-induced activity blockade can scale down miniature inhibitory postsynaptic currents (mIPSC) in pyramidal neurons by decreasing synaptic GABA-A receptors, while increased activity causes the accumulation of these receptors at the synapse (Kilman et al., 2002; Rannals and Kapur, 2011). *In vivo*, whisker deprivation has been shown to decrease the levels of GABA-A receptors and GABAergic puncta in primary somatosensory cortex (S1), while continuous whisker stimulation for 24 hours increases inhibitory synaptic density (Knott et al., 2002). Parallel results have been observed in V1, in which visual deprivation preferentially reduces the recruitment of inhibitory inputs (Gandhi et al., 2008; Maffei et al., 2004). In addition, recent studies have demonstrated that inhibitory transmission responds differentially to dark exposure versus light re-

exposure. In particular, mIPSC frequency decreases in L2/3 pyramidal neurons in V1 after dark exposure while mIPSC amplitude only increases after light exposure during a critical period (Gao et al., 2014).

In contrast, excitatory drive onto inhibitory neurons does not seem to be regulated in the same way. Experiments in cortical dissociated neurons have shown that prolonged periods of enhanced neuronal activity increase excitatory transmission onto inhibitory neurons, but decreased activity does not modulate it (Chang et al., 2010; Ibata et al., 2008; Rutherford et al., 1998). It seems likely that the varied homeostatic regulation between different inhibitory and excitatory inputs can lead to an overall tilt of the balance between excitation and inhibition that governs a particular network such that activity is stabilized.

v. Intrinsic Excitability

Homeostatic balance in neuronal activity can be achieved not only by modification of synaptic physiology, but also by changes in membrane properties. Evidence for changes in neuronal intrinsic excitability comes from experiments performed in both hippocampal (O'Leary et al., 2010) and neocortical cultures (Desai et al., 1999). A chronic decrease in activity by TTX application for 2 days results in increased firing frequency and lower spike threshold (Desai et al., 1999). These changes, at least in part, are attributed to changes in ionic conductance resulting in higher sodium currents (Desai et al., 1999; Wierenga, 2005). On the other hand, increased neuronal depolarization leads to lower resting potentials and an increased action potential threshold (O'Leary et al., 2010). In this case, an increase in potassium conductance is observed (O'Leary et al., 2010). Regulation

of the required current for spiking can provide a global homeostatic mechanism. Changes is overall neuronal intrinsic excitability could lead to an identical scaling of synapses without compromising the inputs' relative weights and with it information storage (D'Angelo, 2010).

It is clear that achieving neuronal firing homeostasis is crucial for neural networks. As I have described, this can be achieved by multiple mechanisms that possibly act in cooperation. This redundancy is likely beneficial especially in cases in which one strategy fails, but complicates the investigation of the underlying mechanisms. In addition, the exact way in which homeostasis is achieved might vary according to brain area, developmental stage and experience.

Section 2: Experience-dependent plasticity in the rodent primary visual cortex (V1)

Primary sensory cortices have been used as a popular model to study experience-dependent synaptic changes mainly due to the detailed knowledge of their anatomy and physiology, as well as the ease to directly manipulate their primary inputs. The pioneering work of Hubel and Wiesel paved the way for the study of "visual-deprivation induced plasticity" and provided invaluable insights into the functional consequences of altered experience on V1 function (Hubel and Wiesel,1959, 1962, 1970). The work presented in the following chapters focused on examining synaptic changes in V1 after sensory deprivation, and thus this section will provide an overview of the circuitry and experience-dependent synaptic changes that take place in V1.

Subsection 1: V1 circuitry overview

Sensory cortical areas, despite of their primary input, share a common laminar organization with slight variations between modalities (Creutzfeldt, 1977). V1 is characterized as having six layers, each with distinct cell types and each participating differentially in sensory processing. Layer 1 (L1) is defined as being the closest to the surface of the brain (pia) while layer 6 (L6) is the deepest and closest to the white matter. The laminar location of cells dictates the type of information they process and where it gets relayed. In general, mouse V1 receives direct input from thalamic nuclei, primarily the dorsal lateral geniculate nucleus (dLGN), and distributes information to higher order cortical and thalamic areas for further processing. Another important feature of V1 is that it maintains reciprocal, recurrent connections within the cortex itself and provides feedback to thalamic nuclei. V1 a major stage of integration in the visual pathway and each layer, with its unique qualities, plays a role in processing these sensory signals.

i. Thalamocortical (TC) input

Information from the periphery reaches most primary sensory cortices through monosynaptic inputs coming from modality-specific relay nuclei in the thalamus. In the case of mouse V1, information from the retina reaches the cortex through dLGN projections mainly onto layer 4 and 6 (Wang et al., 2013). Thalamic afferents comprise the primary driving inputs onto layer 4 (L4) and are considered the first step in the feedforward pathway of information processing in V1. TC inputs represent only about 10% of the excitatory synaptic inputs into the cortex (Ahmed et al., 1994, 1997), yet are very efficient at driving cortical responses (Bagnall et al., 2011; Bruno and Sakmann, 2006; Cruikshank et al., 2007a; Gil et al., 1999).

The organization of dLGN inputs along with the information they relay provide the substrates required to shape cortical receptive field properties in L4. Information regarding spatial localization, as well as eye-specific input is directly relayed onto V1 by TC synapses (Hubel and Wiesel, 1959). Receptive field properties like orientation selectivity are known to arise in the cortex of cats and primates, mainly by the convergence of linearly aligned center-surround LGN inputs (Alonso et al., 2001; Clay Reid and Alonso, 1995; Hubel and Wiesel, 1968). However, studies in mice have shown that orientation selectivity is present in the visual thalamus (Marshel et al., 2012; Piscopo et al., 2013) and can be inherited in V1 directly from the dLGN (Scholl et al., 2013). This implies that although shared features exist in V1, the organization of visual processing can differ according to the species studied.

ii. Layer 4 (L4)

L4 is the major recipient layer of direct sensory input from the dLGN. The principal neurons (PNs) in this layer are spiny stellate cells, although other types of excitatory and inhibitory cells are interspersed in rodent cortex. For example, L4 of rodent somatosensory cortex contains a majority (58%) of spiny stellate cells, about 25% star pyramids and about 17% pyramidal neurons (Staiger et al., 2004). Principal cells and inhibitory parvalbumin positive (PV+) cortical neurons both receive monosynaptic thalamic inputs, however the TC synapses onto PV+ neurons have been shown to be stronger and more reliable (Cruikshank et al., 2007; Kloc and Maffei, 2014). PV+ neurons that receive TC input provide

disynaptic feedforward inhibition within L4 and help shape receptive fields in V1 (Isaacson and Scanziani, 2011).

Stellate cells are characterized as has having a dendritic arbor that remains within layer 4, allowing these cells to receive direct thalamic and within-layer connections (Callaway and Borrell, 2011; Gilbert and Wiesel, 1983). Although intralaminar inputs comprise the majority of synapses for L4 principal neurons, TC inputs are known to dominate cortical drive (Cruikshank et al., 2007; Reinhold et al., 2015). TC synapses are not known to be particularly stronger than other excitatory inputs onto V1 thus, their efficiency is thought to result from recurrent lateral connections within the layer implicating that these intralaminar connections are well suited to amplify the sensory signals that reach the cortex (Douglas et al., 1989, 1995).

iii. Layer 2/3

L2/3 receives strong feedforward input from L4 as well as intralaminar and intracortical connections. Pyramidal excitatory neurons dominate L2/3 with apical dendrites that extend towards the pia and axon terminals into the deeper layers of V1 and other cortical areas (Gilbert and Wiesel, 1983). Inputs from L4 comprise the least number of synapses into L2/3 while intracortical inputs represent the majority (Binzegger, 2004; Douglas and Martin, 2004). However, the feedforward input remains very effective at driving L2/3 responses and thus, receptive fields in L2/3 are thought to arise through combinations of receptive fields of L4 neurons (Hubel and Wiesel, 1962). Intralaminar inputs are reciprocal and represent synapses made locally, between excitatory and inhibitory neurons within L2/3

(Avermann et al., 2012; Dantzker and Callaway, 2000; Olivas et al., 2012; Pala and Petersen, 2015; Thomson and Lamy, 2007; Xu et al., 2016). Intracortical afferents, on the other hand, provide feedback information from other cortical areas like higher order visual cortex. The feedback afferents originate in L5 or L6 of other cortical regions and terminate in L2/3 of V1 (Laramée and Boire, 2014; Rockland and Pandya, 1979). L2/3 in turn sends projections to lower V1 layers as well as higher order cortical areas of sensory processing (Gilbert and Wiesel, 1983; Thomson and Lamy, 2007). Within V1, L2/3 pyramidal neurons send axonal innervation mainly to L5 (Harris and Mrsic-Flogel, 2013) while long efferents to other cortical regions initiate in V1 L2/3 and innervate L4 of the target areas (Gilbert and Wiesel, 1983; Laramée and Boire, 2014).

iv. Layer 5 and 6

Layers 5 and 6 play an important role in maintaining communication between primary sensory cortices and other brain areas. L5 neurons are characterized as having dendrites that span all six layers of the cortex and thus are considered the main integrators in V1 (Shai et al., 2015). Three distinct population of excitatory neurons coexist in L5, differentiated mainly by their outputs. One type is characterized as having a longer apical dendrite and projecting to subcortical regions like superior colliculus and association thalamic nuclei (Hallman et al., 1988). The other types have slightly shorter, non-tufted dendrites and are thought to project to the V1 in the opposite hemisphere or striatum (Hallman et al., 1988; Kim et al., 2015). The diverse inputs and outputs

from L5 pyramidal neurons reveal the importance of these neurons in cortical communication.

L6 in the rodent cortex receives direct thalamocortical input as well as intracortical excitatory drive from L4, L5 and some L2/3 (Beierlein and Connors, 2002; Zarrinpar, 2006). However, it is also one of the important output layers in the cortex from which descending projections to thalamic nuclei arise (Thomson, 2010). In the mouse, three main classes of excitatory neurons have been described in L6. One class is characterized as cortico-cortical (CC). L6 CC neurons send horizontal projections which form synapses across cortical areas and other L6 pyramidal neurons (Thomson, 2010; Thomson and Lamy, 2007; Vélez-Fort and Margrie, 2012). Another class is considered to be cortico-thalamic (CT) and can be further subdivided into 2 classes according to their location within L6 and their final output (Thomson, 2010). Those found in upper L6 have dendritic arbors in L4 and project to dLGN and the thalamic reticular nucleus (TRN) (Bourassa and Deschenes, 1995; Bourassa et al., 1995). The other class, found in deep L6, has dendritic arbors in L5 and L2/3 and projects to primary and association areas of the thalamus (Llano and Sherman, 2009). Since L6 neurons receive both thalamic and cortical input and mainly innervate thalamic nuclei, they are set to establish thalamo-cortico-thalamic loops which fine tune thalamocortical processing (Briggs, 2010; Thomson, 2010).

v. Layer 1 (L1)

L1 in the rodent cortex is the least well studied layer. It has been described as consisting mainly of axon terminals from thalamic, callosal and cortical feedback

projections that synapse onto apical dendrites of pyramidal neurons whose cell bodies lie in deeper layers (e.g. L5) (Ji et al., 2015). However, recent studies have shown the existence of inhibitory cells that reside in this layer. These inhibitory neurons are known to receive thalamic as well as cortical feedback projections and can interact with neurons in other layers of V1 (Roth et al., 2015). The exact role of L1 is still not fully understood, but the pattern of inputs and outputs suggest it could be an important location for bottom up and top-down modulation of cortical function.

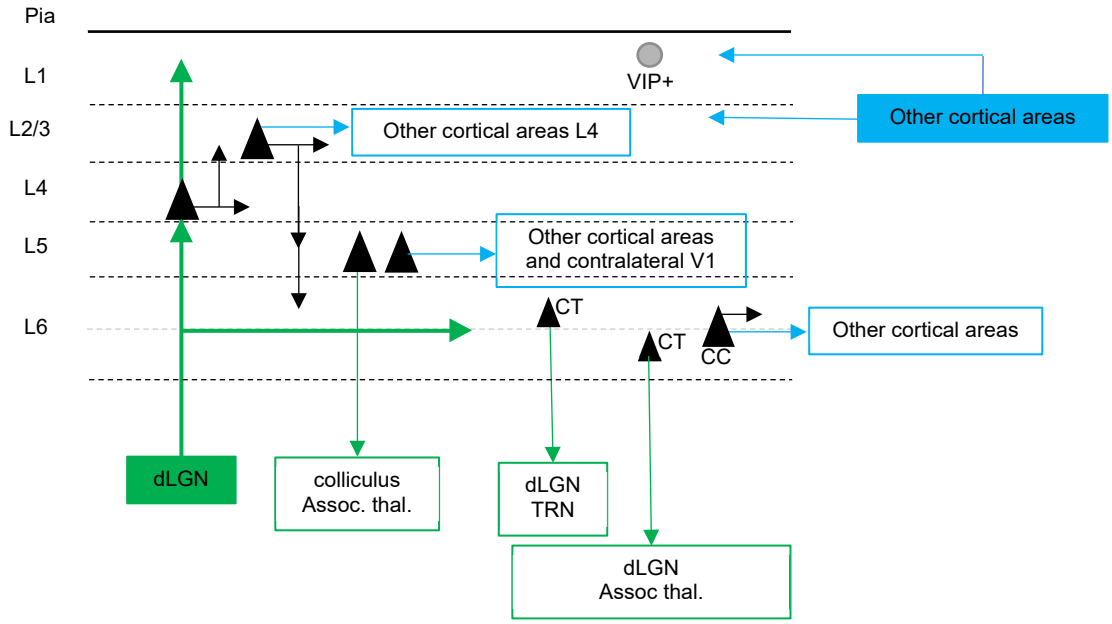

Figure 1.2: **Schematic of primary visual cortex excitatory connectivity**. Triangles represent principal neurons in each layer (CT=corticothalamic, CC=corticocortical). Black arrows represent synapses within V1 and arrow head location indicates layer to which information is transferred. Blue relates to cortical communication while green relates to subcortical (solid boxes represent source of afferents, outlined boxes represent efferent targets).

vi. Inhibition

Inhibitory neurons in the cortex are diverse, and generally are not arranged in particular layers. These neurons can be classified by morphology as basket,

chandelier and Martinotti cells; by biochemical markers as parvalbumin (PV), somatostatin (SST), or vasoactive intestinal peptide (VIP); and by electrophysiological properties as fast spiking or regular spiking (Isaacson and Scanziani, 2011). In V1, PV+ and SST+ neurons are located in most layers, while VIP+ neurons are more restricted to upper layers. It has been suggested that inhibitory neurons – in particular PV+ neurons - have broader response selectivity than excitatory cells (Kerlin et al., 2010; Runyan et al., 2010). PV+ neurons are also considered to be the primary inhibitory cells driven by thalamocortical (TC) inputs, providing feedforward inhibition to principal neurons in the cortex and sharpening L4 receptive fields (Ferster and Jagadeesh, 1992; Krukowski and Miller, 2001). SST-expressing neurons on the other hand, mainly target apical dendrites as well as other inhibitory neurons (van Versendaal and Levelt, 2016). Both of these inhibitory inputs onto excitatory neurons register with a disynaptic delay, allowing for a window of excitatory integration to occur in principal neurons before they are inhibited (Pouille and Scanziani, 2001). A third class of inhibitory neurons, VIP+ cells, are driven by cortical as well as cholinergic inputs and synapse mainly onto other inhibitory synapses, thus mediating disinhibition in V1 (Adesnik et al., 2012).

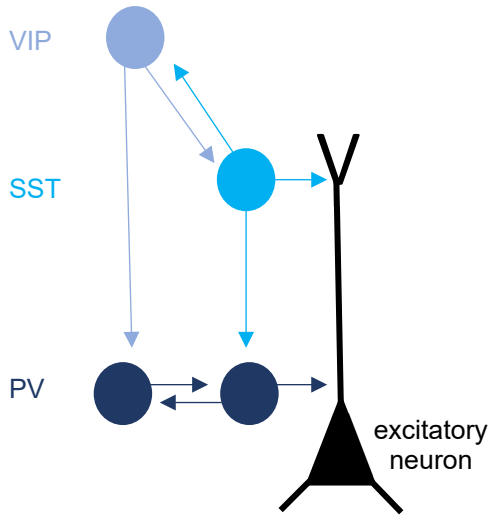

Figure 1.3: **Canonical inhibitory network described in primary sensory cortex.** Circles represent inhibitory neurons; dark blue PV+; medium blue SST+; light blue VIP+.

Although excitatory neurons in different layers receive inhibitory inputs from varied sources within the cortex, an organized pattern of connectivity between molecularly distinct inhibitory neurons has been described (Pfeffer et al., 2013). In general, PV+ interneurons inhibit one another while also providing strong inhibition to principal neurons. SST+ neurons, on the other hand do not contact each other, but instead inhibit all other populations of inhibitory cells as well as distal dendrites of excitatory neurons. VIP+ cells are more selective in their target and mainly inhibit SST+ neurons. This scheme occurs somewhat uniformly across layers, suggesting that inhibitory networks modify cortical inputs and outputs similarly (Pfeffer et al., 2013).

Subsection 2: Experience-dependent changes in V1

Classical studies by Hubel and Wiesel characterized basic features of V1 neurons and how susceptible they are to manipulations of visual experience in cats and primates (Hubel and Wiesel, 1959,1962, 1968, 1970). More recent studies have demonstrated these features to be conserved in rodent V1 (Dräger, 1978; Gordon et al., 1996). Inputs into V1 arise from both the contralateral and ipsilateral eyes. The rodent cortex receives the majority of its afferents from the contralateral eye and devotes a large area to these inputs, while a smaller

binocular area coexists where inputs from both eyes coincide (Dräger, 1975; Kalatsky and Stryker, 2003). Another important characteristic of mouse V1 organization is its preserved retinotopy - inputs are organized in an ordered spatial representation of the external world (Schuett et al., 2002; Wagor et al., 1980). A basic aspect of V1 processing is that pixels of light detected by the retina are transformed into orientation selective responses (Hubel and Wiesel, 1962). Each of these features is malleable by experience at particular periods during development, the so called “critical periods”. It is also worth noting that different cortical layers are susceptible to experience-dependent synaptic changes during different periods (Desai et al., 2002). In the following sections I will discuss some of the best characterized synaptic modifications in V1 resulting from changes in sensory experience.

i. Thalamocortical refinement

The first major change in visually driven experience for rodents occurs at eye opening, which is around post-natal day 14 (P14). Although thalamic innervation is complete at eye-opening, the circuit is not yet mature. Thalamic inputs are broadly connected to neurons in the cortex and require visual experience to refine their arborization in L4 and L6 (Hensch et al., 2004). A window of robust plasticity at thalamocortical (TC) synapses allows these modifications to occur for about a week after eye opening (Jiang et al., 2007). Several independent studies have reported the potential for inducing LTP and LTD at TC synapses onto V1 L4 for a short period of time after eye opening (Dudek and Friedlander, 1996; Jiang et al., 2007; Kirkwood et al., 1995). In particular, LTP is lost at thalamic inputs

at P21 (Jiang et al., 2007). LTD, however, undergoes a more gradual loss and can be elicited up until the fourth week of post-natal development in L4 (Jiang et al., 2007)

This early postnatal TC plasticity in L4 has been shown to be dependent on the activation of NMDARs and on the presence of postsynaptic intracellular calcium, both of which are mechanisms conserved in other sensory cortical areas (Barkat et al., 2011; Crair and Malenka, 1995; Kirkwood and Bear, 1994b). A change correlated with the decline of this period of plasticity is a switch in the composition of NMDARs at TC synapses that is able to change NMDAR function and thus the ease of inducing LTP/LTD (Erisir and Harris, 2003). At birth, NMDARs are comprised of the obligatory NR1 subunit in conjunction with NR2b (Stocca and Vicini, 1998). However, there is a progressive inclusion of NR2a subunits as post-natal development ensues (Monyer et al., 1994; Stocca and Vicini, 1998). Studies in rat V1 have shown that this switch in subunit composition is driven by visually evoked activity (e.g. eye-opening or light exposure) (Philpot et al., 2001; Quinlan et al., 1999). The main consequence of the switch in NMDAR subunit composition is a change in receptor kinetics from longer decay times to shorter ones after the incorporation of NR2a (Carmignoto and Vicini, 1992; Philpot et al., 2003; Quinlan et al., 1999). Although changes in NMDAR subunits have been described in L4 and L2/3 of V1, it is important to note that L2/3 seems to be aplastic during the developmental window for plasticity at TC synapses (Desai et al., 2002). On the other hand, L2/3 synapses remain plastic even after the closure of heightened TC plasticity (Desai et al., 2002; Goel and Lee, 2007), demonstrating a structured

progress of adaptation to sensory experience through layers in V1. Recently, the classically defined “critical period” for TC plasticity has been challenged by studies showing post-critical period LTP at these inputs under particular circumstances (e.g. enriched environment) (Mainardi et al., 2010; Montey and Quinlan, 2011; Petrus et al., 2014). However, whether V1 TC connections have the ability to extend or reopen a “critical period” in adulthood is unclear. I have addressed this possibility in Chapter 4, in which I will discuss in more detail the reemergence of TC plasticity in adult mouse V1 after deafening.

ii. Ocular Dominance Plasticity (ODP)

Visual deprivation paradigms are also used to probe periods for experience-dependent plasticity in V1. Monocular deprivation (MD) was the classical manipulation used to define the critical period of visual cortical plasticity by Hubel and Wiesel(Hubel and Wiesel, 1970). Typically, MD involves surgically closing one eyelid while the other eye is allowed to have normal visual input. Currently, it is still used to interrogate the effects of visual experience within and outside the critical period. However, many other paradigms have been developed over the years like retinal ablations (Gilbert and Wiesel, 1992; Keck et al.), intraocular TTX injections (Desai et al., 2002a; Frenkel and Bear, 2004) and dark exposure (Fagiolini et al., 1994; Mower, 1991). By applying some of these other paradigms to the study of ODP, we now understand that the changes in ocular dominance are governed by competition between inputs from both eyes. This is supported by reports of a lack of ocular dominance shift when manipulations decrease visual input equally from

both eyes (e.g. binocular lid suture) (Frenkel and Bear, 2004; Gordon et al., 1996; Wiesel and Hubel, 1965).

Experiments describing the effects of MD on V1 function led to the categorization of cortical cells into different ocular dominance classes depending on their responsiveness to inputs from either eye (Hubel and Wiesel, 1970). Following MD, the ocular dominance of the neurons shifted such that the majority of neurons preferentially responded to the eye that remained opened. The ability of neurons to undergo this change was termed ocular dominance plasticity (ODP) and was characterized as being heightened during early postnatal development (Gordon et al., 1996; Hubel and Wiesel, 1970). The mechanisms underlying ODP in juveniles imply two phases of ODP, an initial weakening of the inputs coming from the deprived eye followed by strengthening of inputs from the eye that remains open (Frenkel and Bear, 2004; Sato and Stryker, 2008; Sawtell et al., 2003). The classical critical period for ODP is considered to span a period of about 2 weeks from ~P21 to P35 in rodents (Gordon et al., 1996). However, the ability of V1 neurons to change ocular dominance persists into adulthood (Frenkel and Bear, 2004; Ranson et al., 2012; Sato and Stryker, 2008; Sawtell et al., 2003). In general, ODP observed in adult rodent V1 requires a longer duration of monocular deprivation, and depends more exclusively on potentiation of the open eye inputs (Frenkel and Bear, 2004; Sawtell et al., 2003).

As mentioned above, juvenile ODP in mice undergoes changes in strength in two distinct phases, and shifts in ocular dominance occur after just 3 days of MD (Frenkel and Bear, 2004; Gordon et al., 1996). In contrast, the adult cortex lacks

the initial depression of closed-eye inputs, but is able to potentiate those from the open eye in a delayed fashion (5 days) (Frenkel and Bear, 2004; Sato and Stryker, 2008; Sawtell et al., 2003). Although the synaptic changes associated with the two phases of juvenile ODP seem to mimic LTD and LTP, respectively, there is evidence suggesting that both Hebbian and homeostatic synaptic plasticity coordinate these changes. The initial weakening of closed eye inputs present in the juveniles seems to result from NMDAR-dependent LTD due to the degraded quality of the visual input after lid suture (LS) (Rittenhouse et al., 1999). However, the mechanisms underlying the delayed strengthening of the open-eye inputs are more controversial. It was initially proposed that the delayed strengthening was a result of “sliding” the induction threshold for LTP after a prolonged loss of deprived-eye inputs (Frenkel and Bear, 2004). However, this proposal was challenged by studies showing a global strengthening of both closed-eye and open-eye inputs which is reminiscent of the synaptic scaling mechanism (Mrsic-Flogel et al., 2007). This idea is further supported by studies in TNF-alpha knock-out mice which lack both homeostatic upscaling as well as the delayed potentiation after MD (Kaneko et al., 2008; Stellwagen and Malenka, 2006). However, TNF-alpha knock-out mice lack the delayed potentiation of open eye inputs only during the critical period, and have been shown to display normal strengthening as adults (Ranson et al., 2012). These results support the idea that the mechanisms governing ODP following MD change with age, as is data supportive of LTP-like mechanisms driving the delayed potentiation in adults (Ranson et al., 2012).

There is a developmental decrease in plasticity that correlates with closure of the critical period for ODP (Gordon et al., 1996). Several mechanisms are thought to underlie this process. One of them involves the maturation of inhibitory networks within V1 (Hensch, 2005; Hensch et al., 1998; Morales et al., 2002; Sale et al., 2010). In fact, changes in cortical inhibition are involved in both opening and closing the critical period, suggesting that inhibition directly gates this process. Evidence for this argument comes from experiments showing that manipulation of GABA-mediated transmission by genetic deletion of *Gad65*, a GABA-synthase, was effective at delaying the critical period (Hensch et al., 1998). Moreover, dark rearing rodents prevents maturation of inhibitory synapses and also delays the onset of ODP critical period (Morales et al., 2002). Conversely, the critical period can be accelerated by enhancing inhibitory transmission prematurely by application of BDNF or benzodiazepines at eye opening (Fagiolini et al., 2004; Hensch et al., 1998; Huang et al., 1999). It is interesting to note that a single class of interneurons has been implicated most strongly in controlling the critical period for ODP. The onset of the critical period correlates with the emergence of PV+ cells, and interruption of GABA release from this subset of neurons slows the rate of ODP (Hensch, 2005). However, since recent studies have described the potential for other types of inhibitory cells to control the function of PV+ neurons, it is likely that other components of the inhibitory circuit could also be implicated in controlling the critical period.

Some evidence suggests that altering the balance between excitation and inhibition can reinstate several types of synaptic plasticity in the adult cortex,

including ODP. For example, dark exposure and environmental enrichment can result in a decrease of GABAergic transmission and both manipulation can restore ODP and recruit LTP in the adult V1 (Sale et al., 2007; He et al., 2006, 2007). In addition, chronic treatment with the antidepressant fluoxetine restores ocular dominance plasticity in adult rats and allows full recovery of the amblyopic eye in adulthood by decreasing the level of cortical inhibition (Vetencourt et al., 2008).These findings are expected since, as discussed above, the maturation of inhibitory inputs throughout development represents one of the breaks on cortical plasticity. Ultimately, reversing the E/I balance, through decreases in inhibition or increases in excitation, could be permissive for new windows of synaptic plasticity.

Another mechanism involved in the closure of the ODP critical period involves the maturation of the extracellular (ECM) matrix. The organization of chondroitin sulphate proteoglycans (CSPGs) into mature perineuronal nets coincides with the closure of the critical period for ODP (Pizzorusso et al., 2002). A rigid ECM decreases dendritic dynamics and impedes the formation of new synapses, thereby reducing synaptic plasticity (Levy et al., 2014; Senkov et al., 2014). Indeed, disruption of perineuronal nets can restore critical period-like plasticity in adult V1 (Murase et al., 2017; Pizzorusso et al., 2002). In addition, proteolysis by tissue-type plasminogen activator (tPA) is upregulated in V1 after MD during the critical period, but not in adulthood, and evidence shows that ODP is impaired when tPA is blocked (Mataga et al., 2002). More recent studies show that if MD is preceded by a period of DE in adults, juvenile-like ODP can be reintroduced in rodent V1, and this plasticity involves the degradation of ECM by

matrix-metalloproteases (Murase et al., 2017). Together, these results support a role for the maturation of the ECM in closing the critical period for ODP. Understanding the mechanisms that underlie ODP as well as those that lead to the closure of its critical period offers the potential to design paradigms that can reopen windows of plasticity throughput life. This is particularly important in the study of adult brain plasticity and its limits, as well as relevant for conditions such as amblyopia.

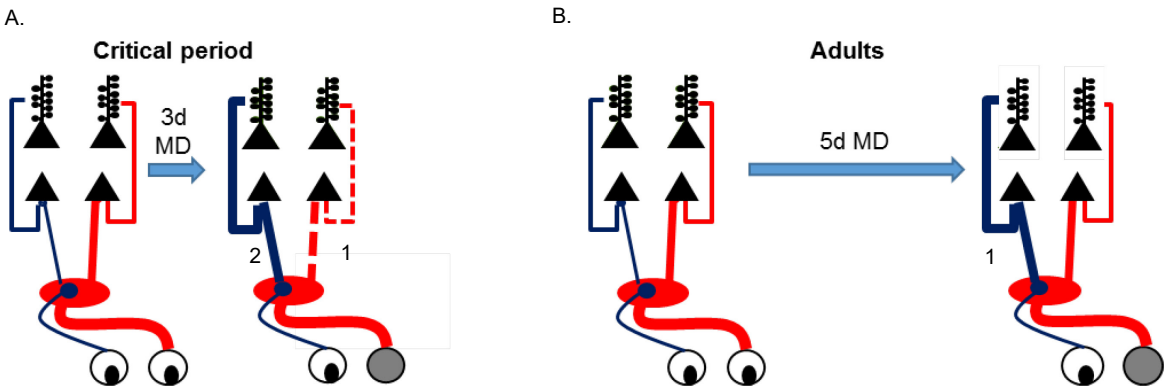

Figure 1.4: **Schematic of the mechanisms driving ODP during the critical period (A) or adults (B).** Dashed line represents LTD; solid bold line represents input strengthening. Red represents inputs from the contralateral eye while blue represents those from the ipsilateral. Numbers designate order of events after MD.

iii. Cross-modal plasticity

Sensory loss not only impacts synaptic plasticity of the deprived cortical area, but also results in compensatory synaptic changes of other sensory cortices. Spared sensory modalities are known to enhance their acuity and functionality (Goldreich and Kanics, 2003; Lessard et al., 1998). The ability of the brain to undergo these compensatory changes is termed “cross-modal plasticity”. Efforts to understand this phenomenon have mainly focused on system-level changes.

However, more recent studies have directed their attention to elucidating its synaptic and circuit mechanisms.

Behavioral and functional magnetic resonance imaging (fMRI) studies in humans reveal enhanced sensory processing in individuals born blind or deaf. For example, blind people have been shown to have more acute pitch recognition, peripheral sound localization and fine tactile discrimination than controls (Gougoux et al., 2004; Lessard et al., 1998; Voss, 2013). Deaf individuals on the other hand, show enhanced tactile sensitivity, as well as better performance on peripheral visual tasks (Bavelier et al.; Dye et al., 2009; Scott et al., 2014). The enhancement of the remaining senses could be due to recruitment of the deprived cortical areas for processing the spared sensory modalities, by stronger activation of the spared cortical areas or a combination of both. Strong evidence exists supporting the idea of deprived areas being recruited to process other types of sensory information. For example, the visual cortex of blind individuals is known to be activated by Braille reading (Merabet et al., 2008) or while performing auditory tasks (Gougoux et al., 2004; Voss, 2013). Moreover, the activation of the visual cortex is required to perform above average in these tasks, suggesting a functional adaptation of the system (Merabet et al., 2008). Other studies also support the hypothesis of enhanced processing in the spared cortical areas. For example, functional reorganization and even expansion of somatosensory and auditory cortices has been described in blind individuals (Elbert and Rockstroh, 2004; Pascual-Leone and Torres, 1993). Additionally, cats blinded early in life show enlarged facial vibrissae and whisker representation (Rauschecker et al., 1992). Observation of

such adaptation across humans and cats suggest that this is likely a fundamental property of the cortex shared across diverse species.

It is important to note that cross-modal recruitment and reorganization occurs in individuals who are born without a sense as well as those who lose a sense as adults. Merabet et al. showed the capacity for the adult cortex to undergo cross-modal plasticity by blindfolding normally-sighted individuals (Merabet et al., 2008). In these experiments, blindfolded people performed better at Braille reading than sighted counterparts after both received Braille comprehension training. This provides insight into how cross-modal re-arrangement in the adult brain might be recruited by attending to or retraining a spared sense.

The synaptic and molecular mechanisms underlying these changes in cortical responses have just recently begun to be uncovered. Cross-modal changes in excitatory synaptic strength were first reported in L2/3 of auditory and somatosensory cortices of DE mice (Goel et al., 2006). Synapses in V1 L2/3 undergo homeostatic increase in synaptic strength after DE, however those in S1 or A1 weaken as measured by mEPSCs (Goel et al., 2006; He et al., 2012; Petrus et al., 2015). Several aspects distinguish the cross-modally induced changes from those that result from unimodal homeostatic adaptation besides the directionality of synaptic strength change. For one, brief DE (2 days) is sufficient to induce homeostatic synaptic plasticity in V1 while a longer period of DE (7 days) is required for cross-modal changes (He et al., 2012). In addition, total deprivation of visual input is required to induce homeostatic changes unimodally, while even mild deprivation paradigms (e.g. lid suture) result in cross-modal weakening of

mEPSCs (He et al., 2012). Based on the latter result, it was suggested that cross-modal plasticity of the spared cortical areas is likely triggered by loss of behaviorally relevant vision, while that in deprived cortex requires complete loss of its own sensory inputs (Whitt et al., 2015).

Cross-modal plasticity at excitatory synapses is not restricted to L2/3 in the spared cortices. Recent studies have provided a detailed description of cross-modally induced synaptic changes throughout the cortical circuitry, including L4 and L2/3. Petrus et al showed that, after DE, spared A1 undergoes synaptic changes in both its feedforward (FF) and intracortical (IC) inputs. Specifically, DE potentiates FF excitatory synapses, including thalamocortical and inputs from L4 to L2/3, as well as IC inputs within L4 of A1 (Petrus et al., 2015). In contrast, IC inputs in A1 L2/3 weaken (Petrus et al., 2014, 2015). This suggests a rearrangement in A1 processing, perhaps to favor the FF auditory input over contextual information arising from IC inputs. Changes in the FF pathway were not unique to A1, since deafened mice also showed potentiation of the TC synapses in V1 (Petrus et al., 2014). This observation, in particular, was unexpected in the adult mice used for this study, since as discussed above the critical period for thalamocortical plasticity ends early during postnatal development. Chapter 3 of this thesis addresses the mechanisms that allow for cross-modally induced TC plasticity. In contrast to spared A1, deprived V1 underwent different changes in which only IC inputs in L2/3 were strengthened, while the FF pathway (i.e. dLGN→L4 and L4→L2/3) was unaltered (Petrus et al., 2014, 2015). This suggests

a preference for processing intracortical information when the primary sensory input is missing.

In addition to the described changes in excitatory inputs, cross-modal plasticity can also impact cortical inhibitory synapses. Petrus and colleagues observed increased evoked inhibitory transmission specifically onto L4 neurons in the spared cortex after deafening (Petrus et al., 2015). Results from other studies also hint at how cross-modal plasticity can impact inhibitory networks. For example, injury to the olfactory epithelium results in an increase of GABAergic neurons in S1 of rodents (Ni et al., 2010). Additionally, sound-evoked responses are found in V1 of normally developed mice, and loud sound can modify V1 neuronal responses by cross-modal activation of inhibitory and disinhibitory circuits (Ibrahim et al., 2016; Iurilli et al., 2012). This suggests that cross-modal adaptation of inhibitory circuits after sensory loss is likely acting on pre-existing functional circuits. The source of these interaereal interactions is unclear. However, there are some clues as to which circuits could potentially mediate them. In particular, direct projections from A1 to V1 were described to activate VIP+ neurons in L1 (Ibrahim et al., 2016). Another locus of potential interactions between cortical areas could include TC and corticothalamic loops. It is possible that different aspects of cross-modal plasticity involve different circuits to ultimately reach brain-wide adaptation to sensory loss.

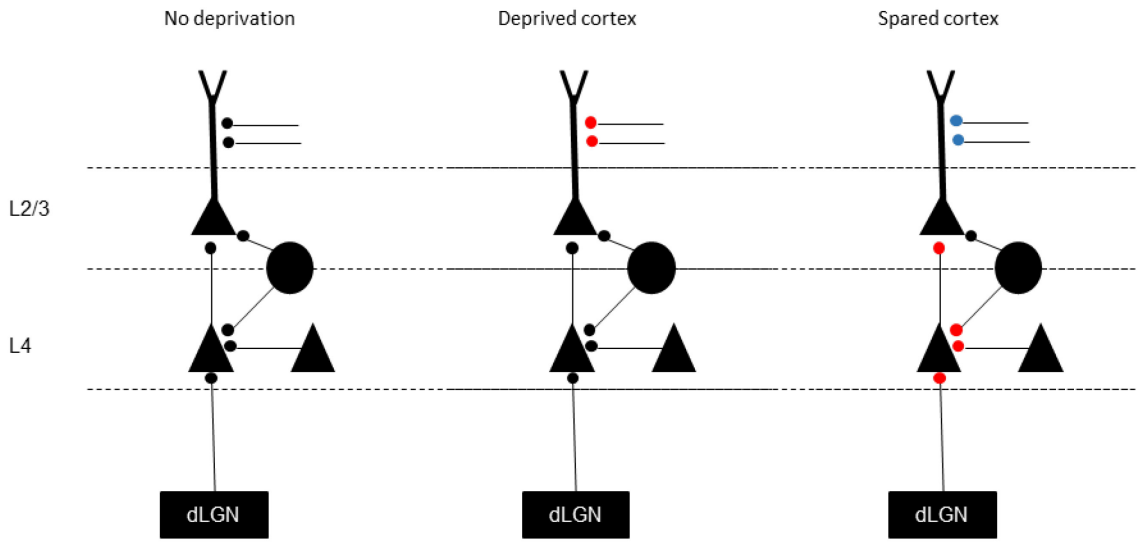

Figure 1.5: **Summary of cross-modal synaptic changes resulting from sensory deprivation in the deprived and spared cortices (Petrus et. al, 2015).** Triangles represent excitatory neurons while circles represent PV+ neurons**.** Small black circles represent synapses that remain the same, red circles represent inputs that strengthen while those in blue weaken.

Chapter 2: Disruption of NMDAR function abolishes experience-dependent homeostatic synaptic plasticity in mouse primary visual cortex

This manuscript is in preparation.

Potential authors: **Gabriela Rodríguez**, Ming Gao, Samuel Parkins and Hey-Kyoung Lee

My contribution: All mEPSC recordings for NR1KO, neighbor, d-CPP and saline groups. Some mEPSC recordings for GFP-only neurons, some c-Fos quantification and some NMDA/AMPA recordings. Experimental design for d-CPP and saline mEPSC recordings as well as c-Fos immunostaining. Analysis of

mEPSCs and NMDA/AMPA responses recorded by me. Statistical analysis of all data.

Section 1: Introduction

Neuronal circuits constantly undergo changes, through development, experience, and learning that allow for adaptation to different environments or internal states. Strengthening or weakening synaptic connections to store information about these changes is largely dependent on Hebbian or "correlation-based" plasticity. However, Hebbian forms of plasticity are known to result in a positive feedback loop that can destabilize neural circuits (Miller and MacKay, 1994). Therefore, additional mechanisms of synaptic plasticity have been proposed to be at play to maintain homeostasis of neural circuits. Several models of homeostatic plasticity can achieve this function, including synaptic scaling (Turrigiano, 2008) and the sliding threshold model (Cooper and Bear, 2012).

According to synaptic scaling, prolonged reduction in neuronal activity leads to an increase in the strength (upscaling) of excitatory synapses, while a period of enhanced activity results in a decrease (downscaling) (Turrigiano et al., 1998). Synaptic scaling was initially proposed to occur globally across the majority of synapses in a multiplicative manner, to preserve relative differences in synaptic weight (Turrigiano et al., 1998). Synaptic scaling was first observed in cultured neurons, in which abolishing or increasing activity by pharmacological means resulted in compensatory changes in synaptic strength as measured by the amplitude of miniature excitatory postsynaptic currents (mEPSC) (O'Brien et al., 1998; Turrigiano et al., 1998). Similar changes in mEPSCs can be induced in

pyramidal neurons of rodent primary visual cortex (V1) *in vivo* by dark exposure (DE) (Goel and Lee 2007; He et al., 2012), intraocular TTX injection (Desai et al., 2002a), enucleation (He et al., 2012) and retinal lesions (Keck et al., 2013). Mechanistically, the synaptic scaling observed across multiple preparations is mediated by the insertion or removal of AMPARs and studies using cortical cultured neurons show that it occurs largely independent of NMDAR activation (Turrigiano et al., 1998).

According to the sliding threshold model, prolonged periods of altered activity result in the modification of the threshold for long-term potentiation (LTP) and long-term depression (LTD) induction. The synaptic modification threshold can shift bidirectionally, depending on the history of neuronal activity: an extended period of low levels of activity results in sliding the threshold to favor LTP, while high activity shifts it to favor LTD (Abraham and Bear, 1996; Cooper and Bear, 2012). This has been shown to happen *in vivo,* in rodent V1, in which DR or DE leads to a lower threshold for LTP induction (Guo et al., 2012; Kirkwood et al., 1996; Philpot et al., 2003). Changes in synaptic modification threshold with previous activity have been shown to be mediated by changes in either the induction mechanisms of LTP/LTD, such as alterations in NMDAR function (Philpot et al., 2003; Quinlan et al., 1999) and inhibition (Steele and Mauk, 1999), or the expression mechanisms of LTP/LTD, such as changes in AMPAR phosphorylation (Huang et al., 2012).

Although seemingly different, both of the proposed models for homeostatic synaptic plasticity promote compensatory changes after continued deviation from

a baseline state of activity to maintain firing rates in a physiologically relevant, yet stable dynamic range. Previous investigations have shown that both changes in mEPSC amplitude and changes in the modification threshold happen *in vivo*. They have, however, failed to address how these two processes interact, if at all, and to which extent. Based on the reported differences in the requirement of NMDAR activation for synaptic scaling and sliding threshold models, we examined the role of NMDARs on visual experience-dependent changes in mEPSCs of L2/3 neurons of mouse V1, which have been interpreted as *in vivo* synaptic scaling (Desai et al., 2002; Goel and Lee, 2007; He et al., 2012). We reasoned that if the observed scaling of mEPSCs with visual experience is a consequence of LTP/LTD due to the sliding threshold, then these changes would be dependent on NMDAR activation. Using cell-type specific knockout mice or an antagonist of NMDARs, we found evidence supporting that experience-dependent homeostatic synaptic plasticity is dependent on functional NMDARs *in vivo*.

Section 2: Materials and Methods

Visual experience manipulation

All animal handling and manipulations were approved by the Institutional Animal Care and Use Committee (IACUC) at Johns Hopkins University and followed the guidelines established by the National Institutes of Health (NIH). Male and female $NR1^{flox}$ mice (B6.129S4-*Grin1tm2Stl*/, The Jackson Laboratory 005246) were raised under a 12 hours light/dark cycle until postnatal day 25-35 (P25-P35). At this point a group of mice was placed in 24-hour dark conditions for 2 days (2 days dark exposure, 2dDE). Animals in the dark were cared for by using infrared vision

goggles. A group of 2dDE mice were taken out of the dark and re-exposed to light for 2 hours (2 hours light-exposed, 2hL). Age matched control animals were continuously raised in the normal 12 hours light/dark cycle (Ctl).

Targeted viral transfection

Male and female $NR1^{flox}$ mice between P23-P27 were bilaterally injected with an adeno-associated viral vector expressing Cre-GFP under the control of CaMKII promoter (AAV9.CaMKII.HI.eGFP-Cre.WPRE.SV40; Penn Vector Core, University of Pennsylvania) in V1. Layer 2/3 of V1 was targeted by using the following stereotaxic coordinates: bregma -3.6mm, lateral 1.5mm, and depth -0.3mm. Mice recovered on a heated pad until movement, eating and drinking behaviors were evident. Animals were returned to the mouse colony after recovery and remained under 12 hours light/dark conditions until experimental use. Viral expression and knockout of NR1 gene was confirmed experimentally 6-7 days after transfection as determined by significantly reduced NMDAR currents (Fig. 1). Manipulation of visual experience therefore commenced 1 week (6-7d) after viral injections. Control mice underwent the same procedure, but instead were injected with a GFP-expressing adeno-associated virus (AAV9.CaMKII0.4.eGFP.WPRE.rBG).

Pharmacology

Alzet mini-osmotic pumps attached to a cannula containing saline or 1μM D-4-[(2*E*)-3-Phosphono-2-propenyl]-2-piperazinecarboxylic acid (d-CPP, Tocris) were

incubated in saline solution at 37˚C at least 5 hours before implantation. Male and female NR1^{flox} mice between P25-P30 were anesthetized with isofluorane gas and head-fixed in a stereotaxic apparatus with constant administration of isoflurane/oxygen mix (1.5-2% isoflurane). The dorsal surface of the head was aseptically cleaned, hair removed and skull exposed. A small hole was drilled in the skull at stereotaxic coordinates -0.22 mm posterior, 1 mm lateral (from bregma) to target the cerebral ventricle, using a dental drill and 0.5 mm drill-bit. The neck was aseptically cleaned, a small cut was made at the base and blunt forceps were used to separate the fascia. An osmotic minipump attached to a cannula was inserted subcutaneously. The cannula was guided to the stereotaxic coordinates previously used, lowered until the cap touched the skull and secured in place with dental cement (TEETS dental material methyl methacrylate). Animals were allowed to recover from the effects of anesthesia until movement and drinking were evident and returned to the animal care facility. While in the care facility, drinking water was supplemented with 0.07 mg/mL carprofen (Sigma) (Ingrao et al., 2013) . Mice were allowed to recover for 12 hours before undergoing manipulations in visual experience. Those animals that were re-exposed to light (2hL) only received an intraperitoneal (ip) injection of 200 µL saline or d-CPP (10mg/kg) 10 min before light exposure.

Primary visual cortex slice preparation

Mice between P25-P35 were deeply anesthetized with isoflurane gas in a chamber placed in a chemical fume hood. Anesthesia was delivered to dark exposed

animals in a light-tight chamber. After confirming the absence of pinch or righting reflex, mice were decapitated and the brain was immediately placed in ice-cold dissection buffer containing the following (in mM): 212.7 sucrose, 10 dextrose, 3 $MgCl_2$, 1 $CaCl_2$, 2.6 KCl, 1.23 $NaH_2PO_4 \bullet H_2O$, and 26 $NaHCO_3$, which was bubbled with 95% O_2/5% CO_2 gas. Blocks containing V1 were rapidly isolated and sectioned coronally into 300 µm thick slices, while submerged in ice-cold dissection buffer, using a vibratome (Pelco easiSlicer, Ted Pella). Slices were transferred to a submersion holding chamber filled with artificial cerebrospinal fluid containing (in mM): 124 NaCl, 5 KCl, 1.25 $NaH_2PO_4 \bullet H_2O$, 26 $NaHCO_3$, 10 dextrose, 2.5 $CaCl_2$, and 1.5 $MgCl_2$, bubbled with 95% O_2/5% CO_2. The slices recovered for 1 hour at room temperature before electrophysiological recordings started.

Electrophysiological recordings

Slices were transferred to a submersion-type recording chamber and perfused with oxygenated ACSF (bubbled 95% O_2/5% CO_2 at 32 ± 2°C) at a rate of 2mL/min. The chamber was mounted on a fixed stage under an upright microscope (E600 FN; Nikon, Tokyo, Japan) with oblique infrared illumination. Pyramidal neurons in L2/3 of V1 were visually identified and patched using a glass pipette with a tip resistance between 3 and 5 MΩ, which was filled with internal solution containing (in mM): 120 CsOH, 120 Gluconic acid, 10 phosphocreatine, 0.5 GTP, 4 ATP, 8 KCl, 1 EGTA,10 HEPES and 5 QX-314. An Axon patch-clamp amplifier 700B (Molecular Devices) was used for voltage-clamp recordings and data was acquired

through Igor Pro software (WaveMetrics). Only data from cells with input resistance (Ri) > 150 MΩ and series resistance (Rs) < 25 MΩ were analyzed.

NMDAR/AMPAR ratio Glutamatergic currents were recorded in response to electric stimulation delivered through a bipolar glass electrode placed in V1 L4 or L2/3. Recordings were done in the presence of 20 μM bicuculline in the ACSF. The stimulation intensity was adjusted so that a single-peak response was produced with an onset latency of 2-3ms. The AMPA receptor component was taken as the average peak amplitude of responses recorded at Vh=-80 mV. The NMDA receptor component was taken as the average amplitude of responses recorded at Vh=+40 mV 70 ms after onset. Responses were recorded every 10 s and a minimum of 10 responses were averaged for each component.

miniature EPSCs AMPA receptor-mediated miniature excitatory postsynaptic currents (mEPSCs) were isolated by recording with 1 μM tetrodotoxin (TTX), 20 μM bicuculline, and 100 μM DL-2-amino-5 phosphonopentanoic acid (DL-APV) in the ACSF. Events were recorded at Vh=-80 mV for a minimum of 4 minutes initiated 1-2 minutes after cell break-in. The recorded data was digitized at 2 kHz by a data acquisition board (National Instruments), acquired with Igor Pro software and analyzed using the MiniAnalysis program (Synaptosoft). The detection threshold for mEPSCs was set to 3 times the root mean square (RMS) noise and events with a rise time > 3 ms were excluded from analysis. Events within bursts (more than 2 events, inter-event-interval < 10 ms) were excluded from the measurement of

amplitudes. The average of total isolated events (200-220) was used to calculate the decay time constant for each neuron. Cells were discarded if Ri or Rs changed more than 15% during the duration of the recording.

Biocytin processing

Slices used for electrophysiological recordings were immediately fixed in 10% formalin solution overnight at 4°C. Slices were rinsed 0.01M phosphate buffered saline (PBS) at room temperature and permeabilized in 2% Triton X-100 in PBS for 1 h. Slices were then incubated in 1:2000 solution of avidin-Texas Red conjugate in 1% Triton X (in PBS) overnight. After incubation, slices were washed in PBS, mounted on glass slides, and coverslipped with Prolong Gold Anti-fade (Invitrogen) mounting medium. Images were taken using a Zeiss LSM 510 META confocal microscope.

Immunohistochemistry

$NR1^{flox}$ mice were deeply anesthetized with isoflurane vapors in a closed chamber placed in a fume hood. DE animals were anesthetized in a light-tight chamber. Animals were perfused transcardially with PBS followed by 10% formalin solution. The brains were then extracted and kept in 10% formalin overnight. V1 was isolated and sectioned coronally in 40 µm thick slices. Free floating slices containing V1 were incubated with 1% sodium borohydride for 15 minutes at room temperature and then washed with PBS. The same slices were blocked for 2 hours in a solution containing 3% goat serum and 0.3% Triton-X in PBS. Cortical slices

were then incubated with antibodies against c-Fos and Neuronal nuclei protein (NeuN) in the blocking buffer overnight. Slices were rinsed and then incubated for 2 hours with fluorescently labeled secondary antibodies. Slices were then washed with PBS, incubated with DAPI and mounted on glass slides with Prolong Gold Anti-fade (Invitrogen) medium. The antibody concentrations were as follows: 1:20,000 rabbit anti-cFos (Calbiochem pAb), 1:200 mouse anti-NeuN (Millipore MAB377; RRID: AB_2298772), 1:200 Alexafluor 633 anti-rabbit (Fisher), 555 anti-mouse (Fisher). Slices were imaged using a Zeiss LSM 700 confocal microscope with a step size of 0.5 µm. All images were analyzed using Volocity software.

Statistical Analysis

Data are presented as mean ± SEM. All statistical analyses were done using Prism 5.0 (GraphPad) software. One-factor analysis of variance (ANOVA) was used to compare multiple groups followed by a Newman–Keuls multiple comparison *post hoc* test. Unpaired Student's t-tests were used for two group comparisons. The Kolmogrov-Smirnov (K-S) test was used to compare cumulative probabilities. A p-value < 0.05 was used as a measure of significance in t-tests, ANOVAs and Newman-Keuls analysis. For K-S tests, p-values < 0.01 were used as a measure of significance.

Section 3: Results

Subsection 1: Cell-specific NMDAR KO confirmation

We used cell type-specific knock-out of NMDA receptors in L2/3 pyramidal neurons of V1 and assessed the ability of these neurons to undergo experience-

dependent homeostatic synaptic plasticity. This was achieved by targeted injection of an adeno-associated viral construct expressing Cre-GFP under the control of the CaMKII promoter (AAV9.CamKII.Cre-eGFP) into V1 L2/3 of $NR1^{flox}$ transgenic mice (Cre-GFP condition) (Tsien et al., 1996). In this scheme, the expression of Cre recombinase leads to excision of the *Grin1* gene, which encodes the obligatory NMDAR NR1 subunit. To control for effects only due to viral transfection, a second group of $NR1^{flox}$ transgenics were injected with a GFP-expressing viral construct (AAV9.CaMKII.GFP) (GFP-only condition). We verified that viral transfection efficiency was similar for both constructs by quantifying the percentage of GFP-positive cells relative to the total number of neurons in a given tissue section (Fig. 2.1 A). Since the expression of GFP does not directly correlate with elimination of NMDAR currents, we used whole-cell voltage clamp to measure NMDAR/AMPAR ratios after viral injections. We corroborated the specificity of the functional NMDAR knockout by also measuring NMDAR/AMPAR ratios from non-GFP expressing neurons that were neighbors to the knockout cells (neighbors) (Fig. 2.1 B and C). We found a significant decrease in NMDAR currents for NMDAR-knockout cells (NR1 KO; Cre-GFP) 7 days after viral injection (Fig. 2.1 B). These results confirm both the specificity and the effectiveness of the virally mediated NR1-knockout used in this study.

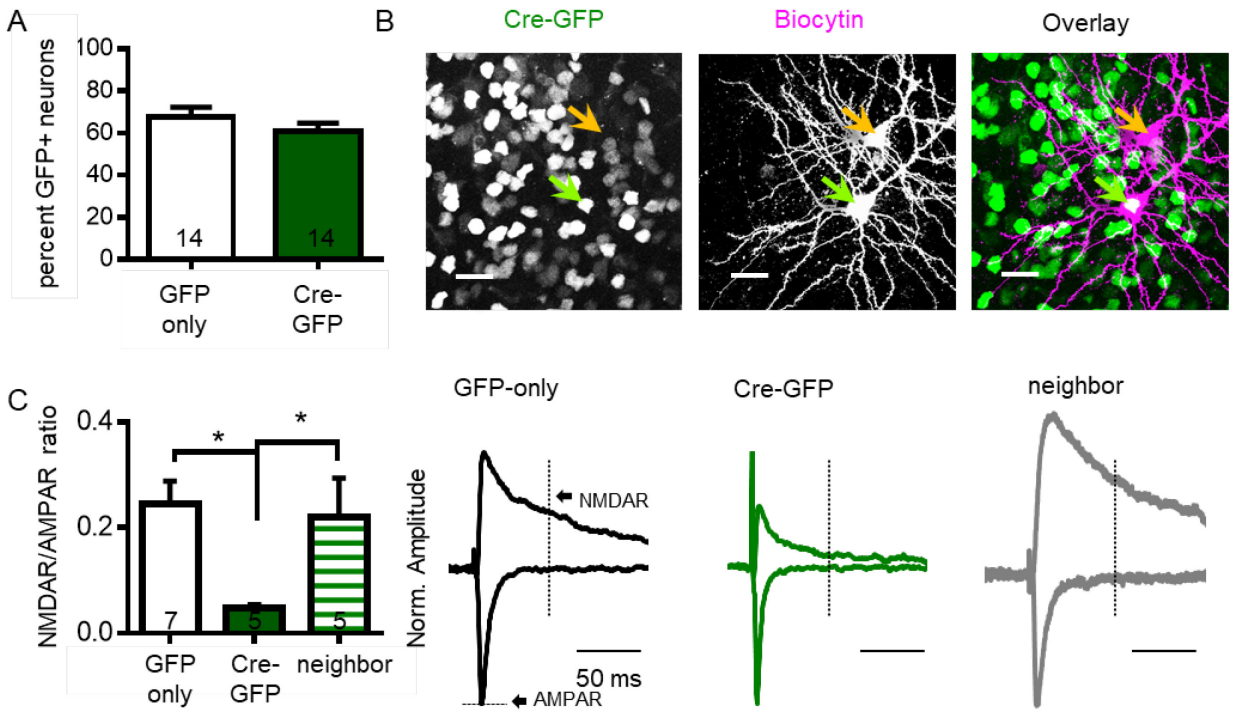

Figure 2.1: Cell specific NMDAR knockout (A) GFP and Cre-GFP expressing viruses result in similar transfection rates of V1 neurons (mean transfection rate: GFP-only 67.7 ± 4.6% ;Cre-GFP 60.8 ± 3.9%; unpaired t-test: p=0.2668; number of slices quantified reported, 6 mice per condition). **(B)** Confocal image of biocytin filled NR1 KO (green arrow, expressing Cre-GFP in the nucleus) and neighbor (orange arrow) neurons in V1 L2/3 (scale bar: 20μm). **(C)** Left: Comparison of average NMDAR/AMPAR ratio for each condition (mean NMDAR/AMPAR ratio for GFP-only 0.25 ± 0.04, NR1 KO 0.05 ± 0.007, neighbor 0.22 ± 0.07; one-way ANOVA p=0.0186; Newman-Keuls *post hoc* *p<0.01; number of cells reported). Right: Example traces of NMDAR and AMPAR mediated currents in GFP-only (black), NR1 KO (green) and neighbor (gray) neurons (Norm Amplitude: trace amplitudes normalized to control AMPAR current).

Sub-section 2: NMDAR KO abolishes experience-dependent homeostatic changes in synaptic strength

In order to test whether NMDARs play a role in homeostatic synaptic plasticity, we measured changes in the strength of excitatory synapses on V1 L2/3 pyramidal neurons following manipulations to visual experience in the presence or absence of NMDAR function. Homeostatic synaptic plasticity has been

characterized, both *in vitro* and *in vivo* (Desai et al., 2002; Goel and Lee, 2007; O'Brien et al., 1998; Turrigiano et al., 1998), as an increase in synaptic strength after prolonged periods of decreased neuronal activity and a decrease in synaptic strength after periods of increased activity. Previous studies have established that 2 days of visual deprivation result in increased excitatory synaptic transmission, as measured by mEPSCs, and that this increase can be reversed by reinstating visual experience for a short period (Gao et al., 2010; Goel and Lee, 2007).

In GFP-only condition cells, the average mEPSC amplitude was significantly increased after 2dDE and returned to normal-reared control (Ctl) values after 2hL (Fig. 2.2 A). Alterations in visual experience had no significant effect on the frequency of mEPSCs of GFP-only condition neurons (Fig. 2.2 A). These results are consistent with previous studies showing that homeostatic synaptic plasticity in V1 L2/3 mainly manifests as a postsynaptic change in mEPSC measurements (Goel et al., 2011; 2006).

On the other hand, mEPSCs recorded from NMDAR KO neurons (NR1 KO; Cre-GFP) lacked regulation by visual experience. Changes in visual experience had no significant effect on either amplitude or frequency measurements (Fig. 2.2 B). We noted a significant increase in baseline frequency of mEPSC in normal-reared NR1 KO neurons when compared to normal-reared GFP-only neurons (GFP-only: 2.5 ± 0.15 Hz, n=9; NR1 KO: 4.9 ± 0.57 Hz, n=14; unpaired Student's t-test *p=0.0038). This is in accordance with a previous study (Adesnik et al., 2008), which implicated NMDARs in regulating the number of functional synapses. However, because there was no significant change in frequency resulting from

changes in visual experience, the basal difference in frequency does not seem to represent a homeostatic adaptation to altered activity levels. These results indicate that knocking out NMDARs results in a deficit of experience-dependent homeostatic synaptic plasticity and therefore suggests that NMDARs are required for this process. Unexpectedly, data from neighbor neurons, which did not express Cre-GFP and have intact NMDAR current (Fig. 2.1B, C), also failed to modulate the average mEPSC amplitude with changes in visual experience (Fig. 2.2 C). However, unlike the NMDAR KO neurons or GFP-only condition, these neighbor neurons showed significant increase in mEPSC frequency after 2dDE that was maintained after light re-exposure (2hL) (Fig. 2.2 C).

To determine whether changes in visual experience impact the overall distribution of mEPSC amplitudes, we analyzed cumulative probability distributions for the different conditions. Comparison of cumulative probability distributions for the GFP-only condition showed significant differences in the amplitude distributions of events from Ctl and 2dDE animals as well as significant differences between events recorded from 2dDE and 2hL groups (Fig. 2.3 A). However, a comparison between data from Ctl and 2hL groups shows no significant difference, supporting the notion that light re-exposure reverses the distribution of synaptic strengths to normal levels. In contrast, mEPSCs recorded from NMDAR KO neurons did not show such change in the amplitude distribution; at most there was a small but significant shift in the cumulative probability curve towards smaller values in the 2dDE group compared to normal controls (Fig. 2.3 B). Similarly, cumulative probability distribution of mEPSCs from NMDAR KO neighbor neurons

showed no significant difference between NR and 2dDE events. Even though there was no statistically significant change in the average mEPSC amplitude in the neighbor neurons with 2hL (Fig. 2.2 C), comparison of the cumulative probabilities of individual mEPSC amplitudes showed a significant increase for the 2hL condition (Fig. 2.3 C). Taken together with the increase in mEPSC frequency in the 2hL condition (Fig. 2.2 C), this result suggests that the neurons with intact NMDARs (Fig. 2.1 C) undergo aberrant plasticity in the absence of homeostatic plasticity in the neighboring NMDAR KO neurons, which constitutes the majority (Fig. 2.1 A).

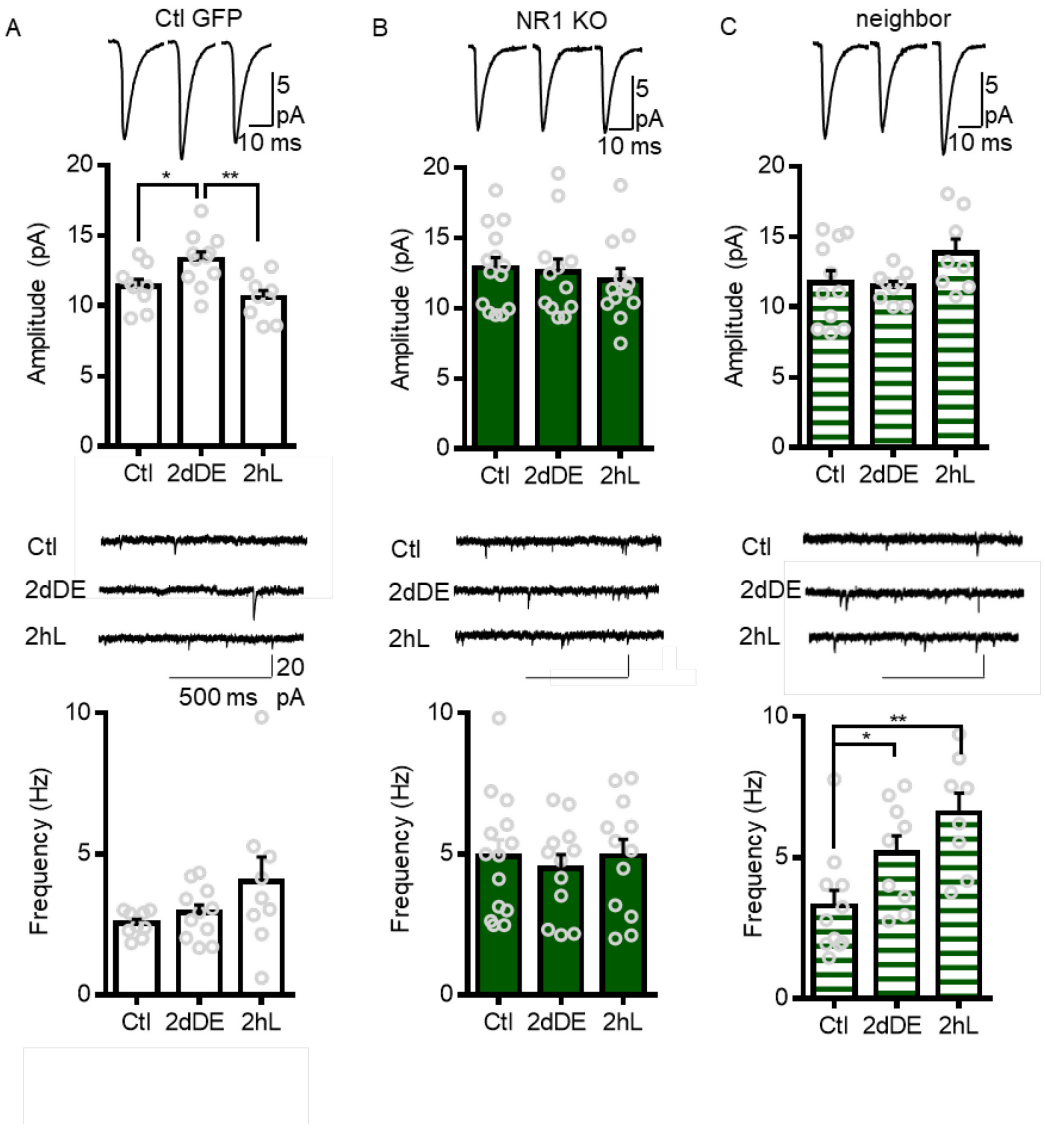

Figure 2.2: Regulation of excitatory synaptic transmission induced by alterations in visual experience Top: average amplitude traces for each condition and comparison of average amplitude values (data points represent cells). Bottom: sample traces for each condition and comparison of average frequency values (data points represent cells). **(A)** Neurons expressing GFP-only virus undergo significant increase in average mEPSCs amplitude after 2dDE which is reversed by 2hL (mean amplitude: Ctl = 11.38 ± 0.51 pA, 2dDE = 13.29 ± 0.55 pA, 2hL = 10.59 ± 0.49 pA; one-way ANOVA **p=0.0032; Newman-Keuls *post-hoc* *p<0.01, **p<0.001). No significant changes in mEPSCs frequency correlated with changes in visual experience (mean frequency: Ctl = 2.43 ± 0.14 Hz, 2dDE = 2.92 ± 0.28 Hz, 2hL = 3.30 ± 0.53 Hz; one-way ANOVA p=0.3192). **(B)** NR1 KO neurons fail to undergo significant changes in mEPSC amplitude (mean amplitude: Ctl = 12.85 ± 0.76 pA, 2dDE = 12.55 ± 0.95 pA, 2hL = 11.96 ± 0.86 pA; one-way ANOVA p=0.7528) or frequency (Ctl = 4.92 ± 0.57 Hz, 2dDE = 4.49 ± 0.48 Hz, 2hL = 4.93 ± 0.58 Hz; one-way ANOVA p=0.8240). **(C)** Neighbor neurons do not undergo significant changes in mEPSCs amplitude (mean amplitude Ctl 11.71 ± 0.88 pA, 2dDE 11.47 ± 0.36 pA, 2hL 13.86 ± 0.97 pA; one-way ANOVA p=0.1054), but undergo changes in frequency after dark exposure that are maintained after light re-exposure (Ctl = 3.28 ± 0.55 Hz, 2dDE = 5.15 ± 0.62 Hz, 2hL = 6.57 ± 0.71 Hz; one-way ANOVA **p=0.0034; Newman-Keuls *post-hoc* *p<0.01, **p<0.001).

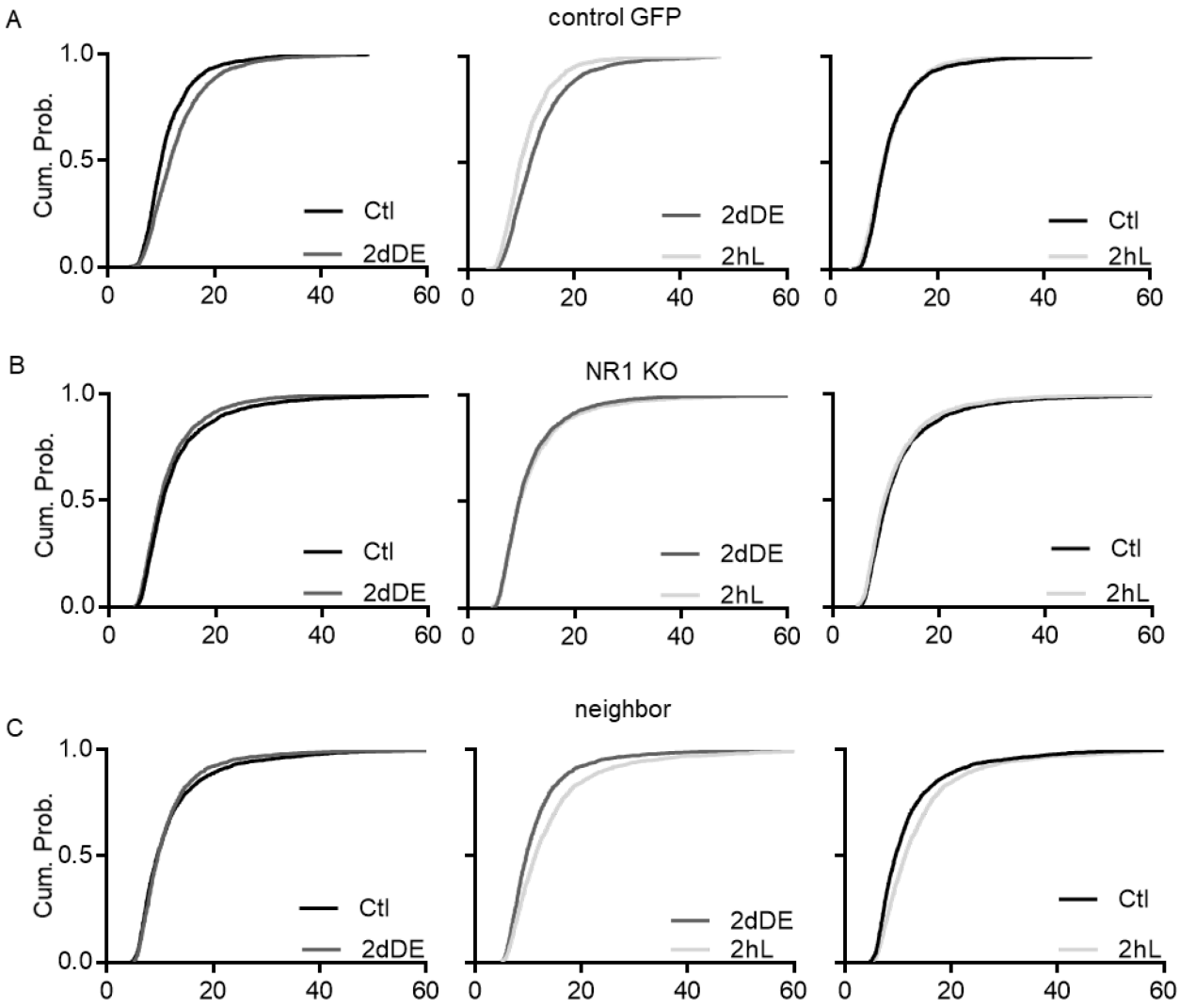

Figure 2.3: Comparison of cumulative probability distributions for mEPSC amplitudes for GFP-only and NR1 KO conditions. (A) GFP-only neurons show differences the distribution of mEPSC amplitudes between normal-reared Ctl and 2dDE distributions (K-S test ****p<0.0001) and between 2dDE and 2hL (K-S test ****p<0.0001). No significant difference between Ctl and 2hL (K-S test p=0.0138). **(B)** Data from Cre-GFP expressing NR1 KO neurons show a slight shift towards higher amplitudes in Ctl data relative to 2dDE (K-S test ***p=0.0005) and 2hL (K-S test ***p=0.0005), but no significant differences between 2dDE and 2hL (K-S test p= 0.1441). **(C)** Data from neighbor neurons show no difference between Ctl and 2dDE values (K-S test p=0.0168), but a significant shift towards larger values for 2hL when compared to 2dDE (K-S test ****p< 0.0001) or to Ctl (K-S test ****p< 0.0001).

Subsection 4: NMDAR function is required to undergo experience-dependent homeostatic synaptic plasticity

Our data so far suggest that NMDAR KO prevents experience-dependent homeostatic synaptic plasticity. One caveat of virally mediated NMDAR KO is that it fails to address whether this is due to missing the NMDAR protein itself, which is known to have a structural role in organizing downstream signaling molecules at synapses via its intracellular domain (Köhr et al., 2003; Sprengel et al., 1998), or absence of NMDAR function. To determine if it is the latter, we blocked NMDAR function pharmacologically by administration of D-4-[(2*E*)-3-Phosphono-2-propenyl]-2-piperazinecarboxylic acid (d-CPP), which is a selective and competitive antagonist of NMDAR (Lehmann et al., 1987). For the purpose of these experiments d-CPP was administered for 2 days via subcutaneous osmotic minipumps to Ctl or 2dDE animals. Mice pertaining to the 2hL group, were placed in the dark room for two days to allow normal scaling up process by 2dDE, and then received d-CPP via an intraperitoneal injection (i.p., 10 mg/kg) 10 minutes before light re-exposure.

To control for osmotic minipump surgery and i.p. injection, we recorded from mice that received saline instead of d-CPP under the same experimental conditions. Saline-treated mice showed a significant increase in the average amplitude of mEPSCs after 2dDE that was reversed after 2hL (Fig. 2.4 A). These results are consistent with our recordings in GFP-only neurons and confirm that our surgical manipulation does not interfere with the ability of the neurons to undergo experience-dependent homeostatic synaptic plasticity.

In comparison, recordings from d-CPP administered mice showed no significant modulation of mEPSC amplitude or frequency with 2dDE (Fig. 2.4 B), demonstrating that NMDAR function is required to undergo homeostatic synaptic upscaling. In addition, mEPSC amplitude measurements for the 2hL group did not show significant change from Ctl values (Fig. 2.4 B). Unlike NR1 KO experiments, we noted a significant increase in mEPSC amplitude under baseline conditions with infusion of d-CPP (saline Ctl: 10.55 ± 0.42 pA, n=9; d-CPP Ctl: 13.19 ± 0.52 pA, n= 10; unpaired Student's t-test *p=0.001). Nonetheless, we did not observe additional modulation of synaptic strength with visual experience. Taken together, these results support the previous conclusion that functional NMDARs are required to undergo proper experience-dependent synaptic scaling.

Cumulative probability distribution plots of mEPSC amplitudes from saline infused mice show significant differences between normal-reared Ctl and 2dDE groups (Fig. 2.5 A). However, no significant amplitude distribution changes are

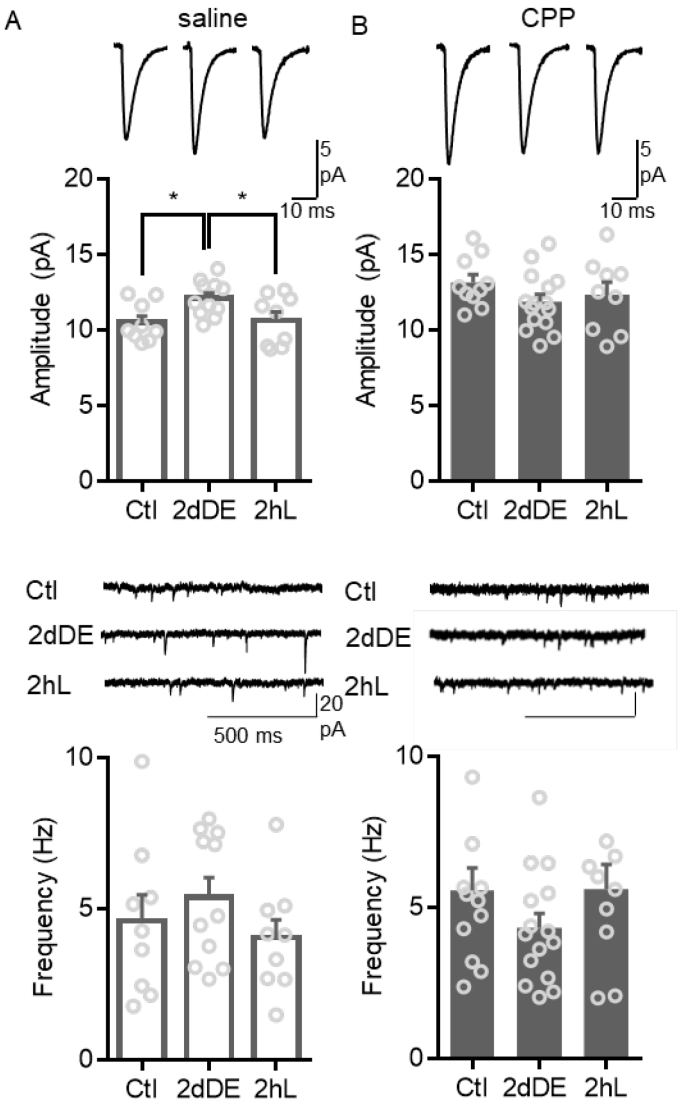

observed between Ctl and 2hL groups (Fig. 2.5 A), suggesting that the distribution of mEPSC amplitude returns to normal levels after brief re-exposure to light. While there was no significant change in the average mEPSC amplitude of d-CPP injected Ctl versus 2dDE conditions, there was a small but statistically significant shift between their cumulative probability curves (Fig. 2.5 B). Also, while the average mEPSC amplitudes for d-CPP

Figure 2.4: Lack of visual experience-dependent changes in excitatory synaptic transmission with NMDAR blockade Top: average amplitude traces for each condition and comparison of average amplitude values (data points represent cells). Bottom: sample traces for each condition and comparison of average frequency values (data points represent cells). **(A)** mEPSC data coming from animals infused with saline show a significant increase in event amplitudes after 2dDE which reverts to control values after 2hL (mean amplitude Ctl 10.55 ± 0.42 pA, 2dDE 12.14 ± 0.35 pA, 2hL 10.69 ± 0.55 pA; ANOVA *p=0.025; Newman-Keuls *p<0.01). No significant changes in frequency associated with changes in visual experience (mean frequency Ctl 4.6 ± 0.86 Hz, 2dDE 5.4 ± 0.64 Hz, 2hL 4.05 ± 0.61 Hz; ANOVA p=0.3952). **(B)** Neurons from CPP treated animals show no significant changes in amplitude (Ctl 13.19 ± 0.52 pA, 2dDE 11.92 ± 0.49 pA, 2hL 12.38 ± 0.81 pA; ANOVA p=0.3052) or frequency (Ctl 5.59 ± 0.73 Hz, 2dDE 4.35 ± 0.48 Hz, 2hL 5.62 ± 0.82 Hz; ANOVA p=0.2793) regardless of visual experience.

injected Ctl and 2hL groups did not differ (Fig. 2.4 B), we observed a small but statistically significant difference in their mEPSC amplitude distributions (Fig. 2.5 B). These results suggest that there is a small shift in mEPSC amplitude distribution when changing visual experience in the presence of d-CPP, but this occurs without affecting the average mEPSC amplitude across conditions.

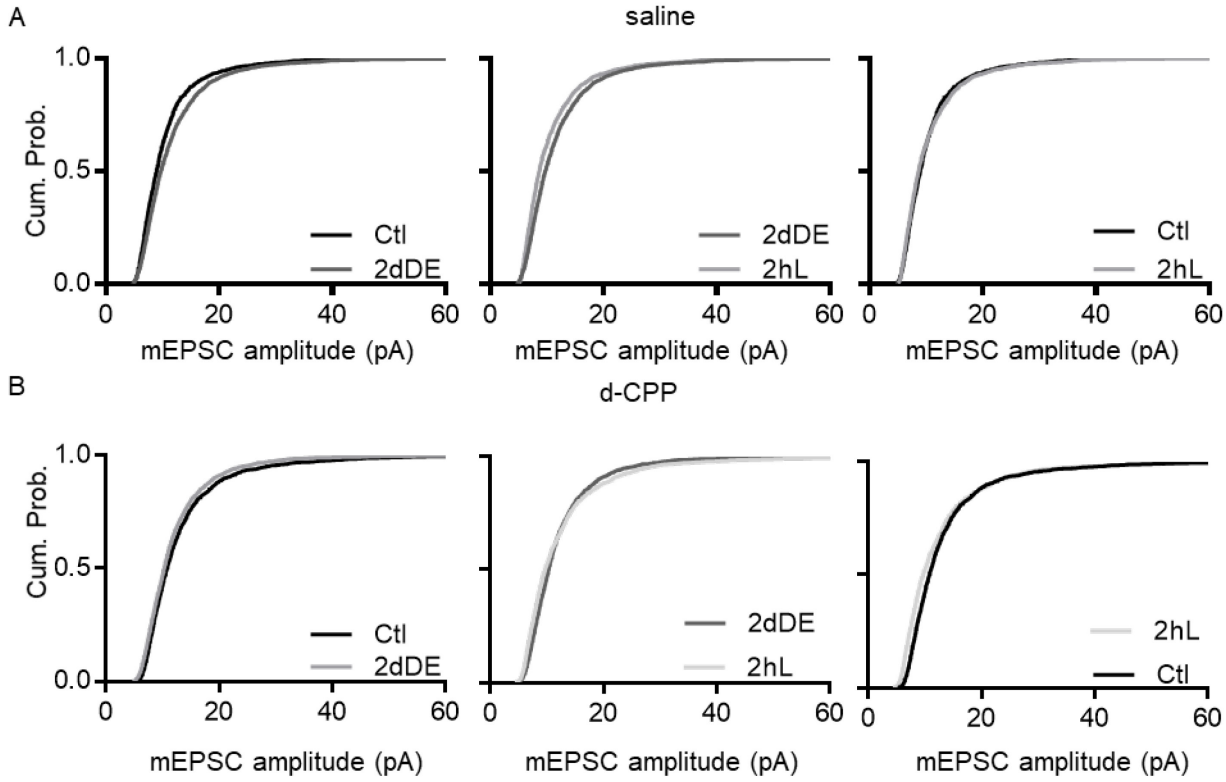

Figure 2.5:. **Comparison of cumulative probability distribution plots for saline and d-CPP treated conditions. (A)** Data from saline infused animals show differences between NR and 2dDE distributions (K-S test ****p<0.0001) and between 2dDE and 2hL (K-S test ****p<0.0001). However, there is no significant difference between NR and 2hL (K-S test p=0.1777). **(B)** Data from d-CPP infused animals show a slight, but significant shift towards lower amplitudes in 2dDE and 2hL events relative to Ctl (K-S test ***p=0.0006;K-S test ****p<0.0001).Comparison between 2dDE and 2hL show significant differences between the distributions (K-S test ****p<0.0001).

Subsection 5: NMDAR disruption does not alter overall postsynaptic activity

A potential concern is that the lack of homeostatic adaptation observed with blocked NMDAR function reflects an inability for the network to modulate activity levels with visual experience. Changes in postsynaptic activity levels are thought to drive homeostatic synaptic plasticity (Goold and Nicoll, 2010; Ibata et al., 2008). Therefore, we investigated whether knocking out altered the overall activity of V1 L2/3 neurons. To do this, we used the expression of the immediate early gene c-Fos as a proxy for neuronal activation under different conditions (Hoffman et al., 1993; Joo et al., 2016). In GFP-only viral expression mice, we did not observe a significant change in the fraction of c-Fos positive neurons between normal-reared (Ctl) and 2dDE groups, but there was a robust increase in the fraction of c-Fos positive neurons after light re-exposure (2hL) as compared to the 2dDE condition (Fig. 2.6 A). When NMDARs were knocked out by expression of Cre-GFP in NR1-flox mice, we detected a small but statistically significant decrease in the fraction of c-Fos positive neurons among the KO neurons in 2dDE group when compared to that of normal-reared (Ctl) values, as well as a significant increase in the fraction of c-Fos positive neurons after light re-exposure relative to 2dDE (Fig. 2.6 B). This suggests that knocking out NMDARs in V1 L2/3 does not grossly interfere with the pattern of changes in of neuronal activation with visual experience. Therefore, the absence of DE-induced scaling up of mEPSCs seen in NMDAR KO neurons (Fig. 2.2 C) cannot be attributed to altered neuronal activity. If at all, the small decrease in the fraction of c-Fos positive NMDAR KO neurons of the DE group, which indicates a reduction in neuronal activity, should have promoted scaling up of mEPSCs. Taken together, our results suggest that the disruption of scaling up of

excitatory synapses in V1 L2/3 neurons after 2dDE in the absence of NMDAR function is not due to major alterations in the overall activity of these neurons, but rather a necessary role for NMDAR in regulating synaptic strength in a homeostatic manner.

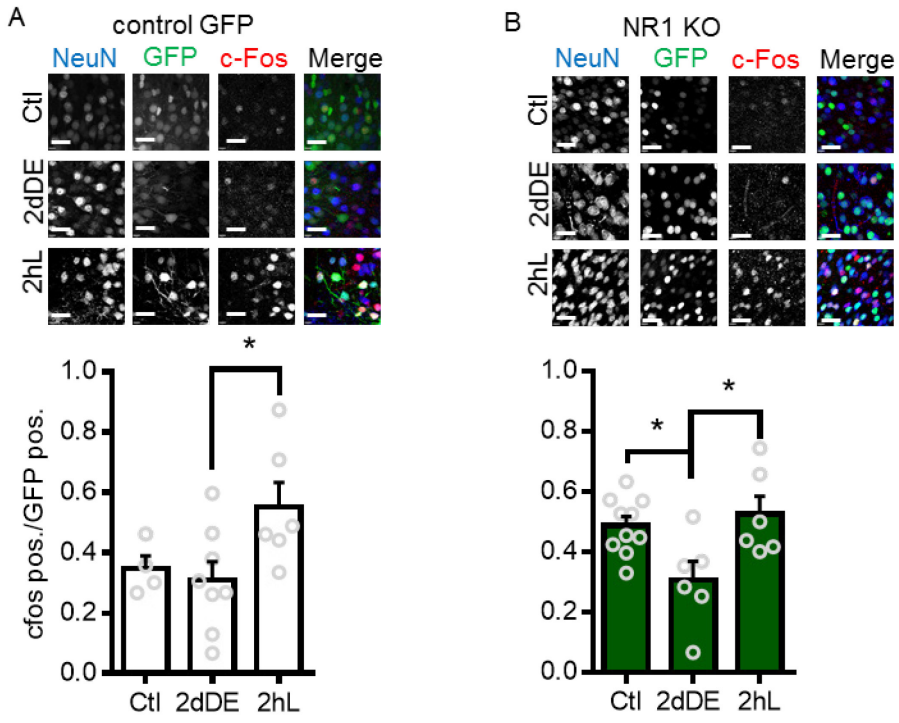

Figure 2.6: Quantification of c-Fos staining Top: representative confocal images, bottom: Bar graph comparison of each condition (data points represent slices quantified). **(A)** V1 L2/3 tissue transfected with GFP-only virus (scale bar= 18 μm) showed a significant increase in the fraction of c-Fos positive neurons in the 2hL in comparison to 2dDE (values = (number of c-Fos positive neurons)/(number of GFP positive neurons): Ctl = 0.35 ± 0.04, 2dDE = 0.31± 0.06, 2hL = 0.55 ± 0.08; ANOVA *p=0.0470; Newman-Keuls *p<0.01) **(B)** In comparison, tissue from NR1 KO mice (scale bar = 18μm) showed a slight decrease in the fraction of c-Fos positive neurons after 2dDE and a significant increase of the fraction of c-Fos positive neurons in the 2hL group (values = (number of c-Fos positive neurons)/(number of Cre-GFP positive neurons): Ctl = 0.48 ± 0.03, 2dDE = 0.31± 0.06, 2hL = 0.53 ± 0.06; ANOVA *p=0.0118; Newman-Keuls *p<0.01).

Section 4: Discussion

In this study, we tested the role of NMDARs in homeostatic synaptic plasticity induced *in vivo* by changes in visual experience. By combining disruption of

NMDAR function, through cell specific knock-out and pharmacology, with brief periods of visual deprivation or light re-exposure, we showed that the principal neurons within L2/3 of V1 require functional NMDARs to undergo proper homeostatic changes in synaptic strength. A targeted and acute manipulation of NMDAR function was achieved by cell-type specific knockout of these receptors. In this case we observed a lack of synaptic strength modulation by visual experience, demonstrating a requirement for NMDARs in regulating homeostatic synaptic plasticity in *vivo*.

We also utilized brain-wide pharmacological blockade of NMDARs to address whether the function or the structure of NMDARs, is essential to allow for experience-dependent homeostatic synaptic plasticity. NMDAR blockade with d-CPP resulted in a baseline increase of synaptic strength under control conditions, which was not seen in cell-specific KO of NR1. Even with this difference, the mean amplitude of mEPSCs was not further modulated by changes in visual activity in the presence of CPP. The aberrant increase in basal synaptic transmission with CPP may suggest that NMDAR blockade mimics the effect of DE. However, the lack of such basal increase with cell-specific KO of NMDAR is inconsistent with this interpretation. Alternatively, a global pharmacological block of NMDAR function may have led to this aberrant change in synaptic transmission with CPP. Hence, our interpretation of CPP experiments is limited by the fact that we cannot distinguish between these two possibilities. Despite this caveat, the data recorded from both NMDAR KO and d-CPP treated neurons point to a deficit in homeostatic synaptic plasticity under conditions of NMDAR disruption.

The involvement of NMDAR activation in homeostatic synaptic plasticity *in vivo* is in line with previous studies showing co-regulation of NMDAR together with AMPAR under inactivity conditions (Watt et al., 2000), as well as changes in NMDAR function after visual deprivation (Philpot et al., 2001; Quinlan et al., 1999). While previous studies in cultured neurons demonstrated that homeostatic synaptic scaling is largely independent of NMDAR activity (Turrigiano et al., 1998), the dependence of sensory experience-induced synaptic scaling on NMDAR function had not been addressed. Here we found that NMDAR function is required for proper scaling of mEPSCs in V1 L2/3 neurons following a few days of DE or brief re-exposure to light (2hL). It has previously been proposed that a switch in NMDAR function underlies the slide in the threshold for LTP/LTD induction after DE (Philpot et al., 2003; Quinlan et al., 1999).Our results suggest a possibility that scaling up of mEPSCs could be a consequence of sliding down of synaptic modification threshold promoting LTP. Lowered synaptic modification threshold by DE would promote LTP across a large population of synapses, and hence manifest as global scaling up of excitatory synapses. This would imply that the amount of activity in V1 under DE condition is sufficient to act on the lowered threshold to induce NMDAR-dependent LTP. This contradicts *in vitro* studies done in cultured neurons, where prolonged blockade of action potentials was able to scale up excitatory synapses. Our data suggest that this may not be the case *in vivo*, where we surmise there may be sufficient activity in the deprived cortex that can activate

NMDARs to potentiate synaptic strengths across a large number of synapses following a reduction in LTP threshold.

Some evidence from previous studies *in vitro* have demonstrated interactions between NMDAR function and synaptic scaling. For example, blocking NMDARs has been shown to accelerate synaptic upscaling in cultured neurons (Sutton et al., 2006) and decreasing NMDAR calcium permeability has been shown to downscale AMPAR currents (Pawlak et al., 2005b). Other potential mechanisms relating NMDAR activation with scaling involve regulation of retinoic acid-dependent insertion of AMPARs (Arendt et al., 2015) or the “unsilencing” of synapses after activity blockade *in vitro* (Arendt et al., 2013). These findings suggest that NMDAR activity can have profound influence on synaptic scaling mechanisms in addition to sliding the threshold for LTP/LTD.

Synaptic scaling has been largely considered a cell-autonomous process that is triggered by readout of postsynaptic spikes, or more precisely postsynaptic depolarization (Goold and Nicoll, 2010; Ibata et al., 2008). For example, optogenetic activation of postsynaptic neurons was shown to be sufficient to drive down-scaling of excitatory synapses (Goold and Nicoll, 2010), and blocking somatic spikes was sufficient to scale up synapses (Ibata et al., 2008). However, recent studies suggest that synaptic scaling is not dependent on postsynaptic spike rate per se, but due to changes in glutamatergic inputs (Fong et al., 2015). These results suggest that the level of activation of glutamate receptors could ultimately be the condition monitored by neurons in order to undergo synaptic scaling.

Our data provide *in vivo* evidence for a homeostatic mechanism that requires NMDAR activation in order to cope with changes in visual experience. These results suggest either a role for NMDAR function in *in vivo* synaptic scaling or that homeostatic scaling of synapses is a manifestation of Hebbian forms of plasticity triggered by lowered or increased synaptic modification threshold according to changes in visual experience. If it is the latter, a major implication is that *in vivo* homeostasis could be implemented in an input specific manner. Indeed, DE has been shown to increase the synaptic strength of connections between V1 L2/3 neurons without affecting those between L4 and L2/3 (Petrus et al., 2015), which could be the basis for non-multiplicative synaptic scaling observed in adult V1 (Goel and Lee, 2007). Moreover, changes in dendritic spine size correlated with synaptic strengthening have been shown to be regulated at the level of branches and microcircuits after visual deprivation (Barnes et al., 2015, 2017). Together with our results, it seems likely that *in vivo* homeostatic synaptic plasticity primarily results in non-homogenous synaptic changes regulated by NMDAR function.

Chapter 3: Cross-modal reinstatement of thalamocortical plasticity accelerates ocular dominance plasticity in adult mice

This manuscript is in preparation.

Potential authors: **Gabriela Rodríguez**, Katrina Shrode, Amanda Lauer and Hey-Kyoung Lee

My contribution: Performed all experiments except auditory brainstem response measurements. Did all experimental design and data analysis with guidance from Hey-Kyoung Lee.

Section 1: Introduction

Thalamocortical (TC) inputs directly convey salient sensory information to the cortex for further processing. As with other aspects of sensory circuit development, TC innervation is shaped by sensory experience during a well-defined “critical period” (Barkat et al., 2011; Crair and Malenka, 1995). In the mouse visual pathway, TC synapses undergo significant reorganization and refinement from the second to the third week of post-natal development (Gu and Cang, 2016; Jiang et al., 2007). Ascending inputs onto thalamorecipient layer 4 (L4) in particular have been shown to express NMDAR-dependent long-term potentiation and depression (LTP and LTD) during this limited time window, while feedforward inputs from L4 to L2/3 remain plastic into adulthood in mouse primary visual cortex (V1) (Jiang et al. 2007; Kirkwood and Bear, 1994). The same laminar progression of plasticity has been described in studies assessing synaptic scaling, another activity-dependent form of plasticity. Here, scaling displays an early critical period in L4, but persists in L2/3 (Desai et al., 2002; Goel and Lee, 2007). Studies performed *in vivo* also showed that ocular dominance plasticity (ODP) is more robust in L4 early in development, while in adults it is more evident in L2/3 (Pham et al., 2004). Taken together, these cases support the view that thalamocortical

synapses onto V1 L4 undergo plasticity early on and subsequent experience-dependent changes are mainly mediated by intracortical synaptic changes.

Recent studies, however, have challenged the notion that V1 TC plasticity cannot be induced in adults by particular manipulations, such as environmental enrichment (Mainardi et al., 2010) or prolonged visual deprivation (Montey and Quinlan, 2011). Moreover, we have previously shown that cross-modal sensory manipulations result in strengthening of TC synapses in the adult brain (P90-120). In particular, visual deprivation results in strengthening of TC inputs to auditory cortex (A1) while deafening leads to TC potentiation in V1 (Petrus et al., 2014). These studies indicate that reactivation of TC plasticity is a hallmark of cross-modal plasticity induced across sensory cortices and could represent the cellular basis for enhanced processing in spared cortices after sensory loss. However, the synaptic mechanisms underlying this change remain unexplored.

Here, we utilized adult mice (P90-120) deafened for 1 week (6-8 days) to investigate the mechanisms responsible for post-critical period TC strengthening in V1. By combining slice electrophysiology with targeted optogenetic activation of thalamic inputs, we demonstrate the reemergence of NMDAR-dependent LTP at visual TC inputs, similar to the plasticity present early during postnatal development. Furthermore, we explored whether restoration of V1 TC plasticity by cross-modal sensory deprivation would reactivate ODP in adults. Our findings support cross-modal sensory manipulations as a potential method to overcome plasticity restrictions in the adult brain.

Section 2: Methods

Animals

B6 (C57BL/6J, Jackson Laboratories) and PV-*Cre x* Ai14 tdTomato (PV-Cre: Pval$^{btm1(cre)Arbr/J}$; Ai14 tdTomato:_Gt(ROSA)26Sor$^{tm14(CAG-tdTomato)Hze}$) mice were reared in a 12 hours light/dark cycle with water and food pellets *ad libitum*. All protocols were approved by the Institutional Animal Care and Use Committee (IACUC) at Johns Hopkins University and followed the guidelines established by the Animal Care Act and National Institutes of Health (NIH).

Thalamic Viral Transfection

B6 and PV-TdTomato mice (p40-p60) of either sex were anesthetized and head fixed in a stereotaxic device (Kopf Instruments, California) under constant flow of an isoflurane/oxygen mix (1.5-2 % isoflurane). The dorsal lateral geniculate nuclei (dLGN) were bilaterally injected with an adeno-associated virus expressing channelrhodopsin (ChR2) under the control of the human synapsin (hSyn) promoter (AAV5.hSyn.ChR2(H134R)-YFP.WPRE.hGH, Penn Vector Core, University of Pennsylvania). dLGN was targeted with the following coordinates: -2.3 mm, Lateral: 2 mm (from bregma); Depth: 2.42 mm. Mice recovered on a heated pad and were returned to the animal colony, housed with 2-3 same sex mice, until experimental paradigms began.

Deafening

At postnatal days (P) 90-110 male and female mice were deafened as in (Petrus et al., 2014). In brief, animals were anesthetized by exposure to isoflurane vapors

in a closed induction chamber. The absence of the toe pinch reflex was confirmed and the animal was placed in a stereotaxic device (Kopf Instruments, California) under constant administration of an isoflurane/oxygen mix (2 % isoflurane). The pinnae were cut and the ventral surface of the ear was slit to aid visualization of the inner ear. The tympanic membrane was then punctured with a 30-gauge needle, the ear cavity was injected with 50 µL kanamycin (175 mg/mL) and stuffed with kanamycin soaked gel foam (Pfizer) (Hashimoto et al., 2007). The ventral incision and remainder of pinnae were sutured shut (PSDII; Ethicon) and animals were allowed to recover on a heating pad until movement and drinking behaviors were evident.

Auditory Brainstem Responses

Auditory brainstem responses (ABRs) were measured for a subset of animals as described previously (McGuire et al., 2015). Mice were anesthetized with an i.p. injection of 100 mg/kg ketamine and 20 mg/kg xylazine, then placed on a heating pad inside a sound-attenuating chamber (IAC) lined with Sonex Acoustic foam to reduce acoustic reflections. Mice were placed facing a speaker (FT28D; Fostex, Tokyo, Japan) with the speaker positioned 30 cm from the pinnae. Temperature was monitored via a rectal probe and maintained at 36°C ±1°. Subcutaneous platinum needle electrodes were placed over the left bulla and at the vertex of the skull, and a ground electrode was inserted into the leg muscle. The electrodes were attached to a preamplifier and amplifier (ISO-80; World Precision Instruments, Sarasota, FL). Stimulus generation, presentation and response

acquisition were controlled using custom Matlab-based software, Tucker Davis technologies programming modules (Tucker-Davis Technologies, Alachua, FL), and a PC.

Stimuli consisting of clicks and 5-ms tones (0.5 ms onset/offset) at frequencies of 8, 12, 16, 24 and were presented. Stimuli were generated with a sampling frequency of 195 kHz, and presented at a rate of 20/s. We sampled responses at 9.5 kHz, bandpass filtered from 300-3000 kHz, and averaged over 300 stimulus repetitions. Clicks were tested first to verify electrode placement and the presence of a clearly observable response, and then tones were tested in random order of frequency. We presented a tone of a given frequency at a sound level of 85-105 dB SPL (depending on frequency), and then continued presenting the same tone at lower sound levels until a threshold was reached. Threshold was defined as the sound level at which the peak-to-peak (any peak) amplitude of the response was two standard deviations above the average baseline noise amplitude during a time window when no sound stimulus was present. Testing lasted approximately 40-60 minutes; mice were returned to their home cages following testing and monitored until recovery.

Cochlea stain

The effectiveness of our deafening protocol was also confirmed by observation of hair cell loss using phalloidin staining. Whole cochleae were dissected from experimental animals and stored in 10% formalin solution (Sigma) at 4℃. Before staining cochleae were washed in 0.1 M PB and decalcified in 3% EDTA for 48

hours. Apical, middle and basal turns were dissected. Each turn was permeabilized with 0.2% Triton-X for 1 hour and subsequently incubated with Alexa Fluor 488-phalloidin (Invitrogen; 1:200) and DAPI (1:5000) for 2 hours. Cochlear turns were whole mounted on glass slides using ProLong Gold antifade mounting medium (Life Technologies).

Cortical slice preparation

Mice were deeply anesthetized using isoflurane vapors in a closed chamber placed in a fume hood. After confirming absence of corneal reflex and toe pinch response, animals were perfused with ice cold artificial cerebrospinal fluid (ACSF, in mM: 124 NaCl, 5 KCl, 1.25 $NaH_2PO_4 \cdot H_2O$, 26 $NaHCO_3$, 10 dextrose, 2.5 $CaCl_2$ 1.5 $MgCl_2$, bubbled with 95% O_2/5% CO_2) and immediately decapitated. The brain was removed and immersed in ice-cold dissection buffer (in mM: 212.7 sucrose, 10 dextrose, 3 $MgCl_2$, 1 $CaCl_2$, 2.6 KCl, 1.23 $NaH_2PO_4 \cdot H_2O$, 26 $NaHCO_3$, bubbled with 95% O_2/5% CO_2). Blocks containing V1 were isolated and sectioned coronally into 300 µm thick slices using a vibratome (Pelco easiSlicer, Ted Pella). Slices were incubated in a light-tight holding chamber filled with ACSF at 30 ° C for 30 minutes and then allowed to recover at room temperature for at least 30 minutes. The slices were then transferred to a submersion-type chamber mounted on the fixed stage of an upright microscope (Nikon, E600FN) with oblique infrared illumination.

Whole-cell current clamp recordings

Whole cell recordings were targeted at a 40-50% depth from the pia corresponding to L4 and principal neurons were visually identified. The location of the majority of recorded cells was confirmed post-hoc by biocytin labelling. Recording pipettes (3-5 MΩ) were filled with an internal solution consisting of (in Mm): 130 K-gluconate, 8 NaCl, 0.2 EGTA, 10 HEPES, 3 ATP, 10 Na-phosphocreatine, and 0.5 GTP, pH 7.4, 275–285 mOsm. Excitatory postsynaptic potential (EPSPs) were evoked by shining blue light (Thorlabs 455 nm LED, 5 ms duration) through a 40x objective (Nikon fluor 40x/0.8W DIC WD 2.0) to activate thalamic terminals. Stimulus intensity was adjusted to the minimum required to reliably produce single-peaked, short-onset latency (< 4 ms) excitatory postsynaptic potentials (EPSPs).

LTP induction (pairing conditioning)

Recording configuration switched from current-clamp to voltage-clamp for the plasticity induction protocol. The paired stimulus protocol entailed 200 pulses of presynaptic stimulation at 1 Hz coupled with continuous postsynaptic depolarization to 0 mV (Choi, 2005; Jiang et al., 2007). Changes in synaptic strength were quantified as changes in the initial slope of the EPSP normalized by the average baseline slope obtained during the first 5 minutes of stable recordings. Cells were discarded if the resting membrane potential was higher than -65 mV or if the resistance values changed more than 30% during the experiment.

NMDAR kinetics

NMDAR currents were pharmacologically isolated in the presence of 2,3-dihydroxy-6-nitro-7-sulfamoyl-benzo[f]quinoxaline-2,3-dione (NBQX, 10 μM), picrotoxin (50 μM) and glycine (1μM). Responses were recorded at +40 mV, with 4 mM Ca^{2+} and 4 mM Mg^{2+} in ACSF to reduce polysynaptic responses and using internal solution consisting of (in mM): 102 cesium gluconate, 5 TEA-chloride, 3.7 NaCl, 20 Hepes, 0.3 sodium guanosine triphosphate, 4 magnesium adenosine triphosphate, 0.2 EGTA, 10 BAPTA, and 5 QX-314 chloride, pH 7.2, 300 mOsm. A minimum of 15 traces (15-30) were averaged per cell and the decay was fitted with a double exponential equation using Igor. Slow (s) and fast (f) exponential values were then used to calculate a weighted time constant (τw) as in (Philpot et al., 2001; Rumbaugh and Vicini, 1999) following: $\tau_w = \tau_f [I_f /(I_f + I_s)] + \tau_s [I_s /(I_f + I_s)]$ where I_f and I_s are the amplitudes for fast and slow components respectively.

NMDAR/AMPAR ratio

Isolated monosynaptic glutamatergic (AMPA/ NMDA) currents were recorded in the presence of bicuculline (20 μM) in ACSF with 4 mM Ca^{2+} and 4 mM Mg^{2+}. The internal solution used to record responses consisted of (mM): 102 cesium gluconate, 5 TEA-chloride, 3.7 NaCl, 20 Hepes, 0.3 sodium guanosine triphosphate, 4 magnesium adenosine triphosphate, 0.2 EGTA, 10 BAPTA, and 5 QX-314 chloride, pH 7.2, 300 mOsm. The LED intensity was adjusted to twice the value of the minimum required to consistently produce single-peaked, short-onset latency (< 4 ms) AMPAR mediated EPSCs. NMDAR and AMPAR responses were distinguished based on their kinetics and voltage dependence. The NMDAR component was taken as the amplitude at holding potential (Vh) +40 mV, 70 ms

after the response onset, whereas the AMPAR component was taken as the peak amplitude recorded at Vh -80 mV.

Light evoked Sr^{2+} mEPSCs (LEv-Sr mEPSCs)

Slices were incubated in the recording chamber in bubbled (95% O2/5% CO2) in Ca^{2+}-free ACSF containing 4 mM Sr^{2+} and 4 mM Mg^{2+} for 20 minutes to equilibrate before initiation of recordings. AMPAR mediated responses were recorded under two conditions: 1) pharmacologically isolated with 20 µM bicuculline and 100 µM DL-2-amino-5 phosphonopentanoic acid (APV) and 2) isolated with the same drugs with the addition of 1 µM tetrodotoxin (TTX), which was done to confirm monosynaptic responses resulting from ChR2 activation of presynaptic inputs. Recording pipettes (3-5 MΩ) were filled with internal solution containing (in mM): 130 Cs-gluconate, 8 KCl, 1 EGTA, 10 HEPES, 4 ATP, and 5 QX-314, pH 7.4, 285–295 mOsm. Target neurons were identified visually and voltage clamped at Vh -80mV. Only recordings with series resistance <25 MΩ and input resistance >150MΩ that changed less than 15% were included in the analysis. The responses were evoked using a 455-nm LED (Thor labs) illuminated through a 40x objective lens (Nikon fluor 40x/0.8W DIC WD 2.0). Stimulation intensity was set to the minimal light required to produce a reliable response with 5 ms stimulus duration. Traces were recorded every 10 s for a duration of 1200 ms which included a seal test pulse, 500 ms window before LED stimulation and 500 ms after stimulation. Spontaneous events were quantified during a 400 ms time window before LED illumination (preLED) and LED-evoked Sr^{2+} desynchronized (LEv-Sr) events were

quantified in a 400 ms window that started 50ms from LED onset (postLED). Events were selected using MiniAnalysis (Synaptososft) with threshold set to 3 times the root mean square (RMS) noise. Cells with an RMS noise higher than 2 were excluded. To calculate the mean amplitude of evoked desynchronized events without baseline spontaneous activity, we used the following equation: [(postLED amp x postLED frq) - (preLED amp x preLED frq)] / (postLED frq -preLEDfrq) where amp is amplitude and frq is frequency. Calculated LEv-Sr^{2+} mEPSC amplitudes between the two recording conditions (with and without TTX) showed no significant changes (mean NR 21.02 ± 2.8 pA, NR_{TTX} 16.44 ± 1.4 pA, unpaired Student's t-test p=0.2080; mean DF 18.61 ± 2.4 pA, DF_{TTX} 20.8 ± 2.3 pA, unpaired t-test p=0.5200). Therefore, the data were pooled for Figure 3.5.

E/I ratio

Cortical L4 principal neurons were patched in voltage-clamp configuration with internal solution consisting of (in mM): 130 Cs-gluconate, 8 KCl, 1 EGTA, 10 HEPES, 4 ATP, and 5 QX-314, pH 7.4, 285–295 mOsm. Only recordings with series resistance < 25 MΩ and input resistance > 150 MΩ were included in the analysis. Monosynaptic EPSCs and disynaptic inhibitory postsynaptic currents (IPSCs) were recorded from each cell at the reversal potential for inhibitory currents and excitatory currents, respectively. After compensation for the junction potential, the reversal potential for inhibitory currents was -52 mV and the reversal potential for excitatory currents was 0 mV. Thalamic terminals were activated with light flashes (LED 455 nm) of 5ms duration delivered at several intensities until

responses maximized, but did not evoke polysynaptic events. E/I ratios were calculated at each stimulation intensity for each cell. We noticed a tendency for E/I values to increase along with stimulation power until eventually saturating at higher intensities. Therefore, we averaged three E/I ratio values at consecutive saturating intensities for each cell and report this as the E/I ratio of the cell (Fig.3.1).

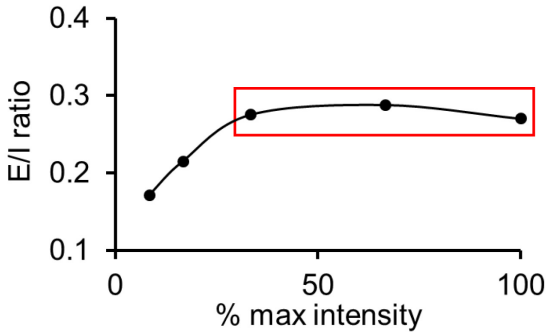

Figure 3.1: **E/I ratio saturates at higher stimulation intensities.** Example plot of E/I ratio values recorded for a single cell. Notice the values plateau at higher stimulation intensities. The values within the red rectangle were averaged and recorded as the E/I ratio for this cell.

Monocular deprivation

Mice were deeply anesthetized with isoflurane gas (3 %) in a sealed induction chamber. Once absence of toe pinch response was confirmed, animals were transferred to a stereotaxic apparatus where oxygen supply was constantly supplemented with isoflurane (1-2 %). The upper and lower margins of one eyelid were trimmed and sutured (PSD II; Ethicon) shut. The eye contralateral to the hemisphere being imaged was always sutured. Animals of the same sex were housed together (2-3 mice/cage) and disqualified if sutures opened.

Optical imaging of intrinsic signals

Mice were placed in a stereotaxic apparatus under constant supply of an oxygen/isoflurane mixture (0.7-1.5 % isoflurane), supplemented by a single injection of chlorprothixene (0.2 µg/g ip). Their temperature was maintained at

37°C and heart rate was monitored throughout the experiment. The skull over V1 on the left hemisphere (contralateral to lid suture) was exposed and washed with hydrogen peroxide. Low melting point agarose (3%) and a glass coverslip were placed over the exposed area and allowed to solidify.

V1 responses were recorded using the method previously developed by Kalatsky and Stryker (Kalatsky and Stryker, 2003) and optimized for ocular dominance (OD) measurements by Cang and colleagues (Cang et al., 2005). Optical images of cortical intrinsic signals were acquired using a Dalsa CCD camera (Dalsa, Waterloo, Canada) controlled by custom software. The surface vasculature and intrinsic signals were visualized with illumination wavelengths of 555nm and 610nm, respectively. After focusing on prominent vasculature marks, the camera was focused 600 μm below the surface. A high refresh rate monitor (ViewSonic) was placed 25 cm in front of the animal for stimulus presentation. The visual stimulus presented was restricted to the binocular visual field (5° to +15° azimuth) and consisted of a horizontal bar (x= 5°, y= 0º, width= 20) continuously presented for 5 minutes in upward (90º) and downward (270º) directions to each eye separately. The cortical response at the stimulus frequency was extracted by Fourier analysis and used to calculate the ocular dominance index (ODI). Two maps were averaged per eye for each animal to compute the ODI following the formula: (C-I)/(C+I) where C and I are the response magnitudes of each pixel to visual stimulation to the contralateral (C) and ipsilateral (I) eye respectively. The binocular area was selected as a region of interest (ROI) in the ODI map and the ODI values within this region were averaged.

Biocytin labeling

Biocytin was added to the internal solution during most experiments to allow confirmation of neuronal location and morphology. Previously recorded cortical slices were fixed in 4% paraformaldehyde overnight at 4°C. Slices were rinsed 10 minutes in 0.1 M phosphate buffer (PB) at room temperature and permeabilized in 2% Triton X-100 for one hour. Slices were then incubated in avidin-AlexaFluor 633 conjugate (Fisher) diluted 1:2000 in 1% Triton X-100 overnight at 4°C. Slices were washed twice in 0.1 M PB and mounted on glass slides with Prolong Gold antifade (Invitrogen). Images were taken on a laser scanning confocal microscope (Zeiss LSM 700) to confirm location of recorded cells post-hoc.

Statistics

All data are presented as ± SEM. Unpaired Student's t-test was used to compare recordings between NR and DF groups. Paired t-tests were used to compare ODI and eye-specific cortical activation responses measured from the same animals before and after monocular deprivation. In all cases $p < 0.05$ was considered statistically significant.

Section 3: Results

Subsection1: Reemergence of LTP at V1 TC synapses in L4 after deafening

Previous work demonstrated that sensory deprivation can lead to cross-modal strengthening of TC synapses in the adult rodent brain, which challenges

the classical view of a brief and early window for TC plasticity (Petrus et al., 2014). Hebbian forms of synaptic plasticity have been established as the mechanisms driving experience-dependent changes of TC inputs to L4 in primary sensory cortices during the critical period (Crair and Malenka, 1995; Dudek and Friedlander, 1996; Kirkwood et al., 1995). Therefore, we tested the hypothesis that post-critical period strengthening of TC synapses after deafening results from reengagement of long-term potentiation (LTP) mechanisms in adult V1.

For the purpose of our study we induced hearing loss in adult animals (P90-120) via ototoxic lesioning of hair cells by injection of kanamycin (175 mg/mL) into the inner ear coupled with tympanic rupture. High concentrations of kanamycin have been shown to significantly affect hair cell morphology and thus, induce deafness (Hashimoto et al., 2007; Hashino et al., 1991). Therefore, we confirmed the efficiency of our approach by measuring auditory brainstem responses (ABRs) and examining the presence of hair cells with phalloidin stain. We observed a significant increase in the threshold to induce ABRs in DF mice indicating that their hearing was impaired (Fig 3.2 A). Moreover, we confirmed cochlear damage in the DF group by phalloidin staining of hair cells (Fig 3.2 B).

In order to selectively activate thalamic inputs we used an optogenetic approach that targeted dLGN terminals in V1 (Wang et al., 2013). Earlier efforts at inducing TC LTP in slices with high frequency stimulation (HFS) have failed in rodent visual cortex (Wang and Daw, 2003). However, pairing low frequency presynaptic stimulation with strong postsynaptic depolarization has proven successful in cortical slices from young (P8-17) mice (Crozier et al., 2007; Jiang et

al., 2007). Therefore, we tested the ability to induce LTP at TC synapses in L4 of V1 in slices from normal reared (NR) or deafened (DF) adult mice (P90-120) by using a pairing protocol for LTP induction. In brief, we paired continuous postsynaptic (L4) cell depolarization (0 mV) with 200 illumination pulses (455 nm LED) at 1Hz to activate thalamic presynaptic terminals expressing channelrhodopsin (ChR2) (Fig. 3.3 A, B). In a pilot experiment, we verified that activation of ChR2 through LED illumination could faithfully generate action potentials up to 40 Hz frequency. We then demonstrated that the pairing conditioning was able to induce LTP at TC inputs onto V1 L4 in DF adult animals (163.5 ± 2.4% of baseline), but not in control NR animals (99.8 ± 1.5% of baseline) (Fig. 3.3 C).

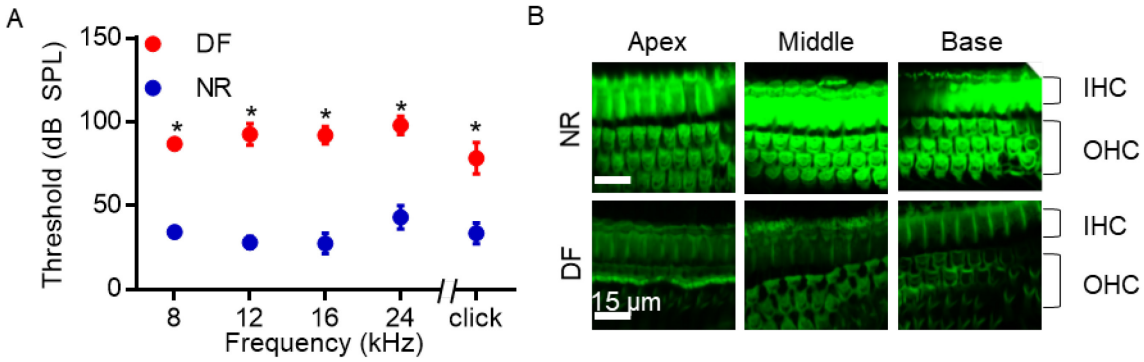

Figure 3.2: **Confirmation of deafening. (A)** Increased threshold to elicit ABRs in DF mice (n=3 animals in all cases; unpaired Student's t-test 8kHz *p= 4.90e-006, 12kHz *p=0.0001, 16kHz *p=0.0002, 24kHz *p=0.0004, click *p=0.0023). **(B)** Confirmation of cochlear damage by phalloidin staining of hair cells from NR (top) and DF (bottom) animals. Note absence (apex) and decreased (middle and base) stain intensity in hair cells from DF. mouse (IHC=

LTP at TC synapses during the early critical period is known to be dependent on NMDAR function in multiple sensory cortices (Barth and Malenka, 2001; Crair and Malenka, 1995; Heynen and Bear, 2001). Therefore, we examined the ability to induce LTP at TC synapses in slices from DF adult mice while blocking NMDARs with DL-2-amino-5 phosphonopentanoic acid (APV). Blockade with APV prevented LTP in slices from DF animals (98.5± 1.1% of baseline) indicating that the induction of LTP in deafened adult mice is dependent on NMDAR activation, similar to what has been described in normal juvenile mice during the critical period (Fig. 3.3 C).

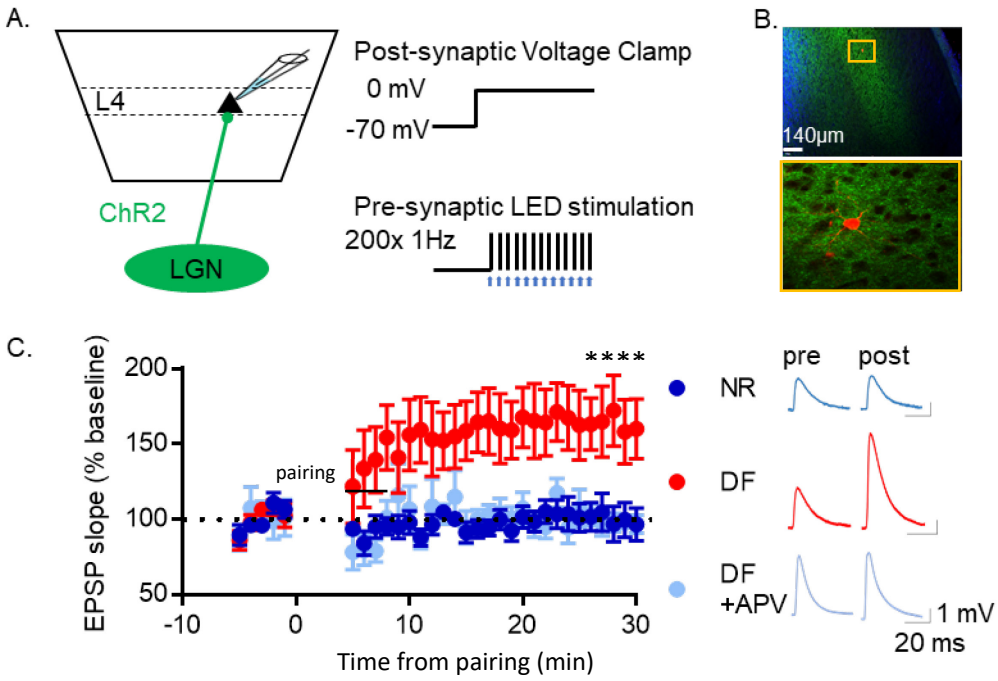

Figure 3.3: **LTP induction at TC→ L4 inputs in adult V1 slices. (A)** Schematic of V1 recordings in which thalamic terminals expressed ChR2. Right: schematic of pairing conditioning used to induce LTP. Briefly, constant postsynaptic depolarization (0 mV) was paired with presynaptic stimulation with light pulses (455 nm; 5 ms; 200 trains at 1 Hz). **(B)** Top: V1 cortical slice expressing ChR2-YFP in thalamic terminals stained for biocytin (TxRed) and counterstained for DAPI. Yellow outline denotes recorded cell. Bottom: Higher magnification image of recorded L4 principal neuron (PN). **(C)** Left: LTP induction in slices from adult mice (data are presented as mean ± SEM; unpaired Student's t-test between baseline and last 5 minutes of recording, DF: n=9 cells, **** p<0.0001; NR: n= 9 cells, n.s. p= 0.9834; DF+APV: n= 6 cells, n.s. p= 0.6972). Right: Example EPSPs averaged 5 minutes before pairing (pre) and last 5 minutes of recording (post).

Subsection 2: Cross-modal regulation of NMDARs at TC synapses to V1 L4 following deafening

Since NMDAR activation is critical for the cross-modal resurgence of TC LTP we investigated what aspect of NMDAR function, if any, was regulated by deafening. First, we determined the relative contribution of NMDARs to EPSCs evoked from thalamic terminals by measuring the NMDA/AMPA ratio (N/A ratio). There was no significant change in the average ratio between NR and DF groups (Fig. 3.4 A). Previous experiments demonstrated increased AMPAR-mediated currents at TC synapses after deafening (Petrus et. al, 2014). Therefore, our results suggest that NMDAR current is co-regulated with potentiation of AMPAR current to maintain a constant N/A ratio.

A switch in NMDAR subunit composition is known to coincide with decreased synaptic plasticity and the closure of the established critical period (Barth and Malenka, 2001; Hensch, 2005; Quinlan et al., 1999; Sheng et al., 1994). In particular, a switch in NR2 subunit composition has been consistently reported during V1 development (Philpot et al., 2003; Quinlan et al., 1999). Previous studies showed that NR2b-containing NMDARs predominate at synapses early on, but

undergo a developmental switch to incorporate NR2a subunits (Monyer et al., 1994; Sheng et al., 1994). NMDAR subunit composition alters receptor decay kinetics such that they become faster over time, which has been implicated in changing the activity threshold for LTP/LTD induction (Philpot et al., 2001, 2003; Quinlan et al., 1999). Therefore, we measured isolated NMDAR evoked responses at TC synapses onto L4 in V1 and compared their weighted decay time constants between groups as reported previously (Philpot et al., 2001, 2003; Rumbaugh and Vicini, 1999). We observed no significant changes in the NMDAR decay kinetics at TC synapses between NR and DF groups (Fig 3.4 B). Our results suggest that cross-modal sensory deprivation in adults may regulate the function of synaptic NMDARs without changes in NR2 subunit composition, which contrasts what is observed early on in development.

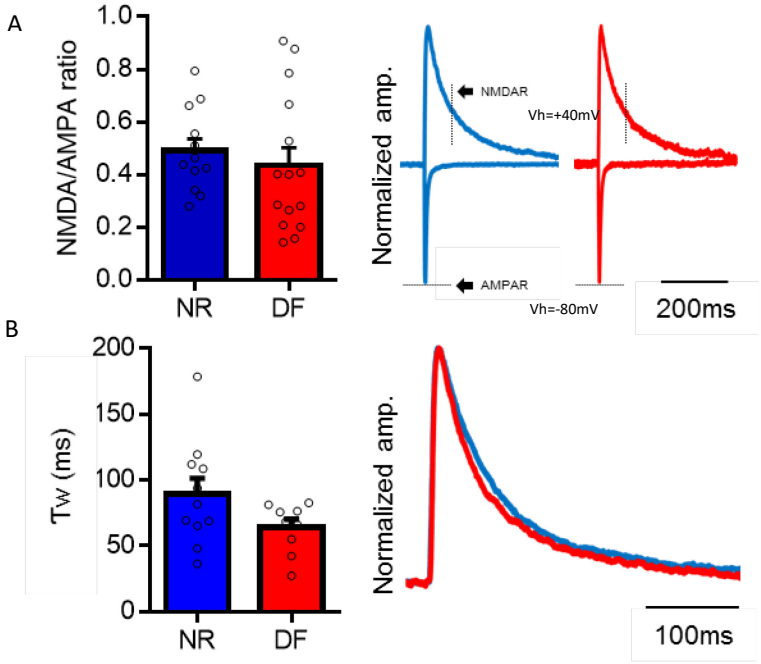

Figure 3.4: **NMDAR regulation at visual TC synapses after deafening. (A)** Left: NMDA/AMPA ratio measurements for NR and DF groups (open circles represent recorded cells; NR mean 0.49 ± 0.045 pA, DF mean 0.43 ± 0.067 pA; unpaired Student's t-test p=0.5173). Right: Averaged example traces for a NR (blue) and a DF (red) cell normalized to AMPAR component in NR (dashed lines point out time after stimulation at which AMPAR and NMDAR components were measured). **(B)** Left: Weighted decay times for NR and DF groups (open circles represent cells; NR mean 89.31 ± 11.97 ms, DF mean 63.93 ± 6.3 ms; unpaired Student's t-test p=0.0961). Right: Averaged NMDAR responses for NR (Blue) and DF (red) groups normalized to respective maximum amplitudes and superimposed.

Subsection 3: V1 TC inputs to inhibitory PV+ neurons remain unchanged after deafening

Thalamic inputs strongly drive feedforward inhibition onto cortical L4 neurons, which serves to regulate coincidence detection and truncate visually evoked EPSPs (Chittajallu and Isaac, 2010; Cruikshank et al., 2007a; Daw et al., 2007; Kloc and Maffei, 2014). In V1, as well as somatosensory cortex, TC inputs recruit feedforward inhibition mainly by activating fast spiking parvalbumin positive (PV+) cells in the cortex (Cruikshank et al., 2007a; Daw et al., 2007; Kloc and

Maffei, 2014; Lintas et al., 2013). Maturation of cortical inhibition mediated by PV+ neurons is also implicated in gating cortical plasticity (Fagiolini et al., 2004; Hensch, 2005; Hensch et al., 1998; Huang et al., 1999; Jiang et al., 2005; Kirkwood and Bear, 1994b; Trachtenberg, 2015). Therefore, we examined if deafening could lead to changes in thalamic engagement of cortical inhibition.

In order to test potential modulation of thalamic input to cortical PV+ cells after deafening, we targeted recordings to this class of inhibitory cells in visual cortical slices by using mice expressing Td-Tomato in PV+ neurons (PV-tdT; offspring of PV-Cre crossed with Ai14). As in previous experiments, ChR2 was expressed in TC terminals of PV-tdT mice, and we stimulated ChR2-expressing dLGN terminals with a 455 nm LED (Fig. 3.5 A, B). To compare the strength of individual synapses regardless of ChR2 expression or stimulation level, we recorded LED-evoked, Sr^{2+} desynchronized (LEv-Sr^{2+}) mEPSCs as described previously (Petrus et al., 2014; 2015) (for detailed explanation see Methods section). In this scheme, LED-evoked responses are desynchronized such that recorded events represent single-vesicle release and thus, quantal synaptic response size can be determined (Gil et al., 1999). We found no significant differences between the amplitudes of LEv-Sr^{2+} mEPSCs recorded from PV+ neurons in NR and DF groups (Fig. 3.5 C).

Our results in Figure 3.5 C and Figure 3.3 C, together with our previous studies (Petrus et al., 2014) reveal differential regulation of thalamocortical recruitment of excitation and inhibition as a result of cross-modal sensory deprivation. Therefore, we examined the excitation to inhibition (E/I) ratio across

principal neurons (PNs) in V1 L4. Briefly, pure inhibitory or excitatory responses were isolated from the same cell by recording in voltage-clamp configuration while holding membrane potentials at the reversal for excitation or inhibition, respectively. We observed a significant increase in E/I ratio values in V1 L4 PNs after deafening (Fig 3.5 D, E). Based on our previous study (Petrus et al., 2014) and the results from this study, the altered E/I ratio balance is likely driven by potentiation of thalamic drive onto excitatory L4 PNs.

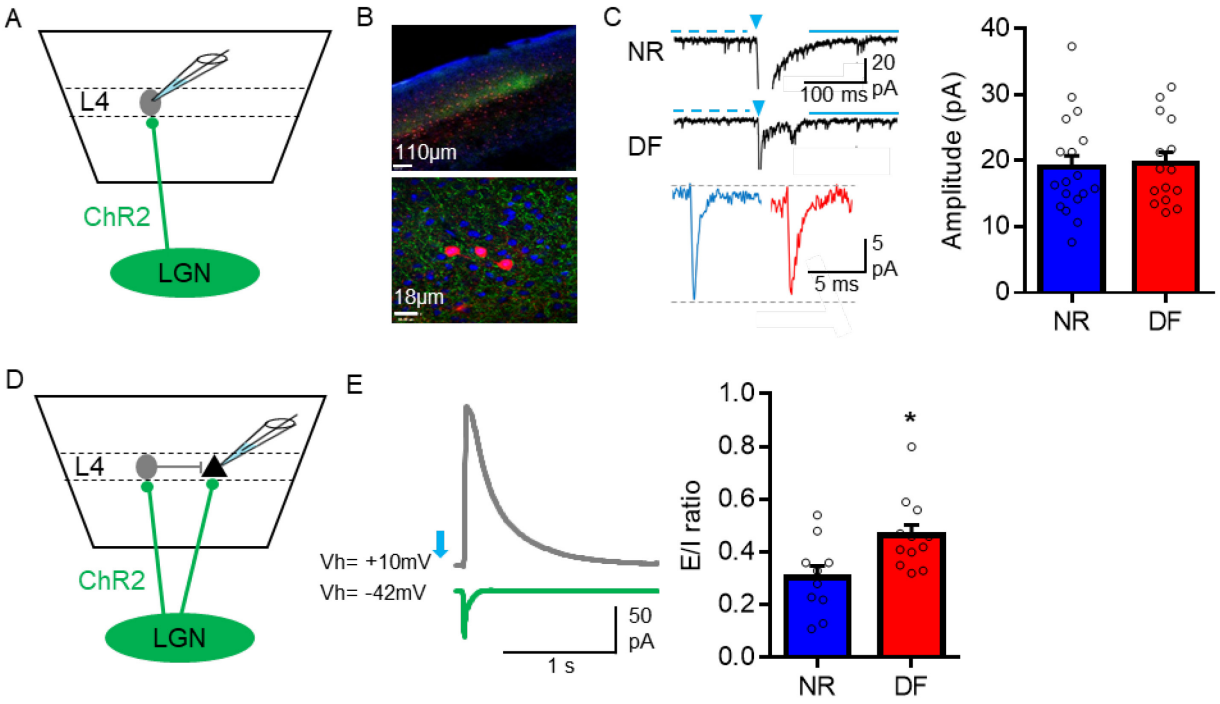

Figure 3.5: **Differential regulation of TC inputs between principal neurons and PV+ cells results in increased E/I ratio. (A)** Schematic of PV+ neuron (gray circle) targeted in V1 L4 for LEv-Sr^{2+} mEPSCs recording. **(B)** Confocal image of a V1 slice showing thalamic terminals expressing ChR2-YFP (green), PV+ neurons expressing Td-Tomato (red) and counterstained for DAPI. Top: 10x magnification; bottom: 63x. **(C)** Left top: Example traces of LEv-Sr^{2+} mEPSCs recordings from NR (top) and DF (bottom) groups. Dashed line demarcates events before LED stimulation (blue triangle) and solid line demarcates events 50 ms after stimulation. Left bottom: Average traces of the calculated amplitudes for LEv-Sr^{2+} mEPSCs for NR (blue) and DF (red) groups. Right: Average LEv-Sr^{2+} mEPSCs amplitude comparison between NR and DF groups (open circles represent cells; NR mean 18.9 ± 1.7 pA, DF mean 19.6 ± 1.65 pA; unpaired Student's t-test n.s. p= 0.7893). **(D)** Schematic showing targeted V1 L4 principal neurons for E/I ratio recording where thalamic terminals (green) were stimulated with light (455 nm) to evoke responses in L4. **(E)** Left: Average trace of recorded monosynaptic excitatory response (green) and disynaptic inhibitory response (gray) from the same cell after light stimulation (blue arrow). Holding potentials to record isolated inhibitory or excitatory responses shown (reversal potential for excitation +10mV and reversal potential for inhibition -42mV measured for our cesium based internal solution). Right: Significant increase in average E/I ratio values after deafening (open circles represent cells; unpaired Student's t-test *p= 0.0127).

Subsection 4: Deafening restores rapid ocular dominance plasticity (ODP) in adult V1

Based on our result that short-term deafening of adult mice restores TC LTP in V1, we next tested whether deafening could restore experience-dependent V1 plasticity. ODP is a classic approach to studying experience-dependent synaptic plasticity in V1, and the mechanisms underlying it in both young and adults have been well characterized (Frenkel and Bear, 2004; Gordon et al., 1996; Sato and Stryker, 2008; Sawtell et al., 2003). It is well established that a short period (3-4 days) of monocular deprivation (MD) elicits quick and robust OD shift in V1 during the critical period for ODP, which in mice starts at P19 and extends until P35 (Gordon et al., 1996). In adults (P60-90), however, ODP requires a longer period of MD (5-7 days) (Frenkel and Bear, 2004; Sato and Stryker, 2008; Sawtell et al., 2003). The mechanisms underlying ODP in young animals and adults appear to differ: ODP in young animals is initiated by weakening of closed eye inputs

followed by a delayed potentiation of open eye inputs (Sato and Stryker, 2008; Sawtell et al., 2003). In adults, mainly the delayed potentiation of open eye inputs is observed and correlates with OD shift (Sato and Stryker, 2008; Sawtell et al., 2003). Since deafening promotes potentiation of inputs to L4 in adult V1, we reasoned that deafening may accelerate the emergence of open eye potentiation in adults and allow ODP with shorter duration of MD, which is normally ineffective.

We measured ODP using optical imaging of V1 intrinsic signals before and after periods of MD (Fig. 3.6 A, B) and calculated an ocular dominance index value (ODI) at each time point (Fig. 3.6 C). First, we observed the changes elicited by brief (3-4d) MD on the OD of mice within the established critical period. Indeed, as reported previously (Gordon et al., 1996), this short duration deprivation was sufficient to induce a significant shift in ODI values (Fig. 3.7 A i). Next, we tested whether the same brief MD could produce ODP in deafened adults. We observed a significant decrease in ODI after 3-4 days of MD indicative of an OD shift towards the eye which remained open (ipsilateral) (Fig. 3.7 A ii). Consistent with previous studies, the same short duration MD failed to change ODI in V1 of age matched adult NR mice (Fig. 3.7 A iii). However, longer deprivation periods (5-7d) resulted in a significant shift of ODI values in NR adults (Fig. 3.7 A iv), supporting previous reports indicating that adult V1 still has the potential for ODP, but occurs in a delayed manner (Frenkel and Bear, 2004; Sato and Stryker, 2008; Sawtell et al., 2003).

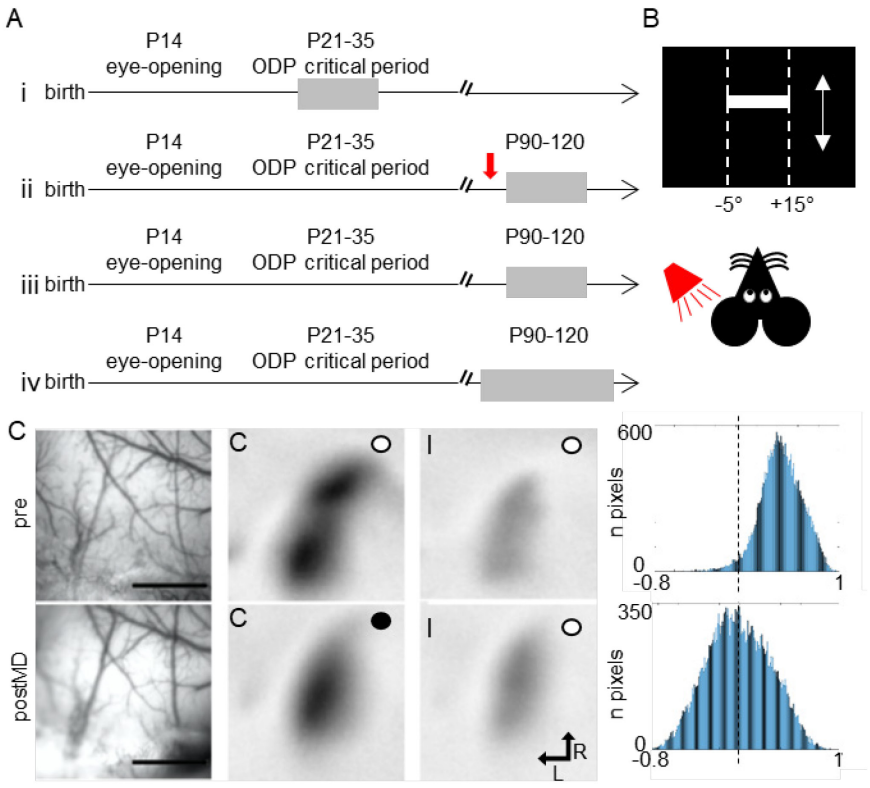

Figure 3.6: **Ocular dominance measured by cortical intrinsic signal imaging. (A)** Experimental timeline for MD during: i) critical period, ii) DF adults (P90-120; red arrow signifies deafening) and iii & iv) NR adulthood. Gray lines represent MD (short lines 3-4 d, long line 5-7 d). **(B)** Schematic of visual stimulus presented while recording V1 intrinsic signals. **(C)** All images and data are from the same animal (critical period MD). Left: Surface vasculature used to guide imaging in the same animal before (top) and after (bottom) MD. Scale bar is 1mm. Middle: V1 intrinsic signals recorded before (top) and after (bottom) MD for contralateral (C) and ipsilateral (I) eyes (white circles indicate open eye; black circle indicates closed eye). Right: Histogram showing the distribution of pixels corresponding to ODI values. Note a left shift in the distribution after MD indicating more pixels have a lower ODI (dashed line indicates binocularity ODI=0).

While our results demonstrate that deafening accelerates ODP in the adult cortex, whether this is through re-establishing "juvenile-like" plasticity in the adult V1 is not known. ODP can be distinguished at different developmental stages based on the mechanisms that underlie it. In essence, "juvenile-like" or critical period ODP relies on an initial depression of closed-eye (contralateral) inputs followed by strengthening of open-eye (ipsilateral) projections (Ranson et al.,

2012; Sato and Stryker, 2008). On the other hand, adult ODP is mainly mediated by a delayed potentiation of open-eye (ipsilateral) inputs (Frenkel and Bear, 2004; Ranson et al., 2012; Sato and Stryker, 2008; Sawtell et al., 2003). Therefore, we examined the magnitude of visually evoked cortical activation through each eye before and after MD in young and adult mice. As expected, we observed both a decrease in V1 activation when a stimulus was presented to the previously deprived eye (contralateral), as well as an increase in cortical activation corresponding to inputs from the open eye when deprivation occurred during the critical period for ODP (Fig. 3.7 B i). In DF adult animals, we detected a robust increase in V1 activation through the open eye with no significant changes in the closed-eye inputs (Fig. 3.7 B ii). Age matched NR adults showed no significant changes in eye-specific V1 activation after brief MD, but increased open-eye activation intensity after long-term MD (Fig. 3.7 B iii, iv). These results suggest that deafening accelerates the emergence of open-eye potentiation in the adults, but does not engage the fast depression of the closed-eye inputs as observed in critical period juveniles.

Subsection 5: Deafening does not allow recovery from chronic monocular deprivation (MD)

Next, we asked whether the plasticity recruited in V1 by deafening would allow for recovery of deprived eye inputs following chronic MD. Previous work has established that chronic MD before eye opening is resilient to recovery later on across different species (He et al., 2006; Hubel and Wiesel, 1970; Liao et al., 2004) and recent work has implicated TC plasticity as a key component for recovery (He, 2006; Montey and Quinlan, 2011). Based on the ability of deafening to promote

potentiation of TC inputs in adult V1, we wanted to test whether this would allow potentiation of the previously weak chronically-deprived eye inputs to normal levels.

To test our idea, we sutured the contralateral eye of mice closed before eye-opening (~P12) and kept it closed until P120 or older. A group of mice were deafened for a week (DF) before reopening of the chronically deprived eye. We observed a drastic shift in baseline OD, in both NR and DF groups, to lower ODI values following chronic MD indicating ipsilateral inputs dominated V1 after chronic MD of the contralateral eye, just as reported previously (Fig 3.8 A, B) (He et al., 2006; Hubel and Wiesel, 1970; Liao et al., 2004). Opening the contralateral eye and allowing animals to have binocular vision (BV) did not recover normal level of contralateral bias in either NR or DF animals even if the period of BV was extended beyond a week (Fig. 3.8 A, B). These results suggest that although deafening can reactivate TC plasticity in a cross-modal fashion, it is not sufficient to drive plasticity of the previously closed eye inputs and suggests that additional mechanisms might be required to recover deprived-eye inputs following chronic MD.

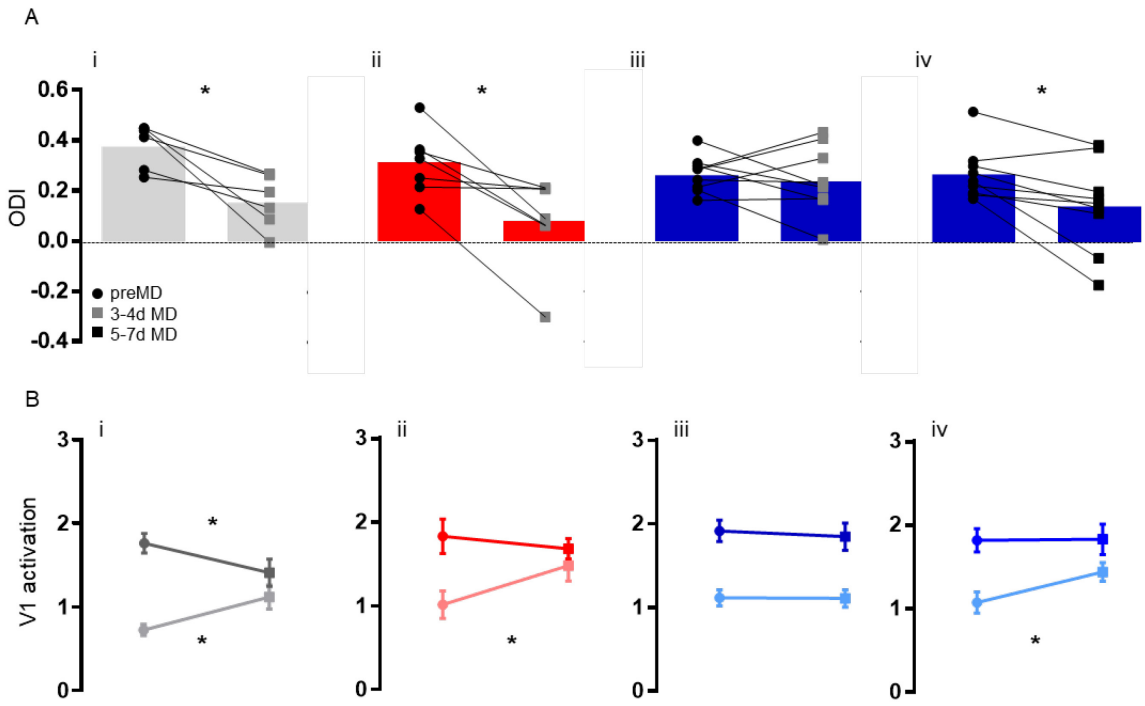

Figure 3.7: **Deafening accelerates ODP in the adult V1. (A)** Ocular Dominance index where ODI=(C-I)/(C+I), before and after MD for: **i)** critical period 3-4d MD (bars show mean, preMD = 0.378 ± 0.036 , postMD = 0.1534 ± 0.044 data point represent animals; paired t-test *p=0.0132), **ii)** DF adults 3-4dMD (mean: preMD = 0.3164 ± 0.048, postMD = 0.083 ± 0.068; paired t-test *p=0.0121); **iii)** NR adults 3-4dMD (mean: preMD = 0.264 ± 0.023, postMD = 0.2389 ± 0.044; paired t-test n.s. p=0.5892); and **iv)** NR adults 5-7dMD (mean: preMD = 0.2682 ± 0.035 postMD = 0.1411 ± 0.060; paired t-test *p=0.170). **(B)** Average eye-specific V1 activation intensity where darker shade represents contralateral eye and soft shade represents ipsilateral for: **i)** critical period 3-4dMD (mean contralateral: preMD = 1.76 ± 0.12, postMD = 1.41 ± 0.16, paired t-test *p = 0.0204; mean ipsilateral: preMD = 0.72 ± 0.16, postMD = 1.21 ± 0.35, paired t-test *p = 0.0213), **ii)** DF adults 3-4dMD (mean contralateral: preMD = 1.83 ±0.21, postMD = 1.68 ±0.12, paired t-test p = 0.5200; ipsilateral preMD = 1.02 ±0.16, postMD = 1.48 ±0.18, paired t-test *p = 0.0207), **iii)** NR adults 3-4dMD (mean contralateral: preMD = 1.9±0.13, postMD = 1.84 ±0.16, paired t-test p = 0.6782; mean ipsilateral: preMD = 1.12 ± 0.09, postMD = 1.12 ± 0.10, paired t-test p = 0.9168 and **iv)** NR adults 5-7dMD (mean contralateral: preMD = 1.81 ± 0.14, postMD = 1.82 ± 0.18, paired t-test p = 0.9629; mean ipsilateral: preMD = 1.08 ± 0.13, postMD = 1.45 ± 0.11, paired t-test *p=0.0328.

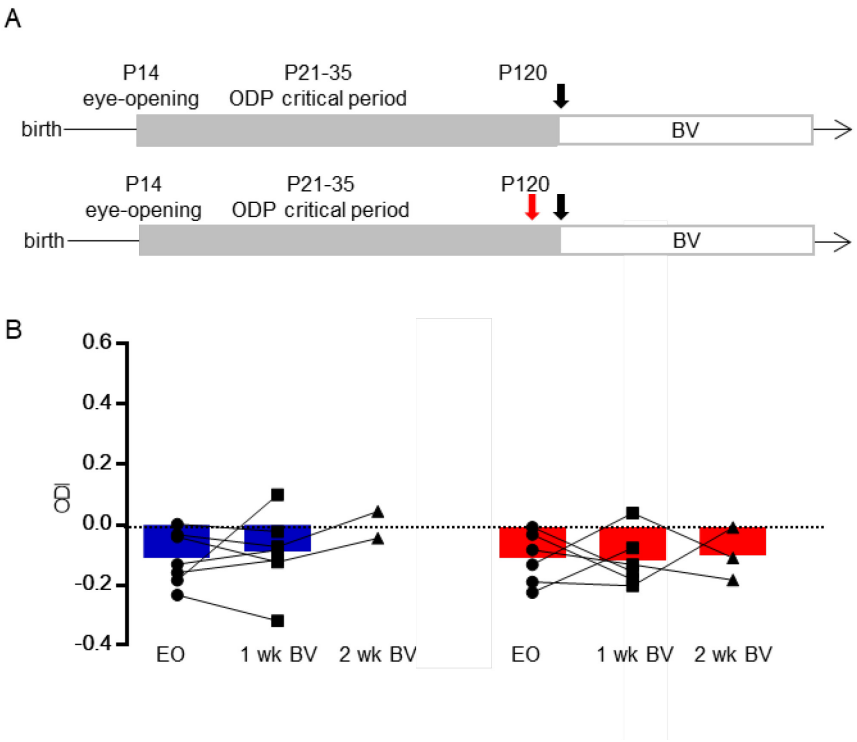

Figure 3.8: **Recovery after chronic MD is resilient to deafening. (A)** Timeline showing chronic MD (gray line) paradigm where lid suture was performed at eye opening (P12-14) and eye was opened at P120 (black arrow) for NR (top) and DF (bottom, red arrow represents deafening) groups. **(B)** ODI comparison for NR (left, blue) and DF (right, red) groups along the time allowed for binocular vision (BV). There were no significant changes in ODI between the time of eye opening (EO) and 1 week of BV (1wkBV) (bars indicate mean; NR mean: EO = -0.111 ±0.03, 1wkBV = -0.091 ± 0.04, paired t-test p=0.6947; DF mean: EO = -0.104 ±0.03, 1wkBV = -0.111 ± 0.36, paired t-test p=0.9070) or between 1wk and 2wkBV (NR mean: 1wkBV = -0.098 ±0.025, 2wkBV = 0.000 ±0.04, paired t-test p= 0.1203; DF mean: 1wk BV = -0.092 ± 0.07, 2wkBV = -0.094 ±0.05) for either condition.

Section 4: Discussion

In this study we investigated the molecular mechanisms underlying the reactivation of TC plasticity by cross-modal sensory manipulations. In particular, we addressed the impact deafening has on TC plasticity in spared mouse V1. Notably, the mechanisms we describe here allow for TC plasticity 10-12 weeks after the defined critical period for TC synapses. Overall, we observed a reemergence of NMDAR-dependent LTP induction at TC synapses which is driven by potentiation of NMDAR currents and an increase in E/I ratio. Moreover, we

demonstrated that hearing loss can accelerate ocular dominance plasticity (ODP) in adult mice through potentiation of open eye inputs. However, the plasticity recruited is not sufficient to recover deprived-eye inputs after chronic MD.

Recent studies have begun to highlight the potential for TC synapses to undergo plasticity in adulthood under certain conditions (Mainardi et al., 2010; Montey and Quinlan, 2011; Petrus et al., 2014; Pizzorusso et al., 2002) The molecular mechanisms underlying it remain largely unexplored. Our findings are in agreement with one of the few other studies describing post-critical period mechanisms of TC synaptic plasticity (Chung et al., 2017). In this case, Chung and colleagues induced adult TC LTP in the spared whisker barrel after infraorbital nerve (ION) lesions. Together with our observations, these results suggest that adult TC LTP is more readily recruited in spared cortical areas rather than within the deprived regions.

Our studies not only reveal a requirement for NMDARs in adult TC LTP induction, but also a potential regulation of NMDAR function as a result of cross-modal sensory deprivation. We observed evidence for potentiation of NMDAR current at TC synapses, in conjunction to previously reported potentiation of AMPAR current (Petrus et al., 2014), which resulted in preservation of NMDA/AMPA ratios between NR and DF groups (Fig. 3.4). However, we did not observe a change in the kinetics of NMDAR current, which argues against a change in NR2 subunit composition. This differs from the findings reported by Chung and colleagues, which showed increased ifenprodil sensitivity at spared TC synapses after ION lesions, indicative of a switch in NMDAR composition (Chung

et al., 2017). Our results would suggest that cross-modal NMDAR regulation is either mediated by a change in the number or function of NMDARs. Therefore, our findings are more in line with previous studies describing concomitant regulation of AMPAR and NMDAR synaptic components in an activity dependent manner (Bashir et al., 1991; von Engelhardt et al., 2009; Watt et al., 2000), which has been shown to be driven mainly by modulation in the number of open NMDAR channels (Watt et al., 2000).

We also report differential regulation of TC synapses dependent on postsynaptic cell identity. While thalamic input to L4 PNs strengthens, input to PV+ inhibitory cells remains unaltered after DF (Fig 3.5). This suggests that the principal regulation during cross-modal reactivation of TC plasticity is specific to the postsynaptic cell-type despite sharing the same presynaptic origin of axons. One implication of this differential regulation is that the balance in feedforward excitation and inhibition recruited by thalamic input to V1 could be altered. Indeed, our data show increased E/I ratio experienced by L4 principal neurons after deafening. Increased E/I ratio is reminiscent of early developmental stages, during which the initially readily available potential for plasticity is becoming restricted as inhibitory inputs mature and decrease E/I (Zhang et al., 2011). Previous work has demonstrated the importance of E/I balance maintenance in the mature cortex (Azouz et al., 1999; Dehghani et al., 2016; Okun and Lampl, 2008; Xue et al., 2014), yet our results show a deviation from baseline (NR) equilibrium. Changes in E/I balance have been implicated previously in recruitment of TC plasticity after environmental enrichment (Mainardi et al., 2010). Our results similarly suggest that

E/I ratio is not fixed even in adults, and can deviate based on sensory experience, which could allow opening of the window of opportunity for plasticity to sculpt neural circuits in accordance to environmental changes and the need of the cortical network for sensory processing.

While the consequences of cross-modal plasticity on V1 function are still unclear, here we demonstrate that loss of hearing can accelerate ODP in V1 of adult mice. This effect was driven by accelerated potentiation of open-eye inputs without major changes in those from the deprived eye. Taken together with reinstatement of TC LTP in V1 by deafening, these results suggest a model in which TC LTP may be driving potentiation of open-eye inputs in V1. In addition, our data indicate that the mechanisms by which rapid ODP occurs with cross-modal sensory deprivation differ from those active during the critical period for ODP, and are likely an acceleration of adult mechanisms of ODP.

Our findings of enhanced ODP in the adult V1 after deafening led us to test its potential for recovering deprived-eye inputs after chronic MD. Chronic MD leads to amblyopia that is resistant to spontaneous recovery after vision is reinstated in the deprived eye (Liao et al., 2004; Montey and Quinlan, 2011; Pizzorusso et al., 2002). The limitations to recovery include the reduction in anatomical and functional plasticity of the adult cortex as well as the degradation of feedforward inputs from the deprived eye. Recent work has demonstrated that visual stimulation to the deprived eye can still evoke TC synaptic potentials indicating that some feedforward excitation persists (Montey and Quinlan, 2011). Potentiation of these inputs could therefore possibly allow recovery of the chronically deprived

eye inputs to V1. We found that short-term deafening, while promoting TC LTP, does not engage sufficient plasticity to allow recovery from chronic MD. This suggests that additional mechanisms of plasticity may need to be engaged for effective recovery. For instance, a reduction in TC afferents serving the deprived eye has been shown to occur as a result of axonal retraction or an inhibition of axonal outgrowth (Antonini and Stryker, 1993; Antonini et al., 1999; Tieman, 1984; Le Vay et al., 1980). This implies that axonal growth might need to be induced in order to fully recover those inputs.

Chapter 4: General discussion and future directions

Sensory experience is crucial for cortical development and circuit maintenance. The importance of sensory-driven activity is highlighted by experiments in which manipulations of these inputs have been shown to cause profound changes in the organization and function of cortical networks. It is now well established that sensory loss not only leads to adaptation of deprived regions, but also impacts spared cortical areas. The main goal of this project was to explore the mechanisms that underlie both forms of adaptation in the mouse V1. My results reveal a requirement for NMDARs in both types of adaptations and shed light on the potential use of sensory manipulations to recruit plasticity in the adult brain. This section will discuss some of our major findings, their implications and future directions.

Section 1: Shared mechanisms between homeostatic and Hebbian plasticity

The studies in both Chapter 2 and 3 reveal the necessity of NMDARs for unimodal as well as cross-modal adaptations in V1. In the case of cross-modal adjustments in V1 after deafening, NMDARs are required to induce Hebbian plasticity at TC synapses. On the other hand, NMDARs are required for homeostatic synaptic plasticity in V1 after DE. These results add to evidence demonstrating that similar mechanisms are utilized for both Hebbian and homeostatic forms of plasticity (Barnes et al., 2015; Goel et al., 2011; Huang et al., 2012).

Although NMDARs have been clearly implicated in the induction of LTP/LTD, previous studies in cultured neurons demonstrated that synaptic scaling, as a result of activity blockade by TTX, was independent of NMDARs (Turrigiano et al., 1998). In our experiments, we tested the dependence of visual deprivation-induced synaptic scaling on NMDAR function, which had not been addressed before. Indeed, our data support a necessary role for these receptors during homeostatic adaption *in vivo*. One possible explanation for this discrepancy involves the differences in residual levels of neuronal activity in each of these manipulations. While activity blockade by TTX abolishes all action potentials (Turrigiano et al., 1998), DE decreases, but does not block all activity within V1 (Czepita et al., 1994; Chapter 2 Fig. 2.6). Therefore, this suggests that V1 in DE animals could have enough residual neuronal activity to allow for NMDAR activation. Since both TTX treatment and DE result in homeostatic adaptations of

excitatory synaptic strength this implies that different mechanisms could coexist and which one is engaged to achieve homeostasis might be dictated by the degree of change in activity. Under our condition of DE, while visually driven activity is missing, there is still activity originating from other brain areas, as well as spontaneous activity that can activate V1 neurons. However, loss of visually driven activity will likely drive metaplasticity to slide the threshold to favor LTP. This would allow active intracortical inputs, which are the majority of synapses, to potentiate hence result in an apparent up-scaling of synapses. On the other hand, if the firing rate approaches zero, as would under TTX application condition, then the neurons would not be able to undergo LTP/LTD and therefore unable to engage the sliding threshold mechanism of metaplasticity. This may trigger neurons to engage in an NMDAR-independent synaptic scaling mechanism to maintain firing rate homeostasis. Such two-stage homeostatic mechanism may provide neural circuits to homeostatically adapt to a much wider range of changes in neuronal activity.

My results suggest either a role for NMDAR function in *in vivo* synaptic scaling or that proper scaling of synapses results from changes in the synaptic modification threshold with visual experience. Potential interactions between NMDARs and homeostatic mechanisms of plasticity have been reported previously. For example, previous work has shown co-regulation of NMDAR and AMPAR after prolonged inactivity (Watt et al., 2000). Additionally, regulation of retinoic acid synthesis, which regulates AMPAR insertion in a homeostatic manner, depends on NMDAR activation (Arendt et al., 2015). Similarly, enhanced LTP after activity blockade can result from “unsilencing” synapses, a process that directly

depends on functional NMDARs (Arendt et al., 2013). Furthermore, NMDARs are the key elements proposed to underlie modification of the threshold for LTP/LTD induction. This is particularly relevant for V1, where manipulations in visual activity have been shown to alter NMDAR subunit composition and thus, function (Philpot et al., 2001, 2003; Quinlan et al., 1999).

A lower threshold for LTP/LTD could promote potentiation of most synapses, which would manifest as an overall scaling up of excitatory inputs. Indeed, previous studies have shown shared final outcomes between LTP and synaptic upscaling, which further supports the idea of mechanistic commonalities. For example, both LTP and synaptic upscaling have been associated with AMPAR GluA1 phosphorylation leading to incorporation of AMPARs to the postsynaptic compartment (Goel et al., 2011; Lee et al., 2000) and both (LTP and upscaling) are correlated with changes in spine size (Keck et al., 2013; De Roo et al., 2008). In addition, neuromodulators acting through cAMP signaling, which promote LTP, also produce scaling up of mEPSCs in L2/3 of V1, while those activating PLC promote LTD (Seol et al., 2007) and result in global downscaling of synaptic strength (Huang et al., 2012; Seol et al., 2007). My data now provide evidence for a potentially shared induction mechanism between scaling and Hebbian plasticity through activation of NMDARs.

It is relevant to point out that distinguishing between Hebbian (LTP/LTD) and homeostatic forms of plasticity is often difficult. This in in part due to the shared molecular mechanisms described for both. Additionally, the changes imposed by homeostatic adjustments inherently affect the induction of Hebbian synaptic

plasticity. This highlights the requirement for both types of plasticity to work at different timescales. It is clear that there is an intricate interaction between Hebbian and homeostatic synaptic plasticity in order to ensure circuit stability. However, the exact way in which these two types of synaptic plasticity cooperate is not fully understood. Our data are consistent with the idea that homeostatic scaling observed in V1 by visual deprivation is simply LTP across many synapses that is triggered by lowering of the sliding threshold. In support of this idea, we recently found that scaling up of V1 synapses following dark exposure is not global across all synapses, but is restricted to intracortical synapses without changes in synapses that serve feedforward circuits (Petrus et al., 2015). It is likely that visual deprivation would preferentially reduce activity of feedforward synapses but would not impact much intracortical activity arising from other brain areas. In this case, a reduction of feedforward activity by visual deprivation is expected to lower the threshold for LTP induction across all synapses, but only the active intracortical synapses would have sufficient activity to recruit NMDAR to express LTP. Whether this is the case would require further studies.

Section 2: Cross-modal reactivation of adult thalamocortical (TC) plasticity

In Chapter 3, I investigated changes in V1 resulting from deafening adult mice. Previous work has provided detailed description of input-specific synaptic changes in spared cortical areas as a consequence of cross-modal plasticity. In general, feedforward excitatory inputs, including TC inputs, strengthen, while intracortical (IC) excitation is enhanced in L4, but decreased in L2/3 (Goel et al., 2006; Petrus et al., 2014, 2015). Notably, these changes can occur in the adult

brain (Petrus et al., 2014, 2015) and suggest cross-modal sensory manipulations might be more efficient than uni-modal deprivation at recruiting mechanisms of plasticity in the adult cortex. Here, I showed cross-modal sensory deprivation can indeed reactivate NMDAR-dependent LTP in V1 TC inputs, and that this reactivation can accelerate adult ocular dominance plasticity through quick potentiation of open-eye inputs.

TC inputs are known to have a very brief window for plasticity during early postnatal development, in which sensory activity can shape and refine the TC circuitry (Crair and Malenka, 1995). Previous experiments have delineated a TC critical period that ends by P18 in V1 (Jiang et al., 2007). During this period LTP and LTD are readily inducible and depend on NMDAR activation (Crozier et al., 2007; Kato et al., 1991). However, LTP induction is unsuccessful at TC synapses in slices taken from older rodents ((Jiang et al., 2007). My results from Chapter 3, however, indicate that V1 TC inputs can become plastic in adulthood, adding to emerging evidence showing reactivation of adult cortical plasticity through different manipulations (Mainardi et al., 2010; Montey and Quinlan, 2011).

The decline of plasticity after critical periods has been attributed to several developmental and cellular factors, in particular those that alter E/I ratio. For example, manipulations that alter inhibition levels are known to modulate plasticity during early development and have been found to restore plasticity in the adult cortex. Acute application of GABA receptor antagonist on V1 slices increases the probability of LTP induction at the end of the critical period (Kirkwood and Bear, 1994b) and *in vivo* infusion of picrotoxin restores ocular dominance plasticity in the

adult brain as well as LTP from white matter to L2/3 (Harauzov et al., 2010). Similarly, enriched environment and dark exposure result in decreased inhibitory transmission and have been shown to recover ODP (He, 2006; Mainardi et al., 2010; Sale et al., 2010). Additionally, the action of neuromodulators has also been implicated in altering E/I balance. In fact treatment with fluoxetine, a serotonin reuptake inhibitor, restores visual cortical plasticity in adults, at least in part by resetting E/I balance (Vetencourt et al., 2008). Our data provide evidence for modulation of the E/I ratio in L4 of adult V1 after deafening. Together with previous observations this would suggest that cross-modal regulation of E/I could be the driver of adult TC LTP reinstatement.

One interesting possibility is that cross-modal changes in V1 TC synapses could depend, in part, on neuromodulation. Indeed, previous studies have identified serotonin as a mediator of cross-modal plasticity in S1 after visual deprivation, although this study did not address changes at TC inputs (Jitsuki et al., 2011). Some of the findings in Chapter 3 certainly fit a few of the changes previously reported as a result of neuromodulatory influence. For example, the regulation of NMDAR currents (Huang et al., 2012; Ji et al., 2008; Liu et al., 2006) and altered E/I balance (Vetencourt et al., 2008) have been observed as a result of adrenergic and serotonergic modulation respectively . In addition, the “pull-push” metaplasticity model is known to gate the threshold for LTP/LTD induction dependent on GPCR signaling mediated by neuromodulators (Huang et al., 2012; Seol et al., 2007). Experiments in mouse V1 have demonstrated that neuromodulators linked to cAMP signaling promote LTP and suppress LTD

(Huang et al., 2012), while those linked to phospholipase C (PLC) enhance LTD and suppress LTP (Huang et al., 2012). Notably, these experiments revealed that the same visual experience could trigger either LTP or LTD depending on the neuromodulators present. Therefore, the accelerated potentiation of open-eye inputs we observed after MD in adults, with no depression of the closed-eye afferents, suggests that a neuromodulatory pull-push mechanism might take place at these synapses, which could gate the state of plasticity to favor potentiation.

Our observed changes in E/I balance seem to be mainly driven by increase of excitatory thalamic drive onto V1 L4 principal neurons. The data in Figure 3.4 provide evidence for a differential regulation of TC inputs dependent on post-synaptic cell type. While inputs to L4 PNs undergo LTP and strengthen, those onto PV+ cells remain the same. This difference in regulation suggests that one of the main modifications during cross-modal reactivation of TC plasticity is specific to the postsynaptic cell identity. Thalamorecipient fast spiking neurons in V1, which are mostly considered to be PV+, have been shown to lack NMDAR components in their EPSCs and NMDA/AMPA measurements at thalamic inputs (Kloc and Maffei, 2014). This observation, together with my results from Figure 3.3 support the idea that one of the principal regulations during cross-modal reinstatement of TC plasticity targets NMDAR-dependent plasticity.

Additionally, an important component of the overall E/I ratio in L4 PNs is evoked lateral inhibition, which plays a critical role in shaping and sharpening receptive fields within V1 (Krukowski and Miller, 2001). From the data presented here, I cannot rule out that changes in lateral inhibition could further impact the

change in E/I balance observed after cross-modal sensory deprivation. Previous work has demonstrated significant changes in cortical inhibition of spared sensory cortices during cross-modal plasticity. For example, injury to the olfactory epithelium increases GABAergic neurons in the primary somatosensory cortex of rodents (Ni et al., 2010). Also, sound-evoked responses have been described in V1 of normally developed mice, for which sound modulates visual responses by activation of disinhibitory circuits (Ibrahim et al., 2016; Iurilli et al., 2012b). In addition, evoked inhibition within L4 of A1 increases after a week of visual deprivation, which is thought to promote sharpening of auditory receptive fields (Petrus et al., 2015), suggesting that a similar change could take place in V1 after deafening. Future experiments could help us determine if these changes are indeed conserved across sensory modalities

Section 3: Cross-modal recovery of adult ocular dominance plasticity (ODP)

In Chapter 3, I tested, for the first time, the effect of cross-modal sensory deprivation on adult ODP. The results demonstrated that short term (3-4d) MD could elicit a robust shift in OD in adult deafened mice. This quick shift was mediated by accelerated potentiation of the open-eye inputs with no change in inputs from the closed eye. These results, together with reinstatement of TC LTP in V1 by deafening, suggest that TC LTP may drive potentiation of open eye inputs in adult V1 of deafened mice. Since this shift is mainly driven by potentiation of the open-eye inputs, we conclude that the mechanisms driving the OD shift in

deafened adult mice are different than those in the juvenile state, in which closed-eye inputs depress followed by strengthening of open-eye inputs.

The enhanced ODP in adults as a result of deafening prompted me to test the ability of deafening to recover visual inputs from the deprived eye after chronic MD. Suturing one eye shut before eye opening and extending the deprivation into adulthood (P120) recapitulates the conditions of amblyopia in the rodent cortex (Liao et al., 2004; Montey and Quinlan, 2011; Pizzorusso et al., 2002). In particular, inputs from the deprived eye lose most of their anatomical and functional connections to V1, although evoked TC potentials from the deprived eye have been reported (Antonini et al., 1999; He, 2006; Le Vay et al., 1980). There was no recovery of responses from the chronically deprived eye even in mice who were allowed to regain binocular vision preceded by a week of deafening, indicating that the plasticity engaged by cross-modal manipulations is not sufficient to recover from chronic MD. This would suggest that additional mechanisms of plasticity are required for recovery. Currently, there is only one manipulation shown to allow full recovery of the deprived eye inputs after chronic MD that begins before eye opening. Montey and colleagues have demonstrated that 10 days of dark exposure followed by reversed deprivation is able to recover inputs from the chronically deprived eye (Montey and Quinlan, 2011). Moreover, they have shown that recovery of cortical dendritic spine density at thalamorecipient layers as well as matrix metalloproteinase activation after light re-exposure are key factors of recovery (Montey and Quinlan, 2011; Montey et al., 2013; Murase et al., 2017). Other studies have shown that the reduction in TC inputs from the deprived eye

occur as a result of axonal retraction (Antonini et al., 1999; Le Vay et al., 1980). Together, these studies suggest that mechanisms promoting structural, in addition to functional plasticity, are necessary for recovery after chronic MD. It would be interesting to explore the potential for cross-modal plasticity to induce structural or anatomical changes in the future.

Another possible explanation for the lack of recovery from chronic MD after deafening could lie in the behavioral relevance carried by inputs from the deprived eye. In our paradigm, the animals are allowed to have binocular vision during the recovery period. However, other studies showing recovery performed reverse lid suture (opened the deprived eye, closed the deprived eye) (Eaton et al., 2016; Montey et al., 2013; Murase et al., 2017), forcing the previously deprived eye to guide behavior. In addition, it is known that repeated training of the deprived eye accelerates recovery (Eaton et al., 2016). This is similar to studies conducted in adult blindfolded subjects, for which 1 week of intensive Braille training proved successful at enhancing their tactile discrimination ability (Merabet et al., 2008). Together, these observations suggest that although synaptic plasticity can be reinstated in the adult cortex by sensory manipulations, engaging those mechanisms for recovery could depend on the necessity of an animal to attend to or use a particular sense.

Conclusion

Studying experience-dependent changes in V1 has provided neuroscience with a wealth of knowledge about synaptic plasticity, development and

maintenance of cortical circuits. Here, I have studied the molecular mechanisms of two different types of adaptions known to occur in V1 after sensory deprivation. Homeostatic adaptations to changes in visual activity provide a constraining balance to the inherently destabilizing effects of Hebbian plasticity. The mechanisms underlying both forms of synaptic changes, Hebbian and homeostatic, share common molecular players *in vivo,* which makes them difficult to dissociate and reinforces the importance of both of these forms of plasticity to act at different timescales. I also addressed some of the adaptations in V1 caused by cross-modal sensory deprivation, in particular deafening. Cross-modal sensory deprivation has the ability to reinstate plasticity at TC synapses in V1, which were previously considered to be aplastic in adults. The reemergence of adult cortical plasticity after deafening has functional consequences on features of V1, like acceleration of ODP. However, the plasticity recruited by deafening has some limitations, as it is unable to recover deprived eye inputs after chronic MD. The experiments presented here, along with previous and future work, will expand our understanding of the brain's capacity for plasticity and potentially help develop non-invasive strategies to effectively manipulate cortical circuits in a targeted manner.

Bibliography

Abbott, L.F., and Nelson, S.B. (2000). Synaptic plasticity: taming the beast. Nat. Neurosci. *3*, 1178–1183.

Abraham, W.C., and Bear, M.F. (1996). Metaplasticity: the plasticity of synaptic plasticity. Trends Neurosci. *19*, 126–130.

Abraham, W.C., and Williams, J.M. (2003). Properties and Mechanisms of LTP Maintenance. Neurosci. *9*, 463–474.

Abraham, W.C., and Williams, J.M. (2008). LTP maintenance and its protein synthesis-dependence. Neurobiol. Learn. Mem. *89*, 260–268.

Adesnik, H., Li, G., During, M.J., Pleasure, S.J., and Nicoll, R.A. NMDA receptors inhibit synapse unsilencing during brain development.

Adesnik, H., Bruns, W., Taniguchi, H., Huang, Z.J., and Scanziani, M. (2012). A neural circuit for spatial summation in visual cortex. Nature *490*, 226–231.

Ahmed, B., Anderson, J.C., Douglas, R.J., Martin, K.A.C., and Nelson, J.C. (1994). Polyneuronal innervation of spiny stellate neurons in cat visual cortex. J. Comp. Neurol. *341*, 39–49.

Ahmed, B., Anderson, J.C., Martin, K.A., and Nelson, J.C. (1997). Map of the synapses onto layer 4 basket cells of the primary visual cortex of the cat. J. Comp. Neurol. *380*, 230–242.

Alonso, J.M., Usrey, W.M., and Reid, R.C. (2001). Rules of connectivity between geniculate cells and simple cells in cat primary visual cortex. J. Neurosci. *21*, 4002–4015.

Antonini, A., and Stryker, M.P. (1993). Rapid remodeling of axonal arbors in the visual cortex. Science *260*, 1819–1821.

Antonini, A., Fagiolini, M., and Stryker, M.P. (1999). Anatomical correlates of functional plasticity in mouse visual cortex. J. Neurosci. *19*, 4388–4406.

Anwyl, R. (2009). Metabotropic glutamate receptor-dependent long-term potentiation. Neuropharmacology *56*, 735–740.

Arendt, K.L., Sarti, F., and Chen, L. (2013). Chronic Inactivation of a Neural Circuit Enhances LTP by Inducing Silent Synapse Formation. J. Neurosci. *33*, 2087–2096.

Arendt, K.L., Zhang, Y., Sü, T.C., Correspondence, L.C., Jurado, S., Malenka, R.C., and Chen, L. (2015). Retinoic Acid and LTP Recruit Postsynaptic AMPA Receptors Using Distinct SNARE-Dependent Mechanisms. Neuron *86*, 442–456.

Artola, A., and Singer, W. (1993). Long-term depression of excitatory synaptic transmission and its relationship to long-term potentiation. Trends Neurosci. *16*, 480–487.

Avermann, M., Tomm, C., Mateo, C., Gerstner, W., and Petersen, C.C.H. (2012). Microcircuits of excitatory and inhibitory neurons in layer 2/3 of mouse barrel cortex. J. Neurophysiol. *107*, 3116–3134.

Azouz, R., Gray, C.M., Hasenstaub, A.R., and McCormick, D.A. (1999). Cellular mechanisms contributing to response variability of cortical neurons in vivo. J. Neurosci. *19*, 2209–2223.

Bagnall, M.W., Hull, C., Bushong, E.A., Ellisman, M.H., and Scanziani, M. (2011). Multiple Clusters of Release Sites Formed by Individual Thalamic

Afferents onto Cortical Interneurons Ensure Reliable Transmission. Neuron *71*, 180–194.
Barkat, T.R., Polley, D.B., and Hensch, T.K. (2011). A critical period for auditory thalamocortical connectivity. Nat. Neurosci. *14*, 1189–1194.
Barnes, S.J., Sammons, R.P., Jacobsen, R.I., Mackie, J., Keller, G.B., and Keck, T. (2015). Subnetwork-Specific Homeostatic Plasticity in Mouse Visual Cortex In Vivo. Neuron *86*, 1290–1303.
Barnes, S.J., Franzoni, E., Jacobsen, R.I., Erdelyi, F., Szabo, G., Clopath, C., Keller, G.B., and Keck, T. (2017). Deprivation-Induced Homeostatic Spine Scaling In Vivo Is Localized to Dendritic Branches that Have Undergone Recent Spine Loss. Neuron *96*, 871–882.e5.
Barth, A.L., and Malenka, R.C. (2001). NMDAR EPSC kinetics do not regulate the critical period for LTP at thalamocortical synapses. Nat. Neurosci. *4*, 235–236.
Bashir, Z.I., Alford, S., Davies, S.N., Randall, A.D., and Collingridge, G.L. (1991). Long-term potentiation of NMDA receptor-mediated synaptic transmission in the hippocampus. Nature *349*, 156–158.
Bavelier, D., Tomann, A., Hutton, C., Mitchell, T., Corina, D., Liu, G., and Neville, H. Visual Attention to the Periphery Is Enhanced in Congenitally Deaf Individuals.
Beierlein, M., and Connors, B.W. (2002). Short-Term Dynamics of Thalamocortical and Intracortical Synapses Onto Layer 6 Neurons in Neocortex. J. Neurophysiol. *88*, 1924–1932.
Bessis, A., Béchade, C., Bernard, D., and Roumier, A. (2007). Microglial control of neuronal death and synaptic properties. Glia *55*, 233–238.
Bi, G.Q., and Poo, M.M. (1998). Synaptic modifications in cultured hippocampal neurons: dependence on spike timing, synaptic strength, and postsynaptic cell type. J. Neurosci. *18*, 10464–10472.
Bienenstock, E.L., Cooper, L.N., and Munro, P.W. (1982). THEORY FOR THE DEVELOPMENT OF NEURON SELECTIVITY: ORIENTATION SPECIFICITY AND BINOCULAR INTERACTION IN VISUAL CORTEX1. J. Neurosci Ence *2*, 32–48.
Binzegger, T. (2004). A Quantitative Map of the Circuit of Cat Primary Visual Cortex. J. Neurosci. *24*, 8441–8453.
Bliss, T. V, and Gardner-Medwin, a R. (1973). Long-lasting potentiation of synaptic transmission in the dentate area of the unanaestetized rabbit following stimulation of the perforant path. J. Physiol. *232*, 357–374.
Boehm, J., Kang, M.-G., Johnson, R.C., Esteban, J., Huganir, R.L., and Malinow, R. (2006). Synaptic incorporation of AMPA receptors during LTP is controlled by a PKC phosphorylation site on GluR1. Neuron *51*, 213–225.
Bourassa, J., and Deschˆnes, M. (1995). Corticothalamic projections from the primary visual cortex in rats: a single fiber study using biocytin as an anterograde tracer. Neuroscience *66*, 253–263.
Bourassa, J., Pinault, D., and Deschênes, M. (1995). Corticothalamic projections from the cortical barrel field to the somatosensory thalamus in rats: a single-fibre study using biocytin as an anterograde tracer. Eur. J.

Neurosci. *7*, 19–30.
Bourtchuladze, R., Frengueili, B., Blendy, J., Cioffi, D., Schutz, G., and Silva, A.J. (1994). Deficient Long-Term Memory in Mice with a Targeted Mutation of the CAMP-Responsive Element-Binding Protein. Cell *79*, 59–68.
Briggs, F. (2010). Organizing principles of cortical layer 6. Front. Neural Circuits *4*, 3.
Bruno, R.M., and Sakmann, B. (2006). Cortex Is Driven by Weak but Synchronously Active Thalamocortical Synapses. Science (80-.). *312*, 1622–1627.
Callaway, E.M., and Borrell, V. (2011). Developmental sculpting of dendritic morphology of layer 4 neurons in visual cortex: influence of retinal input. J. Neurosci. *31*, 7456–7470.
Cang, J., Kalatsky, V.A., Löwel, S., and Stryker, M.P. (2005). Optical imaging of the intrinsic signal as a measure of cortical plasticity in the mouse. Vis. Neurosci. *22*, 685–691.
Carmignoto, G., and Vicini, S. (1992). Activity-dependent decrease in NMDA receptor responses during development of the visual cortex. Science *258*, 1007–1011.
Casimiro, T.M., Sossa, K.G., Uzunova, G., Beattie, J.B., Marsden, K.C., and Carroll, R.C. (2011). mGluR and NMDAR activation internalize distinct populations of AMPARs. Mol. Cell. Neurosci. *48*, 161–170.
Chang, M.C., Park, J.M., Pelkey, K.A., Grabenstatter, H.L., Xu, D., Linden, D.J., Sutula, T.P., McBain, C.J., and Worley, P.F. (2010). Narp regulates homeostatic scaling of excitatory synapses on parvalbumin-expressing interneurons. Nat. Neurosci. *13*, 1090–1097.
Chittajallu, R., and Isaac, J.T.R. (2010). Emergence of cortical inhibition by coordinated sensory-driven plasticity at distinct synaptic loci. Nat. Neurosci. *13*, 1240–1248.
Cho, K., Aggleton, J.P., Brown, M.W., and Bashir, Z.I. (2001). An experimental test of the role of postsynaptic calcium levels in determining synaptic strength using perirhinal cortex of rat. J. Physiol. *532*, 459–466.
Choi, S.-Y. (2005). Multiple Receptors Coupled to Phospholipase C Gate Long-Term Depression in Visual Cortex. J. Neurosci. *25*, 11433–11443.
Chung, S., Jeong, J.-H., Ko, S., Yu, X., Kim, Y.-H., Isaac, J.T.R., and Koretsky, A.P. (2017). Peripheral Sensory Deprivation Restores Critical-Period-like Plasticity to Adult Somatosensory Thalamocortical Inputs. Cell Rep. *19*, 2707–2717.
Cingolani, L.A., Thalhammer, A., Yu, L.M.Y., Catalano, M., Ramos, T., Colicos, M.A., and Goda, Y. (2008). Activity-Dependent Regulation of Synaptic AMPA Receptor Composition and Abundance by β3 Integrins. Neuron *58*, 749–762.
Citri, A., and Malenka, R.C. (2008). Synaptic Plasticity: Multiple Forms, Functions, and Mechanisms. Neuropsychopharmacology *33*, 18–41.
Clay Reid, R., and Alonso, J.-M. (1995). Specificity of monosynaptic connections from thalamus to visual cortex. Nature *378*, 281–284.
Cooper, L.N., and Bear, M.F. (2012). The BCM theory of synapse modification at

30: interaction of theory with experiment. Nat. Rev. Neurosci. *13*, 798–810.
Crair, M.C., and Malenka, R.C. (1995). A critical period for long-term potentiation at thalamocortical synapses. Nature *375*, 325–328.
Creutzfeldt, O.D. (1977). Generality of the functional structure of the neocortex. Naturwissenschaften *64*, 507–517.
Crozier, R.A., Wang, Y., Liu, C.-H., and Bear, M.F. (2007). Deprivation-induced synaptic depression by distinct mechanisms in different layers of mouse visual cortex. Proc. Natl. Acad. Sci. U. S. A. *104*, 1383–1388.
Cruikshank, S.J., Lewis, T.J., and Connors, B.W. (2007a). Synaptic basis for intense thalamocortical activation of feedforward inhibitory cells in neocortex. Nat. Neurosci. *10*, 462–468.
Cruikshank, S.J., Lewis, T.J., and Connors, B.W. (2007b). Synaptic basis for intense thalamocortical activation of feedforward inhibitory cells in neocortex. Nat. Neurosci. *10*, 462–468.
Cummings, J.A., Mulkey, R.M., Nicoll, R.A., and Malenka, R.C. (1996). Ca2+ Signaling Requirements for Long-Term Depression in the Hippocampus. Neuron *16*, 825–833.
Czepita, D., Reid, S.N., and Daw, N.W. (1994). Effect of longer periods of dark rearing on NMDA receptors in cat visual cortex. J. Neurophysiol. *72*, 1220–1226.
D'Angelo, E. (2010). Homeostasis of intrinsic excitability: making the point. J. Physiol. *588*, 901–902.
Dantzker, J.L., and Callaway, E.M. (2000). Laminar sources of synaptic input to cortical inhibitory interneurons and pyramidal neurons. Nat. Neurosci. *3*, 701–707.
Daw, M.I., Ashby, M.C., and Isaac, J.T.R. (2007). Coordinated developmental recruitment of latent fast spiking interneurons in layer IV barrel cortex. Nat. Neurosci. *10*, 453–461.
Dehghani, N., Peyrache, A., Telenczuk, B., Le, M., Quyen, V., Halgren, E., Cash, S.S., Hatsopoulos, N.G., and Destexhe, A. (2016). Dynamic Balance of Excitation and Inhibition in Human and Monkey Neocortex. Nat. Publ. Gr.
Desai, N.S., Rutherford, L.C., and Turrigiano, G.G. (1999). Plasticity in the intrinsic excitability of cortical pyramidal neurons. Nat. Neuronscience *2*, 515–520.
Desai, N.S., Cudmore, R.H., Nelson, S.B., and Turrigiano, G.G. (2002a). Critical periods for experience-dependent synaptic scaling in visual cortex. Nat. Neurosci. *5*, 783–789.
Desai, N.S., Cudmore, R.H., Nelson, S.B., and Turrigiano, G.G. (2002b). Critical periods for experience-dependent synaptic scaling in visual cortex. Nat. Neurosci. *5*, 783–789.
Douglas, R.J., and Martin, K.A.C. (2004). NEURONAL CIRCUITS OF THE NEOCORTEX. Annu. Rev. Neurosci. *27*, 419–451.
Douglas, R.J., Martin, K.A.C., and Whitteridge, D. (1989). A Canonical Microcircuit for Neocortex. Neural Comput. *1*, 480–488.
Douglas, R.J., Koch, C., Mahowald, M., Martin, K.A., and Suarez, H.H. (1995).

Recurrent excitation in neocortical circuits. Science *269*, 981–985.
Dräger, U.C. (1978). Observations on Monocular Deprivation in Mice. J. Neurophysiol. *41*, 28–42.
Dudek, S.M., and Bear, M.F. (1992). Homosynaptic long-term depression in area CA1 of hippocampus and effects of N-methyl-D-aspartate receptor blockade. Proc. Natl. Acad. Sci. U. S. A. *89*, 4363–4367.
Dudek, S.M., and Friedlander, M.J. (1996). Developmental Down-Regulation of LTD in Cortical Layer IV and Its Independence of Modulation by Inhibition. Neuron *16*, 1097–1106.
Dye, M.W.G., Hauser, P.C., and Bavelier, D. (2009). Is Visual Selective Attention in Deaf Individuals Enhanced or Deficient? The Case of the Useful Field of View. PLoS One *4*, e5640.
Eaton, N.C., Sheehan, H.M., and Quinlan, E.M. (2016). Optimization of visual training for full recovery from severe amblyopia in adults. Learn. Mem. *23*, 99–103.
Elbert, T., and Rockstroh, B. (2004). Reorganization of Human Cerebral Cortex: The Range of Changes Following Use and Injury. Neurosci. *10*, 129–141.
von Engelhardt, J., Doganci, B., Seeburg, P.H., and Monyer, H. (2009). Synaptic NR2A- but not NR2B-Containing NMDA Receptors Increase with Blockade of Ionotropic Glutamate Receptors. Front. Mol. Neurosci. *2*, 19.
Erisir, A., and Harris, J.L. (2003). Decline of the critical period of visual plasticity is concurrent with the reduction of NR2B subunit of the synaptic NMDA receptor in layer 4. J. Neurosci. *23*, 5208–5218.
Esteban, J.A., Shi, S.-H., Wilson, C., Nuriya, M., Huganir, R.L., and Malinow, R. (2003). PKA phosphorylation of AMPA receptor subunits controls synaptic trafficking underlying plasticity. Nat. Neurosci. *6*, 136–143.
Evers, D.M., Matta, J.A., Hoe, H.-S., Zarkowsky, D., Lee, S.H., Isaac, J.T., and Pak, D.T.S. (2010). Plk2 attachment to NSF induces homeostatic removal of GluA2 during chronic overexcitation. Nat. Neurosci. *13*, 1199–1207.
Fagiolini, M., Pizzorusso, T., Berardi, N., Domenici, L., and Maffei, L. (1994). Functional postnatal development of the rat primary visual cortex and the role of visual experience: Dark rearing and monocular deprivation. Vision Res. *34*, 709–720.
Fagiolini, M., Fritschy, J.-M., Löw, K., Möhler, H., Rudolph, U., and Hensch, T.K. (2004). Specific GABAA Circuits for Visual Cortical Plasticity. Science (80-.). *303*, 1681–1683.
Feldman, D.E. (2000). Timing-based LTP and LTD at vertical inputs to layer II/III pyramidal cells in rat barrel cortex. Neuron *27*, 45–56.
Feldman, D.E. (2012). The spike-timing dependence of plasticity. Neuron *75*, 556–571.
Ferster, D., and Jagadeesh, B. (1992). EPSP-IPSP interactions in cat visual cortex studied with in vivo whole-cell patch recording. J. Neurosci. *12*, 1262–1274.
Fong, M., Newman, J.P., Potter, S.M., and Wenner, P. (2015). Upward synaptic scaling is dependent on neurotransmission rather than spiking. Nat. Commun. *6*, 6339.

Fox, K., Daw, N., Sato, H., and Czepita, D. (1991). Dark-rearing delays the loss of NMDA-receptor function in kitten visual cortex. Nature *350*, 342–344.
Frankland, P.W., O'Brien, C., Ohno, M., Kirkwood, A., and Silva, A.J. (2001). α-CaMKII-dependent plasticity in the cortex is required for permanent memory. Nature *411*, 309–313.
Frenkel, M.Y., and Bear, M.F. (2004). How Monocular Deprivation Shifts Ocular Dominance in Visual Cortex of Young Mice. Neuron *44*, 917–923.
Frey, U., Krug, M., Reymann, K.G., and Matthies, H. (1988). Anisomycin, an inhibitor of protein synthesis, blocks late phases of LTP phenomena in the hippocampal CA1 region in vitro. Brain Res. *452*, 57–65.
Gandhi, S.P., Yanagawa, Y., and Stryker, M.P. (2008). Delayed plasticity of inhibitory neurons in developing visual cortex. Proc. Natl. Acad. Sci. U. S. A. *105*, 16797–16802.
Gao, M., Sossa, K., Song, L., Errington, L., Cummings, L., Hwang, H., Kuhl, D., Worley, P., and Lee, H.-K. (2010). A specific requirement of Arc/Arg3.1 for visual experience-induced homeostatic synaptic plasticity in mouse primary visual cortex. J. Neurosci. *30*, 7168–7178.
Gao, M., Maynard, K.R., Chokshi, V., Song, L., Jacobs, C., Wang, H., Tran, T., Martinowich, K., and Lee, H.-K. (2014). Rebound potentiation of inhibition in juvenile visual cortex requires vision-induced BDNF expression. J. Neurosci. *34*, 10770–10779.
Gil, Z., Connors, B.W., and Amitai, Y. (1999). Efficacy of Thalamocortical and Intracortical Synaptic Connections: Quanta, Innervation, and Reliability. Neuron *23*, 385–397.
Gilbert, C., and Wiesel, T.N. (1992). Receptive field dynamics in adult primary visual cortex. Nature *356*, 150–152.
Gilbert, C.D., and Wiesel, T.N. (1983). Clustered intrinsic connections in cat visual cortex. J. Neurosci. *3*, 1116–1133.
Goddard, C.A., Butts, D.A., and Shatz, C.J. (2007). Regulation of CNS synapses by neuronal MHC class I. Proc. Natl. Acad. Sci. *104*, 6828–6833.
Goel, A., and Lee, H.-K. (2007). Persistence of Experience-Induced Homeostatic Synaptic Plasticity through Adulthood in Superficial Layers of Mouse Visual Cortex. J. Neurosci. *27*, 6692–6700.
Goel, A., Jiang, B., Xu, L.W., Song, L., Kirkwood, A., and Lee, H.K. (2006). Cross-modal regulation of synaptic AMPA receptors in primary sensory cortices by visual experience. Nat. Neurosci. *9*, 1001–1003.
Goel, A., Xu, L.W., Snyder, K.P., Song, L., Goenaga-Vazquez, Y., Megill, A., Takamiya, K., Huganir, R.L., and Lee, H.-K. (2011). Phosphorylation of AMPA Receptors Is Required for Sensory Deprivation-Induced Homeostatic Synaptic Plasticity. PLoS One *6*, e18264.
Goldreich, D., and Kanics, I.M. (2003). Tactile acuity is enhanced in blindness. J. Neurosci. *23*, 3439–3445.
Goold, C.P., and Nicoll, R.A. (2010). Single-cell optogenetic excitation drives homeostatic synaptic depression. Neuron *68*, 512–528.
Gordon, J.A., Sttyker, M.P., Program, N.G., and Keck, W.M. (1996). Experience-Dependent Plasticity of Binocular Responses in the Primary Visual Cortex

of the Mouse. J. Neurosci. *76*, 3274–3286.
Gougoux, F., Lepore, F., Lassonde, M., Voss, P., Zatorre, R.J., and Belin, P. (2004). Neuropsychology: Pitch discrimination in the early blind. Nature *430*, 309–309.
Gu, Y., and Cang, J. (2016). Binocular matching of thalamocortical and intracortical circuits in the mouse visual cortex. Elife *5*.
Guo, Y., Huang, S., De Pasquale, R., Mcgehrin, K., Lee, H.-K., Zhao, K., and Kirkwood, A. Development/Plasticity/Repair Dark Exposure Extends the Integration Window for Spike-Timing-Dependent Plasticity.
Hallman, L.E., Schofield, B.R., and Lin, C.-S. (1988). Dendritic morphology and axon collaterals of corticotectal, corticopontine, and callosal neurons in layer V of primary visual cortex of the hooded rat. J. Comp. Neurol. *272*, 149–160.
Harauzov, A., Spolidoro, M., DiCristo, G., De Pasquale, R., Cancedda, L., Pizzorusso, T., Viegi, A., Berardi, N., and Maffei, L. (2010). Reducing Intracortical Inhibition in the Adult Visual Cortex Promotes Ocular Dominance Plasticity. J. Neurosci. *30*, 361–371.
Harris, K.D., and Mrsic-Flogel, T.D. (2013). Cortical connectivity and sensory coding. Nature *503*.
Hashimoto, Y., Iwasaki, S., Mizuta, K., Arai, M., and Mineta, H. (2007). Pattern of cochlear damage caused by short-term kanamycin application using the round window microcatheter method. Acta Otolaryngol. *127*, 116–121.
Hashino, E., Tanaka, Y., and Sokabe, M. (1991). Hair cell damage and recovery following chronic application of kanamycin in the chick cochlea. Hear Res *52*, 356–368.
He, H.-Y. (2006). Visual Deprivation Reactivates Rapid Ocular Dominance Plasticity in Adult Visual Cortex. J. Neurosci. *26*, 2951–2955.
He, K., Petrus, E., Gammon, N., and Lee, H.-K. Distinct Sensory Requirements for Unimodal and Cross-Modal Homeostatic Synaptic Plasticity.
He, K., Petrus, E., Gammon, N., and Lee, H.-K. (2012). Distinct Sensory Requirements for Unimodal and Cross-Modal Homeostatic Synaptic Plasticity. J. Neurosci. *32*, 8469–8474.
Henley, J.M., and Wilkinson, K.A. (2013). AMPA receptor trafficking and the mechanisms underlying synaptic plasticity and cognitive aging. Dialogues Clin. Neurosci. *15*, 11–27.
Hensch, T.K. (2005). Critical period plasticity in local cortical circuits. Nat. Rev. Neurosci. *6*, 877–888.
Hensch, T.K., Fagiolini, M., Mataga, N., Stryker, M.P., Baekkeskov, S., and Kash, S.F. (1998). Local GABA circuit control of experience-dependent plasticity in developing visual cortex. Science *282*, 1504–1508.
Hensch, T.K., Stryker, M.P., Notes, 1 U, and Mayor (2004). Columnar architecture sculpted by GABA circuits in developing cat visual cortex. Science (80-.). *303*, 1678–1681.
Heynen, A.J., and Bear, M.F. (2001). Long-term potentiation of thalamocortical transmission in the adult visual cortex in vivo. J. Neurosci. *21*, 9801–9813.
Hoffman, G.E., Smith, M.S., and Verbalis, J.G. (1993). c-Fos and related

immediate early gene products as markers of activity in neuroendocrine systems. Front. Neuroendocrinol.
Hu, J.-H., Park, J.M., Park, S., Xiao, B., Dehoff, M.H., Kim, S., Hayashi, T., Schwarz, M.K., Huganir, R.L., Seeburg, P.H., et al. (2010). Homeostatic Scaling Requires Group I mGluR Activation Mediated by Homer1a. Neuron *68*, 1128–1142.
Huang, E.P. (1997). Synaptic plasticity: A role for nitric oxide in LTP Nitric oxide is back in the spotlight with a new series of studies showing that it plays an important role in long- term potentiation, the best-studied type of synaptic plasticity in the central nervous system thought likely to play an important role in learning and memory. Curr. Biol. *7*, 141–143.
Huang, S., Treviño, M., He, K., Ardiles, A., Pasquale, R. de, Guo, Y., Palacios, A., Huganir, R., and Kirkwood, A. (2012). Pull-push neuromodulation of LTP and LTD enables bidirectional experience-induced synaptic scaling in visual cortex. Neuron *73*, 497–510.
Huang, Z.J., Kirkwood, A., Pizzorusso, T., Porciatti, V., Morales, B., Bear, M.F., Maffei, L., and Tonegawa, S. (1999). BDNF Regulates the Maturation of Inhibition and the Critical Period of Plasticity in Mouse Visual Cortex. Cell *98*, 739–755.
Hubel, D.H., and Wiesel, T.N. (1968). Receptive fields and functional architecture of monkey striate cortex. J. Physiol. *195*, 215–243.
Hubel, D.H., and Wiesel, T.N. (1970). The period of susceptibility to the physiological effects of unilateral eye closure in kittens. J. Physiol. *206*, 419–436.
HUBEL, D.H., and WIESEL, T.N. (1959). Receptive fields of single neurones in the cat's striate cortex. J. Physiol. *148*, 574–591.
HUBEL, D.H., and WIESEL, T.N. (1962). Receptive fields, binocular interaction and functional architecture in the cat's visual cortex. J. Physiol. *160*, 106–154.
Huber, K.M., Sawtell, N.B., and Bear, M.F. (1998). Brain-derived neurotrophic factor alters the synaptic modification threshold in visual cortex. In Neuropharmacology, pp. 571–579.
Huber, K.M., Kayser, M.S., and Bear, M.F. (2000). Role for rapid dendritic protein synthesis in hippocampal mGluR-dependent long-term depression. Science *288*, 1254–1257.
Huemmeke, M., Eysel, U.T., and Mittmann, T. (2002). Metabotropic glutamate receptors mediate expression of LTP in slices of rat visual cortex. Eur. J. Neurosci. *15*, 1641–1645.
Ibata, K., Sun, Q., and Turrigiano, G.G. (2008). Rapid Synaptic Scaling Induced by Changes in Postsynaptic Firing. Neuron *57*, 819–826.
Ibrahim, L.A., Mesik, L., Ji, X., Fang, Q., Li, H., Li, Y., Zingg, B., Zhang, L.I., and Tao, H.W. (2016). Cross-Modality Sharpening of Visual Cortical Processing through Layer-1-Mediated Inhibition and Disinhibition. Neuron *89*, 1031–1045.
Ingrao, J.C., Johnson, R., Tor, E., Gu, Y., Litman, M., and Turner, P. V (2013). Aqueous stability and oral pharmacokinetics of meloxicam and carprofen

in male C57BL/6 mice. J. Am. Assoc. Lab. Anim. Sci. *52*, 553–559.
Isaacson, J.S., and Scanziani, M. (2011). How Inhibition Shapes Cortical Activity. Neuron *72*, 231–243.
Iurilli, G., Ghezzi, D., Olcese, U., Lassi, G., Nazzaro, C., Tonini, R., Tucci, V., Benfenati, F., and Medini, P. (2012a). Sound-driven synaptic inhibition in primary visual cortex. Neuron *73*, 814–828.
Iurilli, G., Ghezzi, D., Olcese, U., Lassi, G., Nazzaro, C., Tonini, R., Tucci, V., Benfenati, F., and Medini, P. (2012b). Sound-driven synaptic inhibition in primary visual cortex. Neuron *73*, 814–828.
Ji, W., Gămănuţ, R., Bista, P., D'Souza, R.D., Wang, Q., and Burkhalter, A. (2015). Modularity in the Organization of Mouse Primary Visual Cortex. Neuron *87*, 632–643.
Ji, X.-H., Cao, X.-H., Zhang, C.-L., Feng, Z.-J., Zhang, X.-H., Ma, L., and Li, B.-M. (2008). Pre- and Postsynaptic -Adrenergic Activation Enhances Excitatory Synaptic Transmission in Layer V/VI Pyramidal Neurons of the Medial Prefrontal Cortex of Rats. Cereb. Cortex *18*, 1506–1520.
Jiang, B., Huang, Z.J., Morales, B., and Kirkwood, A. (2005). Maturation of GABAergic transmission and the timing of plasticity in visual cortex. Brain Res. Rev. *50*, 126–133.
Jiang, B., Treviño, M., and Kirkwood, A. (2007). Sequential development of long-term potentiation and depression in different layers of the mouse visual cortex. J. Neurosci. *27*, 9648–9652.
Jitsuki, S., Takemoto, K., Kawasaki, T., Tada, H., Takahashi, A., Becamel, C., Sano, A., Yuzaki, M., Zukin, R.S., Ziff, E.B., et al. (2011). Serotonin Mediates Cross-Modal Reorganization of Cortical Circuits. Neuron *69*, 780–792.
Jones, M.W., Errington, M.L., French, P.J., Fine, A., Bliss, T.V.P., Garel, S., Charnay, P., Bozon, B., Laroche, S., and Davis, S. (2001). A requirement for the immediate early gene Zif268 in the expression of late LTP and long-term memories. Nat. Neurosci. *4*, 289–296.
Joo, J.-Y., Schaukowitch, K., Farbiak, L., Kilaru, G., and Kim, T.-K. (2016). Stimulus-specific combinatorial functionality of neuronal c-fos enhancers. Nat. Neurosci. *19*, 75–83.
Kalatsky, V.A., and Stryker, M.P. (2003). New paradigm for optical imaging: temporally encoded maps of intrinsic signal. Neuron *38*, 529–545.
Kaneko, M., Stellwagen, D., Malenka, R.C., and Stryker, M.P. (2008). Tumor Necrosis Factor-α Mediates One Component of Competitive, Experience-Dependent Plasticity in Developing Visual Cortex. Neuron *58*, 673–680.
Kato, K., Sekino, Y., Takahashi, H., Yasuda, H., and Shirao, T. (2007). Increase in AMPA receptor-mediated miniature EPSC amplitude after chronic NMDA receptor blockade in cultured hippocampal neurons. Neurosci. Lett. *418*, 4–8.
Kato, N., Artola, A., and Singer, W. (1991). Developmental changes in the susceptibility to long-term potentiation of neurones in rat visual cortex slices. Dev. Brain Res. *60*, 43–50.
Keck, T., Mrsic-Flogel, T.D., Afonso, M.V., Eysel, U.T., Bonhoeffer, T., and

Hübener, M. Massive restructuring of neuronal circuits during functional reorganization of adult visual cortex.
Keck, T., Keller, G.B., Jacobsen, R.I., Eysel, U.T., Bonhoeffer, T., and Hübener, M. (2013). Synaptic Scaling and Homeostatic Plasticity in the Mouse Visual Cortex In Vivo. Neuron *80*, 327–334.
Kerlin, A.M., Andermann, M.L., Berezovskii, V.K., and Reid, R.C. (2010). Broadly Tuned Response Properties of Diverse Inhibitory Neuron Subtypes in Mouse Visual Cortex. Neuron *67*, 858–871.
Kilman, V., van Rossum, M.C.W., and Turrigiano, G.G. (2002). Activity deprivation reduces miniature IPSC amplitude by decreasing the number of postsynaptic GABA(A) receptors clustered at neocortical synapses. J. Neurosci. *22*, 1328–1337.
Kim, E.J., Juavinett, A.L., Kyubwa, E.M., Jacobs, M.W., Callaway Correspondence, E.M., and Callaway, E.M. (2015). Three Types of Cortical Layer 5 Neurons That Differ in Brain-wide Connectivity and Function.
Kirkwood, A., and Bear, M.F. (1994a). Homosynaptic Long-Term Depression in the Visual Cortex. J. Neurosci. *74*.
Kirkwood, A., and Bear, M.F. (1994b). Hebbian synapses in visual cortex. J. Neurosci. *14*, 1634–1645.
Kirkwood, A., Lee, H.-K., and Bear, M.F. (1995). Co-regulation of long-term potentiation and experience-dependent synaptic plasticity in visual cortex by age and experience. Nature *375*, 328–331.
Kirkwood, A., Rioult, M.G., and Bear, M.F. (1996). Experience-dependent modification of synaptic plasticity in visual cortex. Nature *381*, 526–528.
Kloc, M., and Maffei, A. (2014). Target-Specific Properties of Thalamocortical Synapses onto Layer 4 of Mouse Primary Visual Cortex. J. Neurosci. *34*, 15455–15465.
Knott, G.W., Quairiaux, C., Genoud, C., and Welker, E. (2002). Formation of dendritic spines with GABAergic synapses induced by whisker stimulation in adult mice. Neuron *34*, 265–273.
Köhr, G., Jensen, V., Koester, H.J., Mihaljevic, A.L.A., Utvik, J.K., Kvello, A., Ottersen, O.P., Seeburg, P.H., Sprengel, R., and Hvalby, Ø. (2003). Intracellular domains of NMDA receptor subtypes are determinants for long-term potentiation induction. J. Neurosci. *23*, 10791–10799.
Krukowski, A.E., and Miller, K.D. (2001). Thalamocortical NMDA conductances and intracortical inhibition can explain cortical temporal tuning. Nat. Neurosci. *4*, 424–430.
Laramée, M.-E., and Boire, D. (2014). Visual cortical areas of the mouse: comparison of parcellation and network structure with primates. Front. Neural Circuits *8*, 149.
Lee, H.-K. (2006). Synaptic plasticity and phosphorylation. Pharmacol. Ther. *112*, 810–832.
Lee, H.-K., and Kirkwood, A. (2011). AMPA receptor regulation during synaptic plasticity in hippocampus and neocortex. Semin. Cell Dev. Biol. *22*, 514–520.

Lee, H.-K., Gao, M., Whitt, J.L., Huang, S., Lee, A., Mihalas, S., and Kirkwood, A. Experience-dependent homeostasis of “noise” at inhibitory synapses preserves information coding in adult visual cortex.
Lee, H.-K., Barbarosie, M., Kameyama, K., Bear, M.F., and Huganir, R.L. (2000). Regulation of distinct AMPA receptor phosphorylation sites during bidirectional synaptic plasticity. Nature *405*, 955–959.
Lee, H.-K., Takamiya, K., Han, J.-S., Man, H., Kim, C.-H., Rumbaugh, G., Yu, S., Ding, L., He, C., Petralia, R.S., et al. (2003). Phosphorylation of the AMPA Receptor GluR1 Subunit Is Required for Synaptic Plasticity and Retention of Spatial Memory. Cell *112*, 631–643.
Lee, H.K., Kameyama, K., Huganir, R.L., and Bear, M.F. (1998). NMDA induces long-term synaptic depression and dephosphorylation of the GluR1 subunit of AMPA receptors in hippocampus. Neuron *21*, 1151–1162.
Lehmann, J., Schneider, J., McPherson, S., Murphy, D.E., Bernard, P., Tsai, C., Bennett, D.A., Pastor, G., Steel, D.J., and Boehm, C. (1987). CPP, a selective N-methyl-D-aspartate (NMDA)-type receptor antagonist: characterization in vitro and in vivo. J. Pharmacol. Exp. Ther. *240*, 737–746.
Leslie, K.R., Nelson, S.B., and Turrigiano, G.G. (2001). Postsynaptic depolarization scales quantal amplitude in cortical pyramidal neurons. J. Neurosci. *21*, RC170.
Lessard, N., Paré, M., Lepore, F., and Lassonde, M. (1998). Early-blind human subjects localize sound sources better than sighted subjects. Nature *395*, 278–280.
Levy, A.D., Omar, M.H., and Koleske, A.J. (2014). Extracellular matrix control of dendritic spine and synapse structure and plasticity in adulthood. Front. Neuroanat. *8*, 116.
Liao, D.S., Krahe, T.E., Prusky, G.T., Medina, A.E., and Ramoa, A.S. (2004). Recovery of Cortical Binocularity and Orientation Selectivity After the Critical Period for Ocular Dominance Plasticity. J. Neurophysiol. *92*, 2113–2121.
Linden, D.J. (1999). The Return of the Spike: Postsynaptic Action Potentials and the Induction of LTP and LTD. Neuron *22*, 661–666.
Lintas, A., Schwaller, B., and Villa, A.E.P. (2013). Visual thalamocortical circuits in parvalbumin-deficient mice. Brain Res. *1536*, 107–118.
Lisman, J.E., and Zhabotinsky, A.M. (2001). A model of synaptic memory: a CaMKII/PP1 switch that potentiates transmission by organizing an AMPA receptor anchoring assembly. Neuron *31*, 191–201.
Lisman, J., Yasuda, R., and Raghavachari, S. (2012). Mechanisms of CaMKII action in long-term potentiation. Nat. Rev. Neurosci. *13*, 169–182.
Lissin, D. V, Gomperts, S.N., Carroll, R.C., Christine, C.W., Kalman, D., Kitamura, M., Hardy, S., Nicoll, R.A., Malenka, R.C., and von Zastrow, M. (1998). Activity differentially regulates the surface expression of synaptic AMPA and NMDA glutamate receptors. Proc. Natl. Acad. Sci. U. S. A. *95*, 7097–7102.
Liu, W., Yuen, E.Y., Allen, P.B., Feng, J., Greengard, P., and Yan, Z. (2006).

Adrenergic modulation of NMDA receptors in prefrontal cortex is differentially regulated by RGS proteins and spinophilin. Proc. Natl. Acad. Sci. U. S. A. *103*, 18338–18343.

Llano, D.A., and Sherman, S.M. (2009). Differences in intrinsic properties and local network connectivity of identified layer 5 and layer 6 adult mouse auditory corticothalamic neurons support a dual corticothalamic projection hypothesis. Cereb. Cortex *19*, 2810–2826.

Lledo, P.-M., Hjelmstadt, G. 0, Mukherjil, S., Soderlingt, T.R., Malenka, R.C., and Nicoll, R.A. (1995). Calcium/calmodulin-dependent kinase II and long-term potentiation enhance synaptic transmission by the same mechanism. Neurobiology *92*, 11175–11179.

Lu, W., and Roche, K.W. (2012). Posttranslational regulation of AMPA receptor trafficking and function. Curr. Opin. Neurobiol. *22*, 470–479.

Lüscher, C., and Huber, K.M. (2010). Group 1 mGluR-dependent synaptic long-term depression: mechanisms and implications for circuitry and disease. Neuron *65*, 445–459.

Maffei, A., Nelson, S.B., and Turrigiano, G.G. (2004). Selective reconfiguration of layer 4 visual cortical circuitry by visual deprivation. Nat. Neurosci. *7*, 1353–1359.

Magee, J.C., and Johnston, D. (1997). A synaptically controlled, associative signal for Hebbian plasticity in hippocampal neurons. Science *275*, 209–213.

Mainardi, M., Landi, S., Gianfranceschi, L., Baldini, S., De Pasquale, R., Berardi, N., Maffei, L., and Caleo, M. (2010). Environmental enrichment potentiates thalamocortical transmission and plasticity in the adult rat visual cortex. J. Neurosci. Res. *88*, 3048–3059.

Malenka, R.C., and Bear, M.F. (2004). LTP and LTD: An Embarrassment of Riches. Neuron *44*, 5–21.

Malinow, R., Schulman, H., Tsien, R., and Tonegawa, S. (1989). Inhibition of postsynaptic PKC or CaMKII blocks induction but not expression of LTP. Science (80-.). *245*, 862–866.

Markram, H., Lübke, J., Frotscher, M., and Sakmann, B. (1997). Regulation of synaptic efficacy by coincidence of postsynaptic APs and EPSPs. Science *275*, 213–215.

Marshel, J.H., Kaye, A.P., Nauhaus, I., and Callaway, E.M. (2012). Anterior-posterior direction opponency in the superficial mouse lateral geniculate nucleus. Neuron *76*, 713–720.

Mataga, N., Nagai, N., and Hensch, T.K. (2002). Permissive proteolytic activity for visual cortical plasticity. Proc. Natl. Acad. Sci. *99*, 7717–7721.

Mayer, M.L., Westbrook, G.L., and Guthrie, P.B. (1984). Voltage-dependent block by Mg2+ of NMDA responses in spinal cord neurones. Nature *309*, 261–263.

McGuire, B., Fiorillo, B., Ryugo, D.K., and Lauer, A.M. (2015). Auditory nerve synapses persist in ventral cochlear nucleus long after loss of acoustic input in mice with early-onset progressive hearing loss. Brain Res. *1605*, 22–30.

Merabet, L.B., Hamilton, R., Schlaug, G., Swisher, J.D., Kiriakopoulos, E.T., Pitskel, N.B., Kauffman, T., and Pascual-Leone, A. (2008). Rapid and Reversible Recruitment of Early Visual Cortex for Touch. PLoS One *3*, e3046.
Miller, K.D., and MacKay, D.J.C. (1994). The Role of Constraints in Hebbian Learning. Neural Comput. *6*, 100–126.
Montey, K.L., and Quinlan, E.M. (2011). Recovery from chronic monocular deprivation following reactivation of thalamocortical plasticity by dark exposure. Nat. Commun. *2*, 317.
Montey, K.L., Eaton, N.C., and Quinlan, E.M. (2013). Repetitive visual stimulation enhances recovery from severe amblyopia. Learn. Mem. *20*, 311–317.
Monyer, H., Burnashev, N., Laurie, D.J., Sakmann, B., and Seeburg, P.H. (1994). Developmental and regional expression in the rat brain and functional properties of four NMDA receptors. Neuron *12*, 529–540.
Morales, B., Choi, S.-Y., and Kirkwood, A. (2002). Dark rearing alters the development of GABAergic transmission in visual cortex. J. Neurosci. *22*, 8084–8090.
Morris, R.G.M. (1999). D.O. Hebb: The Organization of Behavior, Wiley: New York; 1949. Brain Res. Bull. *50*, 437.
Mower, G.D. (1991). The effect of dark rearing on the time course of the critical period in cat visual cortex. Dev. Brain Res. *58*, 151–158.
Mrsic-Flogel, T.D., Hofer, S.B., Ohki, K., Reid, R.C., Bonhoeffer, T., and Hübener, M. (2007). Homeostatic Regulation of Eye-Specific Responses in Visual Cortex during Ocular Dominance Plasticity. Neuron *54*, 961–972.
Mu, Y., Otsuka, T., Horton, A.C., Scott, D.B., and Ehlers, M.D. (2003). Activity-dependent mRNA splicing controls ER export and synaptic delivery of NMDA receptors. Neuron *40*, 581–594.
Mulkey, R.M., and Malenka, R.C. (1992). Mechanisms underlying induction of homosynaptic long-term depression in area CA1 of the hippocampus. Neuron *9*, 967–975.
Mulkey, R.M., Endo, S., Shenolikar, S., and Malenka, R.C. (1994). Involvement of a calcineurin/ inhibitor-1 phosphatase cascade in hippocampal long-term depression. Nature.
Murase, S., Lantz, C.L., and Quinlan, E.M. (2017). Light reintroduction after dark exposure reactivates plasticity in adults via perisynaptic activation of MMP-9. Elife *6*, e27345.
Murthy, V.N., Schikorski, T., Stevens, C.F., and Zhu, Y. (2001). Inactivity Produces Increases in Neurotransmitter Release and Synapse Size. Neuron *32*, 673–682.
Ni, H., Huang, L., Chen, N., Zhang, F., Liu, D., Ge, M., Guan, S., Zhu, Y., and Wang, J.-H. (2010). Upregulation of Barrel GABAergic Neurons Is Associated with Cross-Modal Plasticity in Olfactory Deficit. PLoS One *5*, e13736.
Nikolaienko, O., Patil, S., Eriksen, M.S., and Bramham, C.R. (2017). Arc protein: a flexible hub for synaptic plasticity and cognition. Semin. Cell Dev. Biol.
O'Brien, R.J., Kamboj, S., Ehlers, M.D., Rosen, K.R., Fischbach, G.D., and

Huganir, R.L. (1998a). Activity-dependent modulation of synaptic AMPA receptor accumulation. Neuron *21*, 1067–1078.
O'Brien, R.J., Kamboj, S., Ehlers, M.D., Rosen, K.R., Fischbach, G.D., and Huganir, R.L. (1998b). Activity-Dependent Modulation of Synaptic AMPA Receptor Accumulation. Neuron *21*, 1067–1078.
O'Brien, R.J., Kamboj, S., Ehlers, M.D., Rosen, K.R., Fischbach, G.D., and Huganir, R.L. (1998c). Activity-dependent modulation of synaptic AMPA receptor accumulation. Neuron *21*, 1067–1078.
O'Leary, T., van Rossum, M.C.W., and Wyllie, D.J.A. (2010). Homeostasis of intrinsic excitability in hippocampal neurones: dynamics and mechanism of the response to chronic depolarization. J. Physiol. *588*, 157–170.
Okun, M., and Lampl, I. (2008). Instantaneous correlation of excitation and inhibition during ongoing and sensory-evoked activities. Nat. Neurosci. *11*, 535–537.
Olivas, N.D., Quintanar-Zilinskas, V., Nenadic, Z., and Xu, X. (2012). Laminar circuit organization and response modulation in mouse visual cortex. Front. Neural Circuits *6*, 70.
Otmakhov, N., Griffith, L.C., and Lisman, J.E. (1997). Postsynaptic inhibitors of calcium/calmodulin-dependent protein kinase type II block induction but not maintenance of pairing-induced long-term potentiation. J. Neurosci. *17*, 5357–5365.
Pala, A., and Petersen, C.C.H. (2015). In vivo measurement of cell-type-specific synaptic connectivity and synaptic transmission in layer 2/3 mouse barrel cortex. Neuron *85*, 68–75.
Pascual-Leone, A., and Torres, F. (1993). Plasticity of the sensorimotor cortex representation of the reading finger in Braille readers. Brain *116 (Pt 1)*, 39–52.
Pawlak, V., Schupp, B.J., Single, F.N., Seeburg, P.H., and Köhr, G. (2005a). Impaired synaptic scaling in mouse hippocampal neurones expressing NMDA receptors with reduced calcium permeability. J. Physiol. *562*, 771–783.
Pawlak, V., Schupp, B.J., Single, F.N., Seeburg, P.H., and Köhr, G. (2005b). Impaired synaptic scaling in mouse hippocampal neurones expressing NMDA receptors with reduced calcium permeability. J. Physiol. *562*, 771–783.
Perez, Y., Morin, F., and Lacaille, J.C. (2001). A hebbian form of long-term potentiation dependent on mGluR1a in hippocampal inhibitory interneurons. Proc. Natl. Acad. Sci. U. S. A. *98*, 9401–9406.
Peter, K., Giese, K.P., Fedorov, N.B., Filipkowski, R.K., and Silva, A.J. (1998). Autophosphorylation at Thr 286 of the alpha Calcium-Calmodulin Kinase II in LTP and Learning. Science (80-.). *279*, 870–873.
Petrus, E., Isaiah, A., Jones, A.P., Li, D., Wang, H., Lee, H.K., and Kanold, P.O. (2014). Crossmodal Induction of Thalamocortical Potentiation Leads to Enhanced Information Processing in the Auditory Cortex. Neuron *81*, 664–673.
Petrus, E., Rodriguez, G., Patterson, R., Connor, B., Kanold, P.O., and Lee, H.-

K. (2015). Vision Loss Shifts the Balance of Feedforward and Intracortical Circuits in Opposite Directions in Mouse Primary Auditory and Visual Cortices. J. Neurosci. *35*, 8790–8801.
Pettit, D.L., Perlman, S., and Malinow, R. (1994). Potentiated transmission and prevention of further LTP by increased CaMKII activity in postsynaptic hippocampal slice neurons. Science *266*, 1881–1885.
Pfeffer, C.K., Xue, M., He, M., Huang, Z.J., and Scanziani, M. (2013). Inhibition of inhibition in visual cortex: the logic of connections between molecularly distinct interneurons. Nat. Neurosci. *16*, 1068–1076.
Pham, T.A., Graham, S.J., Suzuki, S., Barco, A., Kandel, E.R., Gordon, B., and Lickey, M.E. (2004). A semi-persistent adult ocular dominance plasticity in visual cortex is stabilized by activated CREB. Learn. Mem. *11*, 738–747.
Philpot, B.D., Sekhar, A.K., Shouval, H.Z., and Bear, M.F. (2001). Visual Experience and Deprivation Bidirectionally Modify the Composition and Function of NMDA Receptors in Visual Cortex. Neuron *29*, 157–169.
Philpot, B.D.B.D., Espinosa, J.S.J.S., and Bear, M.F.M.F. (2003). Evidence for altered NMDA receptor function as a basis for metaplasticity in visual cortex. J. Neurosci. *23*, 5583.
Pi, H.J., Otmakhov, N., Lemelin, D., De Koninck, P., and Lisman, J. (2010). Autonomous CaMKII Can Promote either Long-Term Potentiation or Long-Term Depression, Depending on the State of T305/T306 Phosphorylation. J. Neurosci. *30*, 8704–8709.
Piscopo, D.M., El-Danaf, R.N., Huberman, A.D., and Niell, C.M. (2013). Diverse Visual Features Encoded in Mouse Lateral Geniculate Nucleus. J. Neurosci. *33*, 4642–4656.
Pizzorusso, T., Medini, P., Berardi, N., Chierzi, S., Fawcett, J.W., and Maffei, L. (2002). Reactivation of Ocular Dominance Plasticity in the Adult Visual Cortex. Source Sci. New Ser. *298*, 1248–1251.
Pouille, F., and Scanziani, M. (2001). Enforcement of Temporal Fidelity in Pyramidal Cells by Somatic Feed-Forward Inhibition. Science (80-.). *293*, 1159–1163.
Quinlan, E.M., Olstein, D.H., and Bear, M.F. (1999). Bidirectional, experience-dependent regulation of N-methyl-D-aspartate receptor subunit composition in the rat visual cortex during postnatal development. Proc. Natl. Acad. Sci. U. S. A. *96*, 12876–12880.
Rannals, M.D., and Kapur, J. (2011). Homeostatic strengthening of inhibitory synapses is mediated by the accumulation of GABA(A) receptors. J. Neurosci. *31*, 17701–17712.
Ranson, A., Cheetham, C.E.J., Fox, K., and Sengpiel, F. (2012). Homeostatic plasticity mechanisms are required for juvenile, but not adult, ocular dominance plasticity. Proc. Natl. Acad. Sci. U. S. A. *109*, 1311–1316.
Rauschecker, J.P., Tian, B., Korte, M., and Egert, U. (1992). Crossmodal changes in the somatosensory vibrissa/barrel system of visually deprived animals. Proc. Natl. Acad. Sci. U. S. A. *89*, 5063–5067.
Regehr, W.G., Carey, M.R., and Best, A.R. (2009). Activity-Dependent Regulation of Synapses by Retrograde Messengers. Neuron *63*, 154–170.

Reinhold, K., Lien, A.D., and Scanziani, M. (2015). Distinct recurrent versus afferent dynamics in cortical visual processing. Nat. Neurosci. *18*, 1789–1797.

Rial Verde, E.M., Lee-Osbourne, J., Worley, P.F., Malinow, R., and Cline, H.T. (2006). Increased Expression of the Immediate-Early Gene Arc/Arg3.1 Reduces AMPA Receptor-Mediated Synaptic Transmission. Neuron *52*, 461–474.

Rittenhouse, C.D., Shouval, H.Z., Paradiso, M.A., and Bear, M.F. (1999). Monocular deprivation induces homosynaptic long-term depression in visual cortex. Nature *397*, 347–350.

Roche, K.W., O'Brien, R.J., Mammen, A.L., Bernhardt, J., and Huganir, R.L. (1996). Characterization of multiple phosphorylation sites on the AMPA receptor GluR1 subunit. Neuron *16*, 1179–1188.

Rockland, K.S., and Pandya, D.N. (1979). Laminar origins and terminations of cortical connections of the occipital lobe in the rhesus monkey. Brain Res. *179*, 3–20.

De Roo, M., Klauser, P., and Muller, D. (2008). LTP Promotes a Selective Long-Term Stabilization and Clustering of Dendritic Spines. PLoS Biol. *6*, e219.

Roth, M.M., Dahmen, J.C., Muir, D.R., Imhof, F., Martini, F.J., and Hofer, S.B. (2015). Thalamic nuclei convey diverse contextual information to layer 1 of visual cortex. Nat. Neurosci. *19*, 299–307.

Rumbaugh, G., and Vicini, S. (1999). Distinct synaptic and extrasynaptic NMDA receptors in developing cerebellar granule neurons. J. Neurosci. *19*, 10603–10610.

Runyan, C.A., Schummers, J., Van Wart, A., Kuhlman, S.J., Wilson, N.R., Huang, Z.J., and Sur, M. (2010). Response features of parvalbumin-expressing interneurons suggest precise roles for subtypes of inhibition in visual cortex. Neuron *67*, 847–857.

Rutherford, L.C., Nelson, S.B., and Turrigiano, G.G. (1998). BDNF has opposite effects on the quantal amplitude of pyramidal neuron and interneuron excitatory synapses. Neuron *21*, 521–530.

Sale, A., Berardi, N., Spolidoro, M., Baroncelli, L., and Maffei, L. (2010). GABAergic inhibition in visual cortical plasticity. Front. Cell. Neurosci. *4*, 10.

Sarihi, A., Jiang, B., Komaki, A., Sohya, K., Yanagawa, Y., and Tsumoto, T. (2008). Metabotropic glutamate receptor type 5-dependent long-term potentiation of excitatory synapses on fast-spiking GABAergic neurons in mouse visual cortex. J. Neurosci. *28*, 1224–1235.

Sato, M., and Stryker, M.P. (2008). Distinctive Features of Adult Ocular Dominance Plasticity. J. Neurosci. *28*, 10278–10286.

Sawtell, N.B., Frenkel, M.Y., Philpot, B.D., Nakazawa, K., Tonegawa, S., and Bear, M.F. (2003). NMDA Receptor-Dependent Ocular Dominance Plasticity in Adult Visual Cortex. Neuron *38*, 977–985.

Scholl, B., Tan, A.Y.Y., Corey, J., and Priebe, N.J. (2013). Emergence of orientation selectivity in the Mammalian visual pathway. J. Neurosci. *33*, 10616–10624.

Schuett, S., Bonhoeffer, T., and Hübener, M. (2002). Mapping retinotopic structure in mouse visual cortex with optical imaging. J. Neurosci. *22*, 6549–6559.
Scott, G.D., Karns, C.M., Dow, M.W., Stevens, C., and Neville, H.J. (2014). Enhanced peripheral visual processing in congenitally deaf humans is supported by multiple brain regions, including primary auditory cortex. Front. Hum. Neurosci. *8*, 177.
Seeburg, D.P., and Sheng, M. (2008). Activity-induced Polo-like kinase 2 is required for homeostatic plasticity of hippocampal neurons during epileptiform activity. J. Neurosci. *28*, 6583–6591.
Senkov, O., Andjus, P., Radenovic, L., and Soriano, E. (2014). Neural ECM molecules in synaptic plasticity, learning, and memory. Prog. Brain Res. *214*, 53–80.
Seol, G.H., Ziburkus, J., Huang, S., Song, L., Kim, I.T., Takamiya, K., Huganir, R.L., Lee, H.K., and Kirkwood, A. (2007). Neuromodulators Control the Polarity of Spike-Timing-Dependent Synaptic Plasticity. Neuron *55*, 919–929.
Shai, A.S., Anastassiou, C.A., Larkum, M.E., and Koch, C. (2015). Physiology of layer 5 pyramidal neurons in mouse primary visual cortex: coincidence detection through bursting. PLoS Comput. Biol. *11*, e1004090.
Sheng, M., Cummings, J., Roldan, L.A., Jan, Y.N., and Jan, L.Y. (1994). Changing subunit composition of heteromeric NMDA receptors during development of rat cortex. Nature *368*, 144–147.
Shepherd, J.D., Rumbaugh, G., Wu, J., Chowdhury, S., Plath, N., Kuhl, D., Huganir, R.L., and Worley, P.F. (2006). Arc/Arg3.1 Mediates Homeostatic Synaptic Scaling of AMPA Receptors. Neuron *52*, 475–484.
Shouval, H.Z., Bear, M.F., and Cooper, L.N. (2002). A unified model of NMDA receptor-dependent bidirectional synaptic plasticity.
Siddoway, B., Hou, H., and Xia, H. (2014). Molecular mechanisms of homeostatic synaptic downscaling. Neuropharmacology *78*, 38–44.
Song, S., Miller, K.D., and Abbott, L.F. (2000). Competitive Hebbian learning through spike-timing-dependent synapticplasticity. Nat. Neurosci. *3*, 919–926.
Sprengel, R., Suchanek, B., Amico, C., Brusa, R., Burnashev, N., Rozov, A., Hvalby, Ø., Jensen, V., Paulsen, O., Andersen, P., et al. (1998). Importance of the Intracellular Domain of NR2 Subunits for NMDA Receptor Function In Vivo. Cell *92*, 279–289.
Staiger, J.F., Flagmeyer, I., Schubert, D., Zilles, K., Kötter, R., and Luhmann, H.J. (2004). Functional Diversity of Layer IV Spiny Neurons in Rat Somatosensory Cortex: Quantitative Morphology of Electrophysiologically Characterized and Biocytin Labeled Cells. Cereb. Cortex *14*, 690–701.
Stanton, P.K., Chattarji, S., and Sejnowski, T.J. (1991). 2-Amino-3-phosphonopropionic acid, an inhibitor of glutamate-stimulated phosphoinositide turnover, blocks induction of homosynaptic long-term depression, but not potentiation, in rat hippocampus. Neurosci. Lett. *127*, 61–66.

Steele, P.M., and Mauk, M.D. (1999). Inhibitory Control of LTP and LTD: Stability of Synapse Strength. J. Neurophysiol. *81*, 1559–1566.
Stellwagen, D., and Malenka, R.C. (2006). Synaptic scaling mediated by glial TNF-α. Nature *440*, 1054–1059.
Stocca, G., and Vicini, S. (1998). Increased contribution of NR2A subunit to synaptic NMDA receptors in developing rat cortical neurons. J. Physiol. *507*, 13–24.
Sutton, M.A., Ito, H.T., Cressy, P., Kempf, C., Woo, J.C., and Schuman, E.M. (2006). Miniature Neurotransmission Stabilizes Synaptic Function via Tonic Suppression of Local Dendritic Protein Synthesis. Cell *125*, 785–799.
Thomson, A.M. (2010). Neocortical layer 6, a review. Front. Neuroanat. *4*, 13.
Thomson, A.M., and Lamy, C. (2007). Functional maps of neocortical local circuitry. Front. Neurosci. *1*, 19–42.
Tieman, S.B. (1984). Effects of monocular deprivation on geniculocortical synapses in the cat. J. Comp. Neurol. *222*, 166–176.
Trachtenberg, J.T. (2015). Competition, inhibition, and critical periods of cortical plasticity. Curr. Opin. Neurobiol. *35*, 44–48.
Tsien, J.Z., Chen, D.F., Gerber, D., Tom, C., Mercer, E.H., Anderson, D.J., Mayford, M., Kandel, E.R., and Tonegawa, S. (1996). Subregion- and cell type-restricted gene knockout in mouse brain. Cell *87*, 1317–1326.
Turrigiano, G.G. (2008). The Self-Tuning Neuron: Synaptic Scaling of Excitatory Synapses. Cell *135*, 422–435.
Turrigiano, G.G., Leslie, K.R., Desai, N.S., Rutherford, L.C., and Nelson, S.B. (1998). Activity-dependent scaling of quantal amplitude in neocortical neurons. Nature *391*, 892–896.
Le Vay, S., Wiesel, T.N., and Hubel, D.H. (1980). The development of ocular dominance columns in normal and visually deprived monkeys. J. Comp. Neurol. *191*, 1–51.
Vélez-Fort, M., and Margrie, T.W. (2012). Cortical Circuits: Layer 6 Is a Gain Changer. CURBIO *22*, R411–R413.
van Versendaal, D., and Levelt, C.N. (2016). Inhibitory interneurons in visual cortical plasticity. Cell. Mol. Life Sci. *73*, 3677–3691.
Vetencourt, J.F.M., Sale, A., Viegi, A., Baroncelli, L., De Pasquale, R., F. O'Leary, O., Castren, E., and Maffei, L. (2008). The Antidepressant Fluoxetine Restores Plasticity in the Adult Visual Cortex. Science (80-.). *320*, 385–388.
Vicini, S., Wang, J.F., Li, J.H., Zhu, W.J., Wang, Y.H., Luo, J.H., Wolfe, B.B., and Grayson, D.R. (1998). Functional and Pharmacological Differences Between Recombinant *N* -Methyl- d -Aspartate Receptors. J. Neurophysiol. *79*, 555–566.
Voss, P. (2013). Sensitive and critical periods in visual sensory deprivation. Front. Psychol. *4*, 664.
Wagor, E., Mangini, N.J., and Pearlman, A.L. (1980). Retinotopic organization of striate and extrastriate visual cortex in the mouse. J. Comp. Neurol. *193*, 187–202.

Walz, C., Jüngling, K., Lessmann, V., and Gottmann, K. (2006). Presynaptic plasticity in an immature neocortical network requires NMDA receptor activation and BDNF release. J. Neurophysiol. *96*, 3512–3516.
Wang, X.F., and Daw, N.W. (2003). Long term potentiation varies with layer in rat visual cortex. Brain Res. *989*, 26–34.
Wang, H., Ardiles, A.O., Yang, S., Tran, T., Posada-Duque, R., Valdivia, G., Baek, M., Chuang, Y.-A., Palacios, A.G., Gallagher, M., et al. (2016). Metabotropic Glutamate Receptors Induce a Form of LTP Controlled by Translation and Arc Signaling in the Hippocampus. J. Neurosci. *36*, 1723–1729.
Wang, L., Kloc, M., Gu, Y., Ge, S., and Maffei, A. (2013). Layer-specific experience-dependent rewiring of thalamocortical circuits. J. Neurosci. *33*, 4181–4191.
Watt, A.J., van Rossum, M.C.., MacLeod, K.M., Nelson, S.B., and Turrigiano, G.G. (2000). Activity Coregulates Quantal AMPA and NMDA Currents at Neocortical Synapses. Neuron *26*, 659–670.
Whitt, J.L., Petrus, E., and Lee, H.K. (2015). Experience-dependent homeostatic synaptic plasticity in neocortex. Neuropharmacology *78*, 45–54.
Wierenga, C.J. (2005). Postsynaptic Expression of Homeostatic Plasticity at Neocortical Synapses. J. Neurosci. *25*, 2895–2905.
Wiesel, T.N., and Hubel, D.H. (1965). Comparison of the effects of unilateral and bilateral eye closure on cortical unit responses in kittens. J. Neurophysiol. *28*, 1029–1040.
Winder, D.G., and Sweatt, J.D. (2001). Roles of serine/threonine phosphatases in hippocampel synaptic plasticity. Nat. Rev. Neurosci. *2*, 461–474.
Xu, X., Olivas, N.D., Ikrar, T., Peng, T., Holmes, T.C., Nie, Q., and Shi, Y. (2016). Primary visual cortex shows laminar-specific and balanced circuit organization of excitatory and inhibitory synaptic connectivity. J. Physiol. *594*, 1891–1910.
Xue, M., Atallah, B. V., and Scanziani, M. (2014). Equalizing excitation–inhibition ratios across visual cortical neurons. Nature *511*, 596–600.
Yang, S.-N., Tang, Y.-G., and Zucker, R.S. (1999). Selective Induction of LTP and LTD by Postsynaptic $[Ca^{2+}]_i$ Elevation. J. Neurophysiol. *81*, 781–787.
Zarrinpar, A. (2006). Local Connections to Specific Types of Layer 6 Neurons in the Rat Visual Cortex. J. Neurophysiol. *95*, 1751–1761.
Zhang, Z., Jiao, Y.-Y., and Sun, Q.-Q. (2011). Developmental maturation of excitation and inhibition balance in principal neurons across four layers of somatosensory cortex. Neuroscience *174*, 10–25.

Curriculum Vitae

Gabriela Rodríguez

Department of Biology, Johns Hopkins University, 3400 N. Charles street, Baltimore, MD 21218
(410) 516-5715 | grodrig9@jhu.edu

EDUCATION:

2012-2018 Ph.D., Biology, Johns Hopkins University, Baltimore, MD
Thesis: Cellular mechanisms underlying homeostatic and cross-modal plasticity in mouse primary visual cortex
Advisor: Dr. Hey-Kyoung Lee, Ph.D.
Expected graduation: May 2018

2007-2012 B.S., *cum laude*, Industrial Biotechnology, University of Puerto Rico, Mayagüez, PR

RESEARCH EXPERIENCE:

2012-present Johns Hopkins University
Graduate researcher; Advisor: Dr. Hey-Kyoung Lee, Ph.D.

- Used whole-cell electrophysiology coupled with optogenetics, *in vivo* imaging of intrinsic signals, and immunohistology with the goal of elucidating mechanisms that underlie cross-modal and homeostatic plasticity in primary visual cortex after sensory loss in mice.

2011-2012 University of Puerto Rico, Mayagüez;
Plant Biotechnology Lab
Undergraduate researcher; Advisor: Dr. Dimuth Siritunga, Ph.D.

- Performed complementation and enzymatic assays to characterize the function of newly identified beta-cyanoalanine synthase and cysteine synthase genes found in cassava (*Manihot esculenta crantz*).

Summer 2011 Arkansas Bioscience Institute
Undergraduate intern; Advisor: Dr. Argelia Lorence, Ph.D.

- Studied the effect of myo-inositol oxygenase over-expression on ascorbic acid levels and biomass in tobacco plants.

2008-2010 University of Puerto Rico, Mayagüez

Center for Chemical Sensors Development

Undergraduate researcher; Advisor: Dr. Samuel P. Hernandez, Ph.D.

- Synthesized and optimized silver nanoparticle colloids as substrates for Surface Enhanced RAMAN Spectroscopy of adenine-based molecules.

PUBLICATIONS:

Petrus, E., **Rodríguez, G.,** Patterson, R., Connor, B., Kanold, P.O., and Lee, H-K. (2015) Vision loss shifts the balance of feedforward and intracortical circuits in opposite directions in mouse primary auditory and visual cortices. *Journal of Neuroscience.* 35 (23): 8790-8801

Primera-Pedrozo, O.M**., Rodríguez-González, G**, Castellanos, J., Felix-Rivera, H, Resto, O., and Hernández-Rivera, S. P. (2012) Increasing the Surface Enhanced Raman Spectroscopy (SERS) effect of RNA & DNA components by changing the silver colloid pH.*Spectrochimica Acta Part A Molecular and Biomolecular Spectroscopy.* 87: 77-85

Félix-Rivera, H., González, R., **Rodríguez-González, G.,** Primera-Pedrozo, O.M., Ríos-Velázquez, C. and Hernández-Rivera, S.P. (2011) Improving SERS Detection of Bacillus thuringiensis Using Silver Nanoparticles Reduced with Hydroxylamine and with Citrate Capped Borohydride. *International Journal of Spectroscopy*. 2011(24)

ABSTRACTS AND INVITED TALKS:

Rodríguez, G. and Lee, H-K. (2016) Cross-modal sensory deprivation promotes plasticity in adult visual cortex, *Society for Neuroscience,* Greater Baltimore Chapter meeting, Baltimore, MD

Rodríguez, G. and Lee, H-K. (2017) Cross-modal sensory deprivation promotes plasticity in adult visual cortex, *Society for Neuroscience,* Washington, DC

Invited Speaker (2017) Deafening promotes thalamocortical plasticity in adult visual cortex, NIH/LFMI, Bethesda, MD

Rodríguez, G. and Lee, H-K. (2016) Cross-modal sensory deprivation promotes plasticity in adult visual cortex, *Society for Neuroscience,* San Diego, CA

Rodríguez, G. and Lee, H-K. (2016) Cross-modal sensory deprivation promotes plasticity in adult visual cortex, *NIH Future Research Leaders Conference*, Bethesda, MD

Rodríguez, G., Petrus, E., Shrode, K., Lauer, A. and Lee, H-K. (2016) Cross-modal regulation of thalamic inputs onto inhibitory neurons in adult primary visual cortex, *Gordon Research Conference: Optogenetic Approaches to Understanding Neural Circuits and Behavior*, Sunday River Newry, ME

Rodríguez, G., Gao, M. and Lee, H-K. (2015) Cell autonomous and network effects of NMDA receptors in experience-dependent homeostatic synaptic scaling, *Greater Baltimore Society for Neuroscience meeting*, Baltimore, MD

Rodríguez, G., Gao, M. and Lee, H-K. (2015) Cell autonomous and network effects of NMDA receptors in experience-dependent homeostatic synaptic scaling, *Society for Neuroscience*, Chicago, IL

Rodríguez, G., Gao, M. and Lee, H-K. (2014) Role of NMDA receptors in experience-dependent homeostatic synaptic scaling, *Greater Baltimore Society for Neuroscience meeting Baltimore*, MD

Rodríguez, G., Gao, M. and Lee, H-K. (2014) Role of NMDA receptors in experience-dependent homeostatic synaptic scaling, *Society for Neuroscience*, Washington, DC

Rodríguez, G, Nessler, C.L. and Lorence, A. (2011) Myo-Inositol Oxygenase expression in tobacco leads to plants with enhanced biomass and vitamin C content. *Annual Biomedical Research Conference for Minority Students* , St. Louis, MO

Rodríguez, G., Martínez-García, R., Félix-Rivera, H., Soto-Feliciano, K., Primera-Pedrozo, O.M., Ríos-Velázquez, C. and Hernández-Rivera, S.P. (2010) *Bacillus thuringiensis* detection and characterization by normal Raman and SERS at the stationary growth stage. *Annual Biomedical Research Conference for Minority Students*, Charlotte, NC

Rodríguez, G., Martínez-García, R., Félix-Rivera, H., Ríos-Velázquez, C. and Hernández-Rivera, S.P. (2010) *Bacillus thuringiensis* detection and characterization by normal Raman and SERS at the stationary growth Stage, *Puerto Rico Junior Technical and Interdisciplinary meeting,* San Juan, PR

Rodríguez, G., Martínez-García, R., Félix-Rivera, H., Soto-Feliciano, K., Primera-Pedrozo, O.M., Ríos-Velázquez, C. and Hernández-Rivera, S.P. (2010) *Bacillus thuringiensis* detection and characterization by normal Raman and SERS at the stationary growth stage. *Northeast Alliance for Graduate Education and the Professoriate NEA Science Day*, Mayagüez, PR

Rodríguez, G., Primera-Pedrozo, O., Hernández-Rivera, S.P., Rivera, N.,

Castellanos, J. and Resto, O. (2009) Surface Enhanced Raman Spectroscopy (SERS) of RNA - DNA components by changing the silver colloid pH, *Annual Biomedical Research Conference for Minority Students,* Phoenix, AZ

HONORS AND AWARDS

2017	Outstanding poster award Baltimore Chapter SfN meeting
2016	Carl Storm Underrepresented Minority Fellowship
2011	Award for best poster in Cellular Biology, ABRCMS
2011	Award for best poster in Interdisciplinary Research, ABRCMS
2010-2012	Minority Access to Research Careers (MARC) fellowship
2009-2010	UPRM/DoE-SRS undergraduate scholarship

TEACHING AND MENTORING EXPERIENCE

2017	Instructor Johns Hopkins University Multisensory integration: functions and dysfunctions
Summer 2016	Mentor Johns Hopkins University Research experience for undergraduates (REU) program
Summer 2015	Mentor Johns Hopkins High school intern
Fall 2015	Teaching Assistant Johns Hopkins University Phage lab (Narrative and Visualization project)

	Supervisor: Dr. Emily Fisher
Spring 2014	Teaching Assistant Johns Hopkins University Cell Biology Lab Supervisor: Dr. Robert Horner
Fall 2013	Teaching Assistant Johns Hopkins University Biochemistry Lab Supervisor: Dr. Robert Horner
Summer 2013	Mentor Johns Hopkins REU program

PROFESIONAL DEVELOPMENT

2015 – 2017 **Neuroscience Scholars Program (NSP) Associate**

Two-year training program funded and organized by the Society for Neuroscience focused on providing career mentorship to graduate students and post-docs from underrepresented groups.

07/2017 **NSP Preparing the Next Generation of Neuroscience Leaders Conference Washington, DC**

Two-day conference focused on discussing the grant application process through the NIH and NSF, science communication and scientific rigor.

11/2016 **NIH Future Leaders in Research Conference Bethesda, MD**

Three-day conference focused on discussing NIH funding options, the intramural research program and career options at the NIH.

05/2015 **Johns Hopkins University Teaching Academy**

Three-day teaching institute designed to improve university-level classroom teaching. Workshops focused on: teaching-as-scholarship, inclusive classrooms, active-learning, assessment, teaching-as-research/evaluation, course planning, teaching statement and teaching portfolios.

07/2014 **Stanford University, Deisseroth Lab's CLARITY workshop**

Workshop leader: Kristin Engberg. Three-day workshop focused on processing tissue with the CLARITY technique and discussion of its applications.

OUTREACH AND PROFESIONAL ASSOCIATIONS:

2017	Volunteer	Sisters Circle Super Science Saturday
2017	Member	Society for Neuroscience
2015	Speaker	University of Puerto Rico-Mayaguez
2015	Speaker	University of Puerto Rico-Humacao
2015	Speaker	University of Puerto Rico-Cayey
2015	Speaker	University of Puerto Rico-Rio Piedras
2014	Organizer	Johns Hopkins, REU program
2014	Speaker	University of Puerto Rico-Rio Piedras
2014	Speaker	University of Puerto Rico-Mayaguez
2013	volunteer	Johns Hopkins, REU program
2013	representative	Annual Biomedical Research Conference for Minority Students (ABRCMS)
2012-present	Member	Mentoring and Inspiring Diversity in Science (MInDS)